2005

EFFECT OF COMBINATION EXPOSURE TO ZIDOVUDINE AND SULFAMETHOXAZOLE-TRIMETHOPRIM ON IMMUNE RESPONSE IN MICE AND HUMANS

David James Feola
University of Kentucky, djfeol2@email.uky.edu

ABSTRACT OF DISSERTATION

David James Feola

The Graduate School

University of Kentucky

2005

EFFECT OF COMBINATION EXPOSURE TO ZIDOVUDINE AND SULFAMETHOXAZOLE-TRIMETHOPRIM ON IMMUNE RESPONSE IN MICE AND HUMANS

ABSTRACT OF DISSERTATION

A dissertation submitted in partial fulfillment of the
requirements for the degree of Doctor of Philosophy in the
College of Pharmacy at the University of Kentucky

By

David James Feola

Lexington, Kentucky

Director: Dr. Robert P. Rapp, Professor of Pharmacy and Medicine

Lexington, Kentucky

2005

EFFECT OF COMBINATION EXPOSURE TO ZIDOVUDINE AND SULFAMETHOXAZOLE-TRIMETHOPRIM ON IMMUNE RESPONSE IN MICE AND HUMANS

ABSTRACT OF DISSERTATION

A dissertation submitted in partial fulfillment of the
requirements for the degree of Doctor of Philosophy in the
College of Pharmacy at the University of Kentucky

By
David James Feola

Lexington, Kentucky

Co-Directors: Dr. Beth A. Garvy, Associate Professor of Medicine
and Dr. Patrick McNamara, Professor of Pharmacy
and Dr. Val Adams, Associate Professor of Pharmacy

Lexington, Kentucky

2005

ABSTRACT OF DISSERTATION

EFFECT OF COMBINATION EXPOSURE TO ZIDOVUDINE AND SULFAMETHOXAZOLE-TRIMETHOPRIM ON IMMUNE RESPONSE IN MICE AND HUMANS

The drug-drug interaction involving zidovudine and sulfamethoxazole-trimethoprim was investigated using an *in vitro* culture system, an *in vivo* mouse model, and a clinical trial in HIV-infected patients. We hypothesized that combination exposure causes immune cell populations in the bone marrow to undergo apoptotic cell death, and that the toxicity would affect the host response to an infectious stimulus.

Mice were dosed with zidovudine, sulfamethoxazole-trimethoprim, the combination of both drugs, or vehicle only control via oral gavage. Focusing on B-lineage cells in the bone marrow, we determined that cells of the rapidly cycling, early pre-B cell subset are targeted, as well as pro-B cells earlier in development. This toxicity was found to be cell cycle dependent, with an increase in percentage of cells in the S/G2/M phases of the cycle. *In vitro* experiments using the drugs in a bone marrow culture system demonstrated that the effect of cytotoxicity with combination exposure is synergistic and concentration-dependent. The mechanism of apoptosis that is induced appears to be caspase-independent.

To measure host response in mice, animals treated with zidovudine plus sulfamethoxazole-trimethoprim were infected with *Pneumocystis murina* pneumonia, and the group that received the combination of agents had a blunted antigen-specific IgG response, possibly due to a decreased number of B cells and activated B cells in the draining lymph nodes of the lungs.

A clinical trial was conducted in HIV-infected patients, dividing subjects into groups receiving zidovudine, sulfamethoxazole-trimethoprim, the combination of both, or neither agent. Upon vaccination with the influenza vaccine, the combination treatment group had a blunted humoral response, with reduced antigen-specific serum IgG titers as compared to the control group. We conclude that the drug-drug interaction involving zidovudine and sulfamethoxazole-trimethoprim is clinically-significant, and clinicians must consider this toxicity when treating patients with these agents concurrently.

KEYWORDS: zidovudine, sulfamethoxazole-trimethoprim, apoptosis, B lymphocytes, humoral immunity

David James Feola

August 31, 2005

EFFECT OF COMBINATION EXPOSURE TO ZIDOVUDINE AND SULFAMETHOXAZOLE-TRIMETHOPRIM ON IMMUNE RESPONSE IN MICE AND HUMANS

By

David James Feola

Robert P. Rapp
Director of Dissertation

Jim R. Pauly
Director of Graduate Studies

August 31, 2005

EFFECT OF COMBINATION EXPOSURE TO ZIDOVUDINE AND SULFAMETHOXAZOLE-TRIMETHOPRIM ON IMMUNE RESPONSE IN MICE AND HUMANS

By

David James Feola

Beth A. Garvy
Co-Director of Dissertation

Patrick J. McNamara
Co-Director of Dissertation

Val R. Adams
Co-Director of Dissertation

Jim R. Pauly
Director of Graduate Studies

August 31, 2005

RULES FOR THE USE OF DISSERTATION

Unpublished dissertations submitted for the Doctor's degree and deposited in the University of Kentucky Library are as a rule open for inspection, but are to be used only with due regard to the rights of the authors. Bibliographical references may be noted, but quotations or summaries of parts may be published only with the permission of the author, and with the usual scholarly acknowledgements.

Extensive copying or publication of the dissertation in whole or in part also requires consent of the Dean of the Graduate School of the University of Kentucky.

A library that borrows this dissertation for use by its patrons is expected to secure the signature of each user.

Name Date

DISSERTATION

David James Feola

The Graduate School

University of Kentucky

2005

EFFECT OF COMBINATION EXPOSURE TO ZIDOVUDINE AND SULFAMETHOXAZOLE-TRIMETHOPRIM ON IMMUNE RESPONSE IN MICE AND HUMANS

DISSERTATION

A dissertation submitted in partial fulfillment of the
requirements for the degree of Doctor of Philosophy in the
College of Pharmacy at the University of Kentucky

By

David James Feola

Lexington, Kentucky

Director: Dr. Robert P. Rapp, Professor of Pharmacy and Medicine

Lexington, Kentucky

2005

EFFECT OF COMBINATION EXPOSURE TO ZIDOVUDINE AND SULFAMETHOXAZOLE-TRIMETHOPRIM ON IMMUNE RESPONSE IN MICE AND HUMANS

DISSERTATION

A dissertation submitted in partial fulfillment of the
requirements for the degree of Doctor of Philosophy in the
College of Pharmacy at the University of Kentucky

By
David James Feola

Lexington, Kentucky

Co-Directors: Dr. Beth A. Garvy, Associate Professor of Medicine
and Dr. Patrick McNamara, Professor of Pharmacy
and Dr. Val Adams, Associate Professor of Pharmacy

Lexington, Kentucky

2005

I dedicate this work to my deceased son, Elijah David,
and to God who shapes us with such wonderful gifts as him.

ACKNOWLEDGEMENTS

The following dissertation, while an individual work, benefited from the insights and direction of several people. First, my Dissertation Chair, Dr. Robert Rapp, exemplifies the high quality scholarship to which I aspire. Most importantly I would like to thank Dr. Beth Garvy for the mentorship, expertise, and understanding at every stage of the dissertation process. I would also like to thank the complete Dissertation Committee, including the outside reader, respectively: Dr. Patrick McNamara, Dr. Val Adams, and Dr. Thomas Roszman. Each of these individuals provided insights and assistance that was invaluable, and guided and challenged my thinking, substantially improving the finished dissertation.

I would also like to thank the exceptional laboratory group with which I had the fortune to work with, including Mr. Kevin Schuer, Mrs. Melissa Hollifield, Mr. Wayne Young, Dr. Mahboob Qureshi, and Dr. Kerry Empey. This process would not have been nearly as productive or enjoyable without them. Additionally I would like to thank Dr. Claire Pomeroy and Dr. Philip Empey for their constant guidance and friendship, and especially Dr. Alice Thornton and the staff at the Bluegrass Care Clinic at the University of Kentucky for their tireless assistance and support.

Finally, I would like to thank my parents, David and Natalie Feola, whose support and guidance are to which all of my accomplishments are credited, and to my wife Katie, whose love, support, and devotion in Christ are my immeasurable strengths.

TABLE OF CONTENTS

LIST OF TABLES

LIST OF FIGURES

CHAPTER 1. Introduction

A. OVERVIEW

Patients infected with human immunodeficiency virus (HIV) undergo worsening of immunosuppression over the course of their illness. While this is mainly a direct result of the virus, iatrogenic causes can be contributory. Two common agents used in the treatment of this patient population include zidovudine (ZDV) and sulfamethoxazole-trimethoprim (SMX-TMP). Investigators recently reported that these agents have an additive toxic effect on immune cell populations in the spleen and peripheral blood (1). The purpose of this dissertation was to investigate the mechanism of this combined toxicity in mice, and to evaluate its impact on host response in both mice and humans.

With the ever-increasing number of agents on the market worldwide, drug-drug interactions continue to be a significant cause of morbidity and mortality among all patient populations, accounting for as much as 3-28% of hospital admissions (2, 3). Adverse drug reactions occur in 5-20% of hospitalized patients, many caused by drug-drug interactions (4, 5). Patients infected with HIV are at a high risk of developing drug-drug interactions due to the large number of agents used to treat them. The medications required to treat HIV-infected patients include antiretroviral drugs comprising highly active antiretroviral therapy (HAART), anti-infectives used for prophylaxis and treatment of opportunistic infections (OI), adjunct treatments for additional disease states, or additional agents to treat iatrogenic toxicities that many of these drugs can cause. Many drug-drug interactions that are typical of patients with acquired immunodeficiency syndrome (AIDS) have been well described and reviewed (6). Iatrogenic effects associated with these agents have the potential to adversely affect clinical outcomes among patients infected with HIV.

Advances in the treatment of HIV infection have increased patient survival and decreased morbidity and mortality so significantly that the disease is now considered to be a chronic condition. With the availability of more effective antiretroviral regimens, researchers and clinicians have prolonged the time interval during which viral replication

is controlled and therefore effective immune function is maintained, prohibiting OI and other complications from HIV infection. HAART benefits these patients by decreasing viral replication of HIV. As a result, these patients are maintained long-term on treatment with a multitude of agents.

However, HAART therapy can also cause a variety of adverse effects that can impact morbidity and quality of life. Bone marrow suppression is associated with the use of many antiretrovirals, with the highest incidence associated with ZDV. It is important for clinicians treating HIV to understand the effects of these agents on the immune system. Further immunosuppression from drug therapy could adversely influence the outcome of HIV treatment and enhance patient susceptibility to OI and malignancy. This work will investigate the hypothesis that ZDV used in combination with SMX-TMP, another agent commonly used in patients infected with HIV, causes clinically-significant alterations to immune function that could contribute to impaired host defense. By way of introduction, aspects of host defense in response to HIV infection will be presented. This will be followed by a discussion of the impact that HIV-infection has on immune cell populations and their functions, including an overview of apoptosis and its role in HIV disease. Drug therapy will then be applied to this overview, and the positive and negative aspects of treatment will be presented. The focus will then turn toward ZDV and SMX-TMP, and the hypothesis that these drugs, when used in combination, adversely affect B cell development in the bone marrow, thus leading to significant immunologic impairment.

B. IMMUNE RESPONSE AND HIV INFECTION

HIV disease is characterized by $CD4^+$ T lymphocyte depletion (7). As the $CD4^+$ cell population declines, it leaves the host susceptible to OI which, along with the patient's $CD4^+$ cell count, defines disease progression toward AIDS. $CD4^+$ cells die via direct cytopathologic effects of the virus, as well as by apoptosis induction due to exposure to viral antigens (8-11). This leads to decreased immune surveillance, and increased incidence of OI and neoplasms.

Primary immune response to HIV is both humoral and cell-mediated. After dissemination of the virus to lymphoid organs and throughout the body, the immune response controls the burst of viral replication. The virus is incompletely eliminated and goes into a state of persistent replication. This characteristic is unique to HIV and is not found among other human viral pathogens (12). During this phase, HIV becomes trapped in germinal centers of the lymph nodes. $CD4^+$ T cells migrate here as part of their normal response to infection, where they then become infected with the virus. It is paradoxical that the very immune response which controls viral spread also effectively propagates the disease. The immune system subsequently remains in an activated state for an extended period (12).

Cellular immune response to HIV infection

The immune system controls the virus to extend the infected host's survival by employing $CD8^+$ T cells upon initial infection. There is an increase in the number of HIV-specific $CD8^+$ cytotoxic T lymphocytes (CTL) that inhibit viral replication by destroying virally-infected cells (13). In addition to these activities, $CD8^+$ cells also release anti-HIV macromolecules that combat the virus, including the chemokines RANTES (regulated on activation, normal T cell expressed and secreted), MIP-1α (macrophage inflammatory protein-1α), and MIP-1β (14). These chemokines inhibit infection of activated $CD4^+$ T cells by HIV by inhibiting chemoattractant cytokine receptor type 5 (CCR5), one of the several seven-transmembrane G-protein coupled chemokine coreceptors utilized by the virus for cell entry (15-17). $CD8^+$ T cell populations remain constant, keeping the patient in a clinical phase of latency for extended time periods.

Over time the $CD8^+$ cell population will decline allowing the virus to increase replication, with resultant declines in $CD4^+$ cell numbers. There is a strong correlation between a decline in HIV-specific CTL activity and progression of the disease (18, 19). This eventually leads to uncontrolled viral replication and lymph node destruction in progressive illness (20). Additionally, $CD4^+$ T cells respond to HIV epitopes presented in the context of MHC class II (21). This causes $CD4^+$ cells to secrete interleukin (IL)-2

which, while helpful to aid cytotoxic responses, has also been shown to increase HIV replication (22).

In addition to death due to direct infection of the virus, cytotoxicity in $CD4^+$ T cells also occurs by indirect means. Infected cells can bind to uninfected $CD4^+$ cells and deplete them (10). This occurs because the molecular events associated with the fusion of the HIV viral envelope and the cell membrane that occur during infection can also occur when an infected $CD4^+$ cell expressing viral envelope proteins comes into contact with an uninfected T cell. This causes a "syncytium" of cells to form, thereby depleting them (23). Another mechanism of indirect depletion occurs when uninfected $CD4^+$ cells that express HIV proteins on their surface are killed by CTL responses in an "innocent bystander" phenomenon (24, 25). The CD4 receptor will cross-link soluble viral proteins such as gp120 that, in the absence of TCR activation, induces apoptosis (26).

Impaired hematopoiesis can also lead to depletion in $CD4^+$ cell numbers due to decreases in production. Some $CD34^+$ lymphoid progenitors in the bone marrow express CD4, and are therefore susceptible to the virus (27, 28). HIV infection also increases Fas expression on $CD34^+$ cells which increases apoptosis in these progenitors (29). Fas is a "death receptor" through which cells are stimulated to undergo programmed cell death. These mechanisms will be discussed below.

Finally, HIV infection can prime $CD4^+$ T cells for apoptosis. T cells from HIV patients undergo higher rates of apoptosis when compared to T cells from normal individuals (30, 31). Infected cells are sensitized to undergo apoptosis if CD4 receptors have been cross-linked to the HIV envelope glycoprotein gp120, followed by T cell receptor ligation (30, 31). Because activation of these cells triggers apoptosis, as T cells respond to an infectious stimulus they are depleted (26). This occurs through the intrinsic mitochondrial pathway of apoptosis, although the details remain unknown (32). The percentage of apoptotic $CD4^+$ and $CD8^+$ T cells in lymph node sections is three to four times higher in HIV-infected patients than in normal individuals (11).

In addition to loss of absolute cell numbers, HIV can also influence $CD4^+$ T cell function through decreased production of IL-2 and decreased expression of the IL-2 receptor (33). This, in addition to the decreased expression of CD40 ligand discussed

below, can decrease the functionality of the remaining $CD4^+$ T cells in HIV-infected patients.

Humoral immunity in HIV infection

Several types of antibodies are produced in response to HIV disease. Beginning with primary infection, antibodies to the viral core protein p24 develop, which decreases viremia in the early stages of infection (34). The eventual decline in response to p24 antigen correlates to disease progression in later stages of illness (35, 36). Other antibodies can be present that neutralize HIV that are viral isolate-specific, most often targeting the HIV envelope protein gp120 (37, 38). Some of these antibodies inhibit the interactions between HIV and CCR5, which prevents the entry of the virus into the $CD4^+$ cell (39). Other antibodies can neutralize a wide range of viral isolates, and the presence of these more broadly-specific antibodies correlates with slower disease progression (35, 40, 41). Despite the positive effects of neutralizing antibodies against HIV, it has also been demonstrated that some antibodies present in HIV-infected individuals can actually enhance replication of HIV *in vitro* (42, 43).

HIV infection severely damages the humoral immune response which incurs phenotypic and functional alterations. HIV infection results in increased proportions of B cells with an activated phenotype, resulting in a hyper-production of gammaglobulin (IgG) (44, 45). Despite having elevated IgG levels, HIV-infected individuals have an impaired ability to produce specific antibodies in response to neo-antigens (46-50). The decrease in antigen-specific IgG titers in HIV-infected individuals has been positively correlated with $CD4^+$ T cell count, and inversely correlated to viral load (51).

B cells in patients infected with HIV do not upregulate CD70 normally after being stimulated by activated T cells, which impairs CD70-dependent immunoglobulin synthesis (52). The interaction which up-regulates CD70 expression, between CD40 on B cells and CD40L on T cells, is also affected by a decrease in CD40L expression on T cells in HIV-positive patients, meaning that the defect in antigen-specific Ig production is also a result of $CD4^+$ T cell dysfunction (52). Additionally investigators have shown that memory B cells ($CD27^+$) are depleted from the blood of HIV-infected individuals, possibly due to persistent T cell activation (53). In clinical trials examining B cell

responses in AIDS patients, it is unknown if drug therapy plays a role in B cell malfunction, since this issue has not been studied (46-50).

Dysfunction of the humoral immune system leads to the inability of the patient to properly control extracellular pathogens (54). These include extracellular bacteria, parasites, and fungi, such as *Streptococcus pneumoniae* and *Pneumocystis* (54-56). Although the rate increases as $CD4^+$ count decreases, bacteria are still the most likely cause of pneumonia in an HIV-infected patient with a high $CD4^+$ cell count, with pneumococcus being the most likely cause in this subset of patients (57). This example illustrates the impact of B cell dysregulation on host defense in HIV disease.

Apoptosis

Apoptosis is an important mechanism of homeostasis in adult tissues by the activation of a controlled cellular self-destruction program. This occurs for the removal of infected, transformed, or damaged cells that can be induced by a variety of stimuli, including death receptor ligation, the absence of growth and survival factors, starvation, DNA damage, viral infection, anticancer drugs, and ultraviolet radiation (58). Apoptotic cells have a distinct morphology which includes membrane blebbing, exposure of phosphatidylserine to the outside of the plasma membrane, nuclear fragmentation, and chromatin condensation (59, 60). Cells ultimately lyse and are fragmented into apoptotic bodies, which are engulfed by macrophages without causing an inflammatory response (61, 62). As mentioned above, apoptosis plays an important role in HIV-infection.

Cell death is divided into two main types: programmed cell death, during which the cell plays an active role in its demise, and passive death (necrosis). Apoptosis occurs as a result of a host of stimuli, and it proceeds through a small number of distinct pathways (58). The two major signaling cascades utilize a family of cysteine proteases called caspases, a group of highly-regulated enzymes that undergo cleavage and activation during apoptosis (63-65). The extrinsic cascade originates from the activation of cell membrane death receptors resulting in caspase activation, and the intrinsic pathway involves mitochondrial release of pro-apoptotic factors to activate caspases to

induce apoptosis (66). Additionally, apoptosis can occur in a caspase-independent manner (discussed in Chapter 6) (67, 68).

The extrinsic pathway originates from the ligation of death receptors on the cell surface, including Fas (CD95), TNF-related apoptosis-inducing ligand receptors (TRAIL-R), and TNF-receptor 1 (TNF-R1) (69, 70). Fas ligand (FasL) is expressed by CTL and some activated $CD4^+$ T cells. They recognize cells to be terminated through antigen presentation in the context of MHC. The TRAIL-receptors function in maintaining immune system homeostasis, so that activated cells can be deleted in a form of regulation (71). These receptors have death domains that trimerize upon ligation, thereby recruiting Fas-associated death domain protein (FADD) or TNF-R-associated death domain protein (TRADD). Pro-caspase-8 is then recruited and activated, which in turn activates caspase-3, the main effector caspase through which both pathways flow, which signals the cell to undergo apoptosis (72, 73).

The intrinsic pathway centers on the mitochondria. Different stressors including ultraviolet radiation, growth factor withdrawal, and drug exposure can cause the release of cytochrome c from the mitochondria via complex mechanism of regulation, governed by proteins in the Bcl-2 family. This family contains anti-apoptotic (Bcl-2, Bcl-XL) and pro-apoptotic (Bax, Bid) members that exert their affect on the mitochondria by preventing or inducing mitochondrial dysfunction (74, 75). These proteins are under the control of p53 gene transcription (76). Increases in cytochrome c release can also be induced through the extrinsic pathway with a “crosstalk” signal utilizing caspase-2 (77). Cytochrome c then activates caspase-9, which in turn activates the effector caspases through caspase-3, causing apoptosis (78). CTL can also induce apoptosis through granzyme B secretion, which directly activates caspase-3 (75). The mitochondria can also be stimulated to release apoptosis-inducing factor (AIF), which is a caspase-independent pathway that can also lead to apoptosis (see Chapter 6 for details).

C. DRUG TREATMENT: THE GOOD AND THE BAD

Efficacy of HAART

HAART controls viral replication in infected patients, thereby increasing $CD4^+$ T cell counts and improving patient survival (79-81). HAART targets a variety of viral processes to decrease the impact of mutations that result in resistance to therapy. Many investigations have shown that the number and function of $CD4^+$ cells increases in response to successful viral load reduction with HAART (82-85). In one example, a study involving 44 HIV-positive patients, Lederman et. al. found that $CD4^+$ cells' proliferative capability and delayed-type hypersensitivity reaction potential were both improved after 12 weeks of treatment with a combination of ZDV, lamivudine, and ritonavir (83). Similarly, HAART not only decreases direct viral attack on $CD4^+$ cells, but also restores T cell proliferation, as Lu et. al. demonstrated in $CD4^+$ and $CD8^+$ T cells *in vivo* and *in vitro* in 99 adults infected with HIV (86). Investigators in this study treated patients with combination therapy for one year, and enhanced ability of T cells to survive *in vitro* was associated with the use of the protease inhibitors (PI) indinavir and ritonavir (86). As a consequence of these effects, the addition of PI to HAART allows for a more effective defense against opportunistic pathogens such as cytomegalovirus (CMV), *Pneumocystis jirovecii*, and *Candida albicans*, resulting in a decrease in patient mortality (82, 87-89).

Antiretroviral therapy has many positive effects on the bone marrow of infected individuals. Bone marrow progenitor cells are adversely affected by HIV causing impaired hematopoiesis. $CD34^+$ progenitor cells in the bone marrow of patients infected with HIV typically have an increase in Fas and Fas ligand expression, and an overproduction of tumor necrosis factor-α (TNF-α), an inflammatory cytokine that can increase toxicity to bone marrow progenitor $CD34^+$ cells (29, 90). HIV infection thereby increases the apoptosis rate of $CD34^+$ progenitor cells in the bone marrow. Isgro et. al. demonstrated that HAART reduces this destruction by decreasing Fas expression on the surface of these progenitors (90). This group showed this using *in vitro* culture of bone marrow aspirates from HIV-infected patients pre- and post-HAART (90). The expression of TNF-α was also decreased as a result of HAART in bone marrow cells

from HIV patients cultured *ex vivo* (90). This effect was postulated by the investigators to be due to the presence of PI (90).

Sloand et. al. demonstrated that these agents can also decrease apoptosis rates and caspase-1 content in $CD4^+$ cells (91). Caspase-1, also known as interleukin-1β-converting enzyme, is a cell signaling protein in $CD4^+$ T cells that is preferentially expressed in cells of HIV-infected patients (91). Caspase-1 mediates apoptosis in these cells, and when inhibited reduces activation-induced cell death (92). This group demonstrated that the addition of ritonavir to cultured bone marrow cells from HIV-infected subjects increased colony formation and decreased apoptosis in $CD34^+$ cells, and that this effect was blocked by the addition of a caspase-1 inhibitor (93). These studies highlight the ability of PI to directly affect cells in the bone marrow.

An additional benefit of HAART and subsequent virologic control is the decreased incidence of AIDS-associated neoplasms. Clinicians use HAART therapy to decrease the occurrence of Kaposi's sarcoma and non-Hodgkin's lymphoma (94, 95). HAART restores immune surveillance which leads to a decrease in incidence of OI and cells that have undergone oncogenic transformation.

Toxicity of HAART

Bone marrow suppression in this patient population can be caused by a variety of insults. In addition to direct viral effects, iatrogenic suppression from HIV therapy, neoplasms, malnutrition, and OI (including cytomegalovirus, Mycobacterium avium complex (MAC), and histoplasmosis) can adversely affect bone marrow cell survival and replication (96). Anemia, thrombocytopenia, lymphopenia, and neutropenia are found in most AIDS patients. Bone marrow in patients with AIDS displays a host of pathologic processes, including lymphocyte infiltration, dysplasia, reticulin fibrosis, granulomatous myelitis, and plasmacytosis (97, 98). HIV-infected patients with advanced disease also have high incidences of the aforementioned neoplasms, particularly Kaposi's sarcoma and non-Hodgkin's lymphoma, hypothesized to be due in part to a decrease in immune surveillance (99). Although many of these maladies are directly associated with the virus, drug regimens also have significant adverse effects on immune functions. Investigators have studied and characterized these adverse effects associated with

drug therapy via *in vitro*, animal, and human studies. Clinicians must also be aware of the potential toxicities associated with the use of these agents.

ZDV is associated with the most potent myelosuppressive effects among available antiretrovirals (100, 101). The reported clinical incidence of bone marrow toxicities associated with ZDV, including anemia, neutropenia, and granulocytopenia, ranges from 2 to 45% (102-105). Increases in the mean corpuscular volume of red blood cells is a hallmark of ZDV therapy, its incidence so reliable that it has been shown to be a valuable marker for HAART adherence (103, 106). Several groups have shown that ZDV affects lymphocytes in their early stages of development in the bone marrow (107-109). The triphosphorylated form of ZDV is the active form of the drug. However, the monophosphorylated form is responsible for its toxicity by inhibiting thymidylate kinase and lowering intracellular thymidine pools (107). This toxicity is associated with an inhibition of hematopoietic progenitors in murine and human bone marrow (108-110). This is likely due to the fact that these progenitors tend to be more actively cycling than are mature lymphocytes.

Nucleoside reverse transcriptase inhibitors (NRTI), especially ZDV, induce apoptosis in immune cell populations of HIV-infected patients (111, 112). Viora et. al. found inhibited cell cycle progression and increased apoptosis in human peripheral blood mononuclear cells exposed to clinically relevant concentrations of ZDV and dideoxycytidine (ddC) *in vitro* (111). Several groups have demonstrated ZDV-induced mitochondrial dysfunction in hematological cells because of the drug's affinity for mitochondrial DNA polymerase gamma (113-116). Other investigators have shown that ZDV makes cells more susceptible to apoptosis by inducing mitochondrial membrane hyperpolarization (112, 117). Additionally, investigators have shown didanosine to cause mitochondrial toxicity in human cell lines (113). Clinical studies examining other cell types have demonstrated that these agents cause mitochondrial toxicity in HIV-positive patients, which is then associated with an increased incidence of hyperlactatemia and lipodystrophy (116, 118). The clinical manifestations of NRTI-induced mitochondrial toxicity resemble those of inherited mitochondrial diseases, including lactic acidosis, myopathy, nephrotoxicity, peripheral neuropathy, and pancreatitis (119).

Conversely, PI prevent ZDV-induced apoptosis (93, 120-122). In a study by Matarrese et. al., apoptosis induced by various stimuli in activated T cells cultured from the peripheral blood of HIV-infected patients was decreased through an increase in mitochondrial membrane potential by saquinavir, lopinavir, and indinavir (120). Interestingly, one of the agents used to induce apoptosis was ZDV (120). The addition of PI in this study decreased lymphocyte apoptosis by influencing mitochondrial homeostasis. Apoptosis in cultured T lymphocytes obtained from HIV-infected subjects in another study decreased with the addition of nelfinavir to combination antiretroviral therapy (122). This mechanism is postulated to be due to activated lymphocytes having hyperpolarized mitochondrial membranes, which make the cells prone to apoptosis. PI are able to stabilize the mitochondria in these cells. Therefore, with combination therapy, the addition of a PI could be beneficial not only to decrease viral replication and mutation, but also through this direct affect on lymphocyte apoptosis.

ZDV also causes a decrease in T cell responses to antigens, as well as a depletion of T cell populations in the thymus in mice (123). $CD4^+CD8^+$ (double-positive) cell numbers in the thymus were decreased as a result of ZDV exposure after mice were dosed via oral gavage for a period of 14 days. However, T cell populations in the peripheral blood of these animals were unaffected. At higher doses (1000 mg/kg/day), thymus atrophy occurred. When cultured from treated animals, T cell proliferation to antigenic stimuli was decreased significantly (123). IL-2 exposure reversed the effects that ZDV had on T cell populations and on their function in this investigation (123). In another study, Gallicchio et. al showed that IL-1 activity decreased the toxicity of ZDV on murine hematopoietic cells *in vitro* (124). These studies conclude that the mechanism of toxicity to T lymphocyte development could be due to inhibition of cytokine production. Investigators have used IL-2 successfully in clinical trials to increase lymphoproliferation in HIV patients, lending further support to this notion (125, 126).

Several other reverse transcriptase inhibitors adversely affect the bone marrow. Zalcitabine-associated neutropenia has been reported in up to 17% of patients in clinical trials (127-129). Didanosine, lamivudine, and delavirdine also cause neutropenia, but incidence rates are less than 10% (129-132). The incidence of granulocytopenia

associated with delavirdine increased from 16% to 63% with ZDV co-administration in a phase I/II trial involving 85 patients (132). PI suppress the bone marrow as well, although at a much lower incidence and severity than ZDV. Indinavir causes neutropenia in rare cases, and is associated with an anemia rate of less than 2% (133, 134). Saquinavir and nelfinavir cause mild dose-related neutropenia in clinical studies, however this is typically not clinically significant (135-137).

Anti-infectives and immunosuppression

Medications commonly used for prophylaxis and treatment of OI in HIV-infected patients can also have adverse effects on bone marrow. Foscarnet is used to treat CMV retinitis and herpes simplex virus in HIV positive patients. Use of this antiviral agent can cause anemia, leucopenia, granulocytopenia, and thrombocytopenia (138, 139). However, it is associated with a much lower incidence of severe, dose-limiting leucopenia than ganciclovir, another agent that is used in this patient population to treat CMV. Foscarnet can be given safely to patients with HIV, as demonstrated in a clinical study of ten patients with newly diagnosed CMV retinitis who received induction and maintenance therapy (140). Additionally, cidofovir causes neutropenia in as many as 20% of patients using the drug for CMV retinitis (141). Much of the toxicity associated with these agents is due to their use in combination with ZDV, which is discussed in the subsequent section.

Agents that affect folic acid synthesis such as dapsone, trimetrexate, pyrimethamine, and SMX-TMP are used in HIV-infected patients for the treatment and prophylaxis of *Pneumocystis jirovecii* pneumonia (PCP) and toxoplasmosis. These agents also cause bone marrow toxicity and may contribute to immunosuppression in this patient population. Dapsone is often used in the prophylaxis of PCP in patients with AIDS who are unable to tolerate SMX-TMP. Severe hematologic effects reported with dapsone use include agranulocytosis, aplastic anemia, and hemolytic anemia at estimated incidences of less than 1% (142-144). Trimetrexate, another agent used in the treatment of moderate to severe PCP, causes a high rate of myelosuppression (145, 146). Sattler et. al. reported that 46% of 25 patients receiving various doses of trimetrexate (ranging from 45 to 90 mg/m^2) in combination with folinic acid

(Leucovorin®) experienced dose-modifying hematologic toxicity (146). Pyrimethamine can also be used in the treatment and prevention of toxoplasmosis and *Pneumocystis* in AIDS patients, and is associated with causing megaloblastic anemia, leucopenia, and thrombocytopenia (147, 148). Folinic acid is often dosed with pyrimethamine in order to decrease these effects. Clinicians must be aware of the bone marrow toxicity associated with the use of these agents, and exercise caution when combining these drugs and ZDV, which can have additive toxicities.

SMX-TMP, the drug of choice for the prophylaxis and treatment of PCP, is particularly problematic with regards to bone marrow suppression. A higher than normal incidence of adverse reactions is associated with the use of SMX-TMP in patients with AIDS (149-151). SMX-TMP treatment-limiting adverse events occur in 60-80% of HIV-infected patients, whereas that rate is approximately 15% in non-HIV infected individuals (149, 150). The toxicities of this combination, based on *in vitro* data, are attributable to the oxidative metabolites of SMX (152). Patients with HIV infection have depleted intracellular glutathione (GSH) concentrations, a molecule utilized by cells as a reducing agent for the detoxification of oxidative species (153, 154). GSH is responsible for the conversion of toxic SMX metabolites back to the parent compound, which is then metabolized to non-toxic species and eliminated (155, 156). Investigators have linked this depletion of GSH by the virus to SMX-TMP intolerance in HIV-infected patients (153, 154). This will be discussed in detail in Chapter 4.

Antiretroviral drug-drug interactions and bone marrow toxicity

When treating patients infected with HIV, clinicians should take caution in considering potential drug-drug interactions that could adversely affect immune function, particularly interactions involving ZDV. Combining ZDV with agents that affect its metabolism can lead to increased toxicity. Fluconazole, atovaquone, and methadone all interfere with the clearance of ZDV (157-159). Fluconazole increased the area under the concentration versus time curve (AUC) by 74% after 7 days of dosing in a randomized, crossover study of 12 men infected with HIV (157). In an open-label, randomized, crossover study of 14 patients examining concurrent atovaquone therapy, the AUC of ZDV was increased by 31% (160). Additionally, probenecid, which is

typically administered with cidofovir to prevent nephrotoxicity, can decrease the renal clearance of ZDV (161, 162). Clinicians should consider these drug combinations when investigating causes of hematologic toxicity in patients who are HIV positive.

Caution must also be taken when prescribing PI, as they have the ability to inhibit cytochrome P450 (CYP) liver enzymes that are responsible for the metabolism of many drugs (163, 164). Ritonavir is the most potent inhibitor, but other PI, including saquinavir, indinavir, and nelfinavir will also inhibit CYP3A4 to a clinically significant degree. This inhibition has the potential to increase the exposure to drugs metabolized by this isoenzyme, which could lead to bone marrow suppression if used with agents that cause this type of toxicity. Additionally, the non-nucleoside reverse transcriptase inhibitor (NNRTI) delavirdine inhibits CYP3A4, and can increase the concentrations and risk of toxicity of the PI (164).

Drugs used in combination with antiretrovirals can also increase hematologic toxicity, independent of pharmacokinetic interactions. These interactions are presumed to be due to additive or synergistic bone marrow toxicity, but the precise mechanisms of the combined toxicities of most of these combinations remain unstudied. Investigators have defined several interactions associated with combination therapy with ZDV that are independent of systemic pharmacokinetic mechanisms. These studies are summarized in Table 1.1. Little is known about the clinical impact of co-treatment with antiretrovirals along with these other medications.

The use of ZDV with ganciclovir caused an incidence of severe to life-threatening hematologic toxicity in 82% of patients in a phase I, multicenter study of 41 patients with AIDS-related CMV infection (165). The conclusions of this study confirmed that patients receiving ganciclovir usually cannot tolerate the full recommended dose of ZDV (600mg/day) (165). In a retrospective study of 32 patients with AIDS, combining didanosine with ganciclovir was much better tolerated than combining ZDV with ganciclovir (166). Nine percent of patients given didanosine plus ganciclovir in this study developed dose-limiting hematologic toxicity versus 28% of patients in the ZDV plus ganciclovir group (166).

Table 1.1 Summary of ZDV drug-drug interaction literature.
Interactions with concomitant exposure with ZDV that are independent of systemic pharmacokinetic mechanisms.

Drug	Effect	Study Type	Refs	Comment
Ganciclovir	Leucopenia, granulocytopenia	Clinical	165, 166, 167	Severe, must decrease AZT dose or discontinue
Foscarnet	Leucopenia, granulocytopenia	Clinical	138, 139, 140, 168	Much lower incidence/ severity than ganciclovir
Dapsone	Decrease T cell *ex vivo* proliferation	Mouse, *ex vivo*	168	
	Hematologic toxicity	Clinical	170	10% incidence
Clarithromycin	Neutropenia, lymphopenia	Mouse	169	Decrease splenic cellularity
TMP/SMX	Decrease B cells/ macrophages in spleen	Mouse	1	
Protease inhibitors	Decrease AZT-induced apoptosis in T cells	Human, *ex vivo*	120, 121	Stabilize mitochondrial membrane hyperpolarization

In a clinical trial comparing the safety and efficacy of foscarnet versus ganciclovir for the treatment of CMV retinitis in patients with AIDS, subjects receiving foscarnet had a mortality rate of 36% as compared to 51% in the patients receiving ganciclovir (167). Subjects receiving ZDV had the drug held in the ganciclovir treatment group during the initial phase of therapy, and then reinstated at a lower dose thereafter (300mg/day). Even with this alteration in antiretroviral therapy, the relative risk of neutropenia (1.88) was higher in the patients receiving ganciclovir compared to foscarnet (167).

In animal models, ZDV used in combination with dapsone, clarithromycin, or TMP/SMX causes hematopoietic toxicity due to additive effects (1, 168, 169). In a study

by Freund et. al., concurrent administration of ZDV and dapsone increased the severity of ZDV-induced macrocytic anemia in normal mice (168). The investigators also demonstrated a decrease in proliferation when T cells were taken from mice treated with the drug combination and stimulated *ex vivo* (168). In a clinical study comparing safety and efficacy of dapsone to pentamidine in HIV-infected patients on ZDV, 6 out of 50 patients receiving dapsone experienced significant hematologic toxicity (170). Dapsone should be utilized with caution in patients receiving ZDV.

Administration of ZDV with clarithromycin is also of concern. Combination dosing in normal mice for 28 days resulted in severe hematotoxicity, with a significant decrease in neutrophil and lymphocyte populations in the peripheral blood, as well as a reduction in splenic cellularity of 67% (169). Although the mechanism for this augmentation of toxicity is unknown, the authors cited the ability of clarithromycin to inhibit cytokine production in several cell types (169, 171-173). While clarithromycin is clinically effective in the treatment of MAC (174, 175), it has also been associated with a possible increased mortality rate in HIV-infected patients (175, 176). This group randomly assigned patients with MAC bacteremia to receive twice-daily clarithromycin at doses of 500mg, 1000mg, and 2000mg for 12 weeks (175). For each group, mycobacteremia decreased during the 12 weeks. Unfortunately, treatment-limiting toxicity caused by clarithromycin occurred in 20% to 40% of patients, and patients receiving the higher doses of clarithromycin had higher death rates than did those treated with the 500-mg dose (175).

ZDV in combination with SMX-TMP

It is common for patients infected with HIV to be treated simultaneously with ZDV and SMX-TMP. However, the impact of concurrent exposure on the bone marrow in these individuals is unknown. Freund et. al. investigated the combined toxicity of ZDV and SMX-TMP in normal mice (1). Exposure to ZDV plus SMX-TMP via oral gavage caused severe pancytopenia, a significant decrease in splenic cellularity, a significant decrease in splenic macrophage number, and a trend toward a decrease in splenic B lymphocytes (1). Since these differences were found in the combination treatment group, yet the single drug groups receiving either SMX-TMP or ZDV did not differ from

control, it was concluded that this drug combination causes a synergistic toxicity to cellular immunity, and could be contributory to the immunosuppressive state of AIDS patients. Additionally, combination treatment did not affect T lymphocyte populations in the spleen (1). This could be because they mature in the thymus instead of the bone marrow, or because in mature animals, T cell development in the thymus decreases, and the T cell repertoire is maintained mainly by dividing T cells in secondary lymphoid sites (177).

Because the cell types that are affected originate in the bone marrow, and because of the known adverse affects of SMX and ZDV, we hypothesized that this is the location of the toxicity. In this work we have extended these studies to investigate whether SMX-TMP in combination with ZDV significantly interferes with development of cells in the bone marrow of mice, while focusing our efforts on those of the B lymphocyte lineage. We speculate that this drug-drug interaction could contribute to the impaired B cell function commonly seen in HIV patients (44, 45).

D. B CELL DEVELOPMENT

Mouse bone marrow contains B lineage cells in all stages of development, as they mature from stem cells, to common lymphoid progenitors, to early immature B cells, to mature B lymphocytes. These cells can be characterized and phenotypically delineated by examination of cell surface markers found on each cell type (178). Development of B cells progresses through a series of checkpoints in which the cells display a certain combination of these surface proteins, each with a particular function.

Cells undergo positive and negative selection processes in order to develop a B lymphocyte population that can respond to environmental pathogens effectively, without reacting with self antigens, thereby preventing autoimmunity. This diverse B cell repertoire is developed by genetic recombination, and kept in check by negative selection, which makes cells that are autoreactive undergo programmed cell death. This is of particular interest to us, because as will be demonstrated in this work, B-lineage cells undergo an increased rate of apoptosis as a result of exposure to ZDV

plus SMX-TMP. Apoptosis occurs as a normal part of homeostasis when cells are in the presence of a death signal or in the absence of a survival signal. We have investigated the mechanism by which ZDV plus SMX-TMP causes apoptosis in B-lineage cells.

Development mechanisms

Immature B cell subsets are defined by the assembly and expression of antigen receptor genes and other surface proteins that distinguish the different functional stages of development (179). Antigen specificity of each cell is determined through the complex genetic rearrangement and recombination of genes in the variable regions of both the heavy and light chains of the B cell receptor (BCR) (180, 181). Antibody diversity is forged here via recombination of different gene segments, and through the addition and subtraction of nucleotides that occurs at the joints of these genes during this process (180).

Genetic recombination begins with the genes at the heavy chain locus under the governance of the proteins RAG-1 and RAG-2, products of the recombination-activation genes (182, 183). This causes the cell to express a heavy chain along with a "surrogate" light chain that makes up the pre-BCR (184, 185). Expression of this receptor constitutes a productive genetic rearrangement at the heavy chain locus, which signals the cell to stop genetic rearrangement and to start dividing, thus allowing the cell to progress to the next stages of development. This signal to stop is manifested by degradation of RAG-2, and by suppression of mRNA synthesis for both RAG-1 and RAG-2 (186). Cells that do not express the pre-BCR will die via apoptosis.

Cells then undergo a burst of proliferation, increasing the number of cells that possess successfully rearranged heavy chains by 30- to 60-fold (178, 187). Cells then upregulate RAG-1 and RAG-2 once again to rearrange the genes at the light chain loci. Rearrangement of genes that make up the light chain will then produce the protein that joins with the heavy chain that leads to surface expression of the BCR (IgM). If the BCR encounters an antigen that it can cross-link to, the cell will either halt its development and be deleted via apoptosis (high-affinity interaction), become anergic, or revise its BCR to eliminate self-reactivity (low-affinity interaction) (188-190). This

process of negative selection will protect the host from the development of self-reactive lymphocytes and therefore prevent autoimmunity. In the absence of BCR binding, genetic rearrangement ceases at this stage, and the immature B cell can be released into the periphery.

The bone marrow contains specialized stromal cells to interact with developing B cells in order to provide signals for growth by binding directly to the B cells, and by secreting growth factors into the bone marrow milieu (191). B cells in their early stages of development rely on stem-cell factor (SCF), which interacts with c-kit, a tyrosine kinase receptor on the surface of the B cell precursor. Another molecule on the surface of stromal cells, VCAM-1, serves as an adhesion molecule that binds to VLA-4 on the surface of early B lineage cells in order to promote the binding of c-kit to SCF (192). B cells in later stages of development require IL-7, a cytokine that is produced by stromal cells to govern the proliferative burst seen in the early pre-B cell stage, discussed below (193).

B lineage classification

Classification of B-lineage cells has been made on the basis of cell-surface proteins, including immunoglobulin heavy and light chains, and other molecules that delineate these cell types. Common lymphoid progenitors, derived from pluripotent stem cells that have not yet differentiated into B-lineage cells, already express the IL-7 receptor α chain and c-kit (194). The earliest B-lineage cells are known as pre-pro B cells and are defined by the appearance of the B220 isoform of CD45 (195). These cells can be identified by the lack of CD19 expression, which characterizes all later B-lineage stages (195). Rearrangement of the immunoglobulin heavy chain locus begins during this pre-pro-B cell stage. B220, a tyrosine phosphatase that is involved in BCR signaling, is expressed until B cells terminally differentiate into plasma cells (178). Initial CD19 expression marks transition to the pro-B cell stage (178). The heavy chain is also being formed here, with RAG-1 and RAG-2 expression remaining high.

Productive intact heavy chain expression marks the transition to the pre-B cells stages. The pre-BCR is expressed (albeit mostly intracellularly) in the early pre-B cell stage, which halts heavy chain gene rearrangement. RAG-1 and RAG-2 down-regulate

here, and the cells then divide several times in a proliferative burst under the influence of IL-7, becoming late pre-B cells. The loss of CD43 expression, the adhesion molecule that has been present since the progenitor stages, marks the transition into this next stage (178). The light chain genes then begin to rearrange in late pre-B cells (with the reemergence of RAG-1 and RAG-2). Once the light chain is fully assembled and the complete IgM molecule is expressed on the cell surface, the cell is termed an immature B cell (178).

Other cell-surface molecules on pre-B cells include BP-1, an aminopeptidase, and heat stable antigen (HSA). The function BP-1 in the context of B cell maturation is unknown, but its presence allows researchers to identify and isolate the different B-lineage subsets. HSA has been demonstrated to aid in cell to cell adhesion (196). BP-1- and HSA-deficient mice phenotypically display no B cell abnormalities, including number or immunologic functions (197, 198). The surface expression of these markers, along with developmental processes occurring at each B-lineage stage is summarized in Figure 1.1. Immature B cells will then undergo negative selection for self-tolerance, and will leave the bone marrow, and further their development into mature B cells in secondary lymphoid tissues. They are considered naïve until they encounter foreign antigen and become activated.

ZDV and SMX-TMP exposure alters the progression of B-lineage cells through these stages. We will demonstrate that specific points in development are targeted for apoptosis as a result. This targeting of cells in sequential stages of development ultimately becomes one hypothesis for apoptotic synergy.

E. PROJECT OVERVIEW

The immune response to HIV is complex, and many factors contribute to the success in controlling not only HIV, but OI that afflict this patient population. Adaptive immunity carries a large burden in protecting hosts exposed to opportunistic and other pathogens. Assault on the bone marrow in these patients is multifactorial. While drug therapy has been extremely effective in allowing patients infected with HIV to live longer and

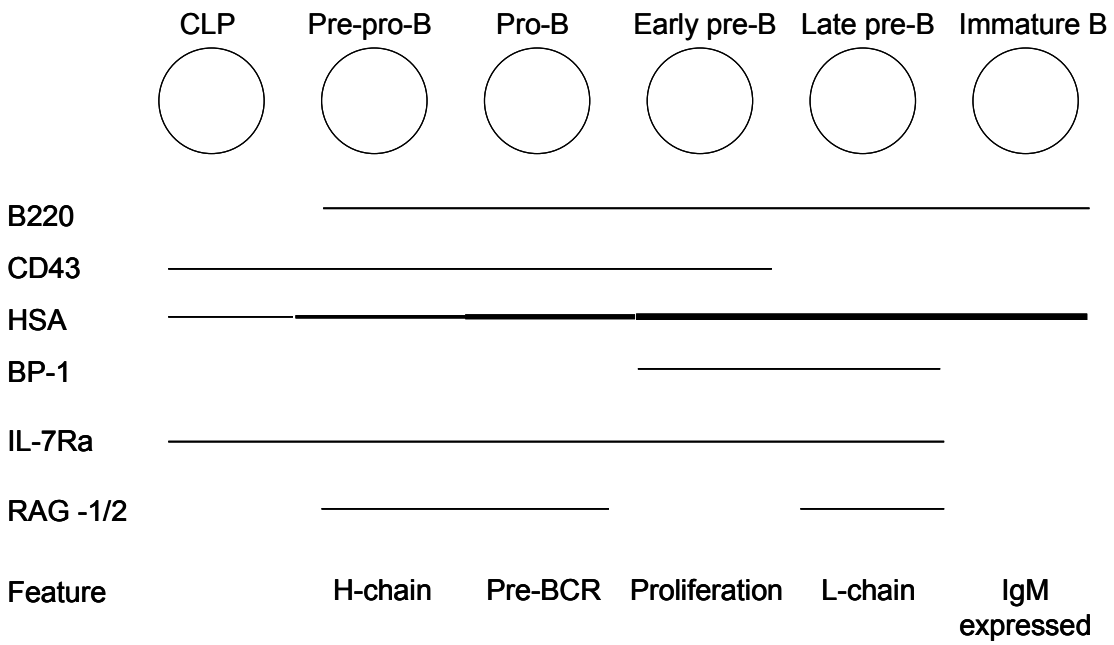

Figure 1.1 Stages of B-lineage development. The cell surface proteins B220, CD43, HSA, and BP-1 can be used to phenotype B-lineage cells via flow cytometry. RAG-1 and RAG-2 expression are up-regulated for heavy- and light-chain gene rearrangement, and down-regulated for the proliferative burst in the early pre-B cell stage. The BCR is then expressed on the cell surface (IgM) in immature B cells. CLP, common lymphoid progenitor. Adapted from Hardy et. al., 1990 (199).

healthier lives, clinicians and researchers must consider that these drugs also alter the number and function of immune cell populations, and can have a negative impact on the treatment of this complex disease state. Patients should be treated cautiously with many of these drug combinations, and any hematological abnormalities identified should be investigated as potential iatrogenic reactions to agents being used.

To this end, we investigated this drug-drug interaction concerning concurrent exposure of ZDV and SMX-TMP. We first began in a mouse dosing model to verify the findings of others concerning peripheral immune cell effects, and then we focused on the bone marrow as a target of this toxicity. This investigation led us to a study of the mechanisms at work in the bone marrow, focusing on B-lineage cell subtypes. Because these drugs in combination were rendering cells in the bone marrow apoptotic, we then investigated the mechanism of apoptosis induction in a series of *in vitro* experiments.

Next we determined that this toxicity has an adverse affect on host defense by examining the immune response in mice challenged with a pulmonary infection with *Pneumocystis murina* after being dosed with ZDV plus SMX-TMP. Because the responses in the mice treated with the drug combination were altered, we conducted a human trial to determine the clinical significance of combining ZDV with SMX-TMP treatment in patients infected with HIV. The humoral response to the yearly influenza vaccine was measured in patients receiving ZDV, SMX-TMP, the combination of both, or neither drug. Data presented suggests a clinically-significant impact on host response due to exposure to ZDV plus SMX-TMP.

CHAPTER 2: Combination exposure to ZDV and SMX-TMP in normal mice

A. OVERVIEW

Our investigation of the toxic effects of combination exposure to ZDV and SMX-TMP in mice began with a characterization of cellular toxicity in the spleen, peripheral blood, and pulmonary tissues to confirm the results of others, and with an in-depth investigation of the effects on bone marrow cell populations in these animals (1). Phenotypic analyses of cell types including neutrophils, monocytes, and T and B lymphocytes in peripheral lymphoid tissues formed the basis of further study directed toward the bone marrow. Because cell types that mature in the bone marrow were most affected, we sought to characterize bone marrow cell population dynamics, as well as to elicit the mechanism of the toxicity, focusing on B lymphocytes.

We hypothesized in Chapter 1 that the site of immunotoxicity in mice as a result of ZDV plus SMX-TMP exposure is the bone marrow. We sought to demonstrate that the mode of cell death (apoptotic versus necrotic) as a result of exposure to ZDV plus SMX-TMP. We then characterized the kinetics of this toxicity in B lineage cell populations as they evolve through the different checkpoints on the way to becoming mature B cells. To explain the mechanism of cell death, we then demonstrated that the effect is cell-cycle specific, primarily affecting early pre-B cells as they undergo the proliferative burst into the late pre-B cell phenotype.

B. MATERIALS AND METHODS

Materials

ZDV (3'-azido-3-deoxythymidine), trimethoprim (2,4-diamino-5-[3,4,5-trimethoxy-benzyl]pyrimidine), SMX (4-amino-N-[5-methyl-3-isoxazolyl]benzenesulfonamide), methylcellulose, sodium azide, DMSO, PBS, ammonium chloride, potassium bicarbonate, EDTA, collagenase A, DNase, caffeine, acetonitrile, acetic acid,

triethylamine, and RNase A were obtained from Sigma-Aldrich (St. Louis, MO). Monoclonal Abs, including FITC-conjugated GR-1, IgD, and BP-1, PE-conjugated CD19 and CD43, APC-conjugated CD11b, B220, and CD8, PE-cyanine-conjugated CD4, and biotinylated CD43 and heat stable antigen (HSA), were obtained from BD Pharmingen (San Diego, CA). Annexin V-FITC/propidium iodide (PI) apoptosis detection kit (BD Pharmingen) was utilized for identifying cells undergoing early stages of apoptosis. RPMI Medium 1640, HBSS, and FCS were purchased from Gibco Invitrogen Corporation, Grand Island, NY.

Animals

Four- to six-week old normal BALB/c mice were obtained from the National Cancer Institute (Raleigh, NC) and isolated for at least 7 days before manipulation. Mice were housed in the Veterans Administration Veterinary Medical Unit under pathogen free conditions with a 12 hour light/dark photocycle and food and water both freely available. This study and all of its procedures were approved by the Veterans Administration Institutional Animal Care and Use Committee.

Drug preparation and dosing design

Drug doses were prepared daily by weighing each powder into polypropylene tubes, SMX and TMP together, and ZDV separately, and suspending each in its appropriate vehicle: ZDV dissolved into sterile-filtered deionized H_20 to a concentration of 50mg/ml, SMX and ZDV suspended in 0.5% methylcellulose in H_20 at concentrations of 106mg/ml and 8mg/ml, respectively. Mice were randomized into four treatment groups, either receiving ZDV or SMX-TMP alone, in combination, or vehicle only (control), at the following doses based on an approximate mean mouse weight of 20 grams: ZDV 240mg/kg (5mg per mouse in 100µl), SMX 840mg/kg (16mg per mouse in 150µl), and TMP 160mg/kg (1.2mg per mouse). Doses were given via oral gavage with an 18-gauge blunt-tipped dosing needle, and mice received each drug or its corresponding vehicle daily.

Tissue processing

Spleens were collected in RPMI-1640 supplemented with 5% FCS, weighed, and pushed through mesh screens to obtain single cell suspensions. Lungs were minced and digested by incubation with 50 U/ml DNase and 1mg/ml collagenase A and pushed through mesh to form single cell suspensions. Peripheral blood specimens were collected from the abdominal aorta and placed in heparinized tubes to prevent clotting. Blood was also collected separately in dry tubes, allowed to clot, and serum was separated by centrifugation and frozen at -80^{0}C until time of SMX concentration analysis. Bone marrow was flushed from femurs and tibias into RPMI-1640 plus 5% FCS, and single cell suspensions were obtained via passage through a 25-gauge needle. Red cells in all samples were lysed with hypotonic buffer consisting of 0.15M ammonium chloride, 10mM potassium bicarbonate, and 0.1mM EDTA. Cells were then washed, enumerated, and transferred into 5ml round-bottom polystyrene tubes for phenotyping via flow cytometry.

Cell phenotyping

Splenocytes and lung digest cells were incubated with fluorescently-labeled mAb specific for murine cell surface markers, including major histocompatibility complex II (MHC II), CD19, CD4, and CD8. Bone marrow cells were incubated with 3 separate panels of Abs to phenotype B lineage cell types in addition to polymorphonuclear cells (PMN). Panel 1 consisted of CD19, granulocyte differentiation antigen (GR-1), and CD11b (component of Mac-1); panel 2 of B220, CD43, BP-1, and HSA; panel 3 of B220, CD43, and IgM. B lineage cells were classified according to nomenclature developed by Hardy et al (178). Cells were washed before and after staining with PBS containing 0.1% BSA and 0.02% sodium azide. All cells were analyzed for phenotype by flow cytometric multiparameter analysis using a FACSCaliber Flow Cytometer (BD Biosciences, Mountain View, CA). Greater than 50 thousand events per sample were routinely examined.

Apoptosis analysis

The proportion of apoptotic cells was quantified using the annexin-V binding protocol with PI exclusion. Annexin binds to phosphatidylserine groups that are externalized on the cell membrane in early stages of apoptosis (59). Samples were analyzed by flow cytometry as above, and cells that fluoresced annexin-V positive/PI negative were considered apoptotic.

Cell cycle analysis

Individual B cell subpopulations were fluorescently labeled as above and sorted using fluorescence-activated cell sorting (FACS) with a MoFlo high speed cell sorter and analyzer from Cytomation (Fort Collins, CO). Subpopulations were then fixed using 95% ethanol, and stored at -20^{0}C. Cell cycle analysis was performed by labeling DNA with PI at 50µg/ml in the presence of 50µg/ml RNase A. A FACSCaliber flow cytometer was used to analyze cell cycle stages with doublet discrimination, using the ModFit software package (Verity Software House, Inc, Topsham, Maine).

Statistical Analysis

Data was compared using one-way ANOVA followed by the Student-Neuman-Keul test for ad hoc pair-wise comparisons. Each treatment group was compared to its corresponding control using commercially available software (Sigmastat, SPSS, Chicago, IL). Data that failed normality testing was compared using the Kruskal-Wallis One Way Analysis of Variance on Ranks method. Results were determined to be statistically significant when a p-value < 0.05 was obtained. Data are expressed as the mean $\pm$ standard deviation.

C. RESULTS

Combination dosing has an overall clinical effect on mice

Mice were dosed with ZDV, SMX-TMP, ZDV plus SMX-TMP, or vehicle only for a period of 28 days. Doses were chosen based on previous studies that produced

significant levels of toxicity. Daily oral gavage of ZDV plus SMX-TMP led to an increase in lethargy, failure to groom, and a hunched appearance by day 28, though no mortality occurred. Mice in this group displayed a decrease in body weight after 28 days of dosing, whereas the ZDV, SMX-TMP, and control groups all gained weight (Table 2.1). Spleen weights and spleen weight expressed as a percentage of body weight were reduced in the combination group compared to the control group, with each single-drug treatment cohort again displaying no difference (Table 2.1). Other organs in the peritoneum did not display any gross changes upon examination.

Table 2.1 Body and spleen weights.

	Mouse weight (grams)			Spleen weight (Day 28)	
Mouse Group	**Day 0[A]**	**Day 28**	**Change**	**Grams**	**Percent body weight**
ZDV	18.73 ± 1.50	19.42 ± 1.41	0.68 ± 0.77	0.078 ± 0.027	0.40 ± 0.14
SMX-TMP	18.43 ± 0.70	20.64 ± 1.06	2.12 ± 0.37	0.086 ± 0.009	0.42 ± 0.03
ZDV + SMX-TMP	17.99 ± 0.49	17.16 ± 1.26[B]	-0.83 ± 1.28[B]	0.040 ± 0.008[B]	0.23 ± 0.04[B]
Control	18.39 ± 1.42	20.28 ± 1.37	1.89 ± 0.73	0.090 ± 0.012	0.44 ± 0.06
p-value	*0.816*	*0.005*	*0.001*	*0.002*	*0.016*

[A]Data expressed as mean ± SD of 5 mice per group.
[B]$p < 0.05$ compared to control group.

B lymphocyte and granulocyte populations are decreased by ZDV plus SMX-TMP treatment, primarily in the bone marrow and spleen

We conducted a phenotypic analysis of immune cell populations in the spleen, lungs, and bone marrow of mice treated with the drug combination. Splenic cellularity decreased 49% in the ZDV plus SMX-TMP group after 28 days of therapy as compared to control, whereas the ZDV and SMX-TMP groups were not significantly affected (Figure 2.1A). The cell types that accounted for this decrease were the splenic monocytes and B lymphocytes in the ZDV plus SMX-TMP group, as shown in Figure 2.1B. No differences were observed in splenic $CD4^+$ and $CD8^+$ T cell numbers. Peripheral blood lymphocyte percentages were not significantly affected at any timepoint examined, with data shown for mice after10 days of drug exposure

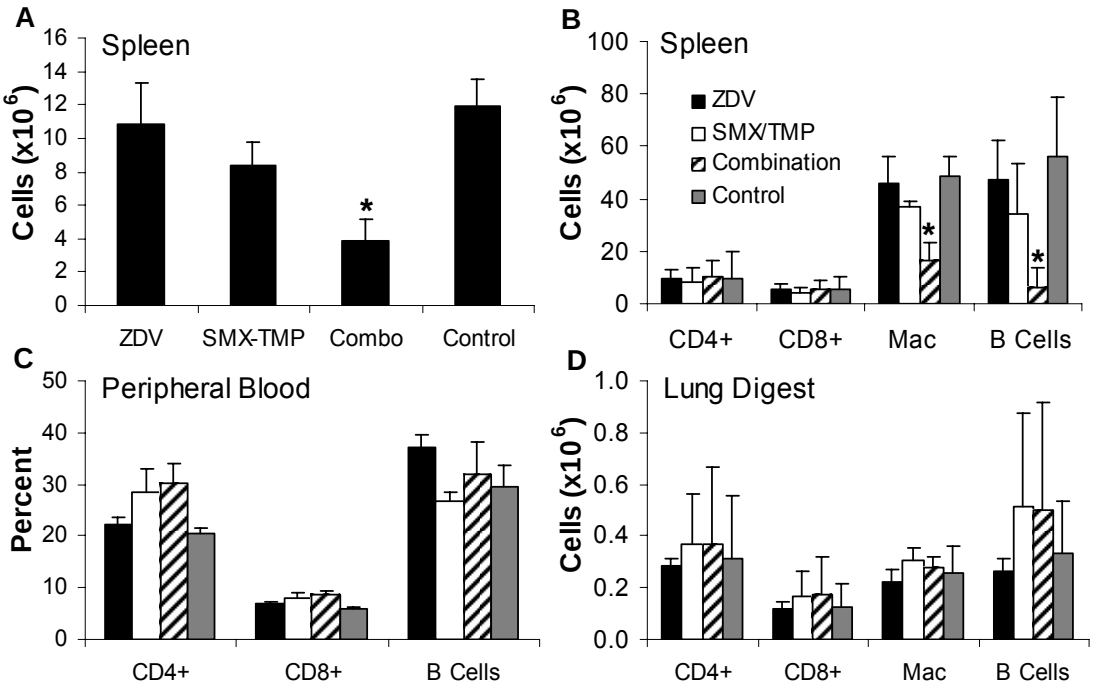

Figure 2.1 Effects of drug dosing on immune cell populations. Mice were treated with either ZDV, SMX-TMP, ZDV plus SMX-TMP, or vehicle only control. Spleen, peripheral blood, and lung digests were processed into single-cell suspensions and phenotyped by flow cytometry. Panels consist of: (A) total splenocytes isolated from mice in each group after 28 days dosing; (B) $CD4^+$ and $CD8^+$ T cells, monocytes (MHC II^+ on non-lymphocyte gate) and $CD19^+$ B cells in spleens; (C) percentages of $CD4^+$, $CD8^+$, and $CD19^+$ cells in peripheral blood after 10 days of dosing; and (D) $CD4^+$ and $CD8^+$ T cells, macrophages (MHC II^+ on non-lymphocyte gate) and $CD19^+$ B cells in lung digests after 28 days drug exposure. Data represent the mean $\pm$ SD of 4 mice per group and are representative of 3 separate experiments. Significant differences from control group (*) were defined at an alpha level of < 0.05.

(Figure 2.1C). Lung digest cell populations (Figure 2.1D) displayed no differences in total cell number or in any subpopulation of cells quantified.

There were significant decreases in all cell lineages examined in the bone marrow in mice receiving combination exposure, including total cells, B lymphocytes, and PMN (Figure 2.2A). There was a dramatic decrease in bone marrow cellularity at all timepoints in the ZDV plus SMX-TMP group as compared to the control group (Figure 2.2B). Bone marrow B cells ($B220^+$) are depicted in Figure 2.2C, demonstrating that they follow the same pattern of depletion over time as the total bone marrow cell

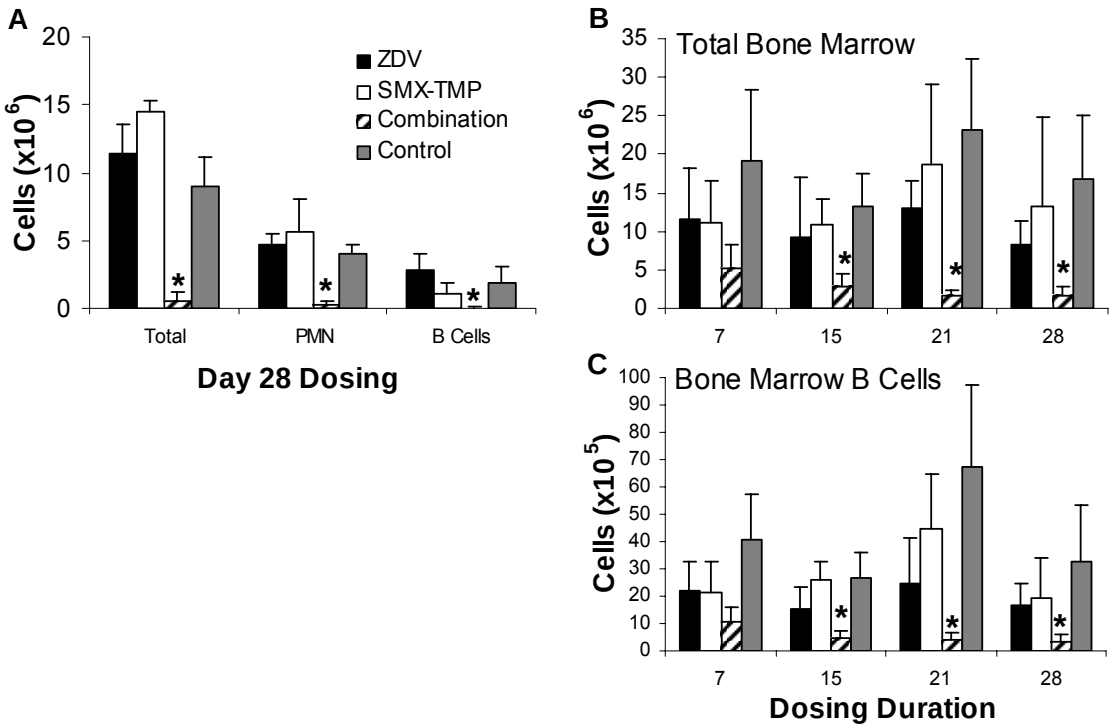

Figure 2.2 Effects of drug dosing on bone marrow B cell populations. Mice were treated with either ZDV, SMX-TMP, ZDV plus SMX-TMP, or vehicle only control. Bone marrow cells were isolated from femurs and tibias of mice and processed into single cell suspensions after RBC lysis. Panel A depicts total cell, PMN (GR-1$^+$/CD11b$^+$), and B cell (B220$^+$) populations in the bone marrow after 28 days of dosing. The next panels show the kinetics of the depletion of total cells (B) and B220$^+$ B cells (C) over time up to day 28 of drug exposure. Data represent the mean ± SD of 4 mice per group and are representative of 3 separate experiments. Significant differences from control group (*) were defined at an alpha level of < 0.05.

populations. Notably, treatment with either drug alone had no statistically significant effect on any cell populations in the bone marrow, spleen, or lung digest at any timepoints examined (Figures 2.1 and 2.2).

B lineage subtypes in the bone marrow are affected primarily at the late pre-B cell stage

B cell development proceeds through discreet stages, allowing us to determine *in vivo* toxic effects of ZDV plus SMX-TMP on B cell maturation. Phenotypic analysis via flow cytometry according to the scheme developed by Hardy et al, 1991 is depicted in

Figure 2.3 (178). When expressed as percentages, large deviations in B lineage cells were not observed, with the exception of late pre-B cells (Figure 2.3B). Representative histograms from flow cytometry analysis show the absence of late pre-B cells in a mouse dosed with ZDV plus SMX-TMP (Panel A, region c, 0.6% of the total bone marrow) compared to a control mouse (Panel B, 6.6% of the total bone marrow).

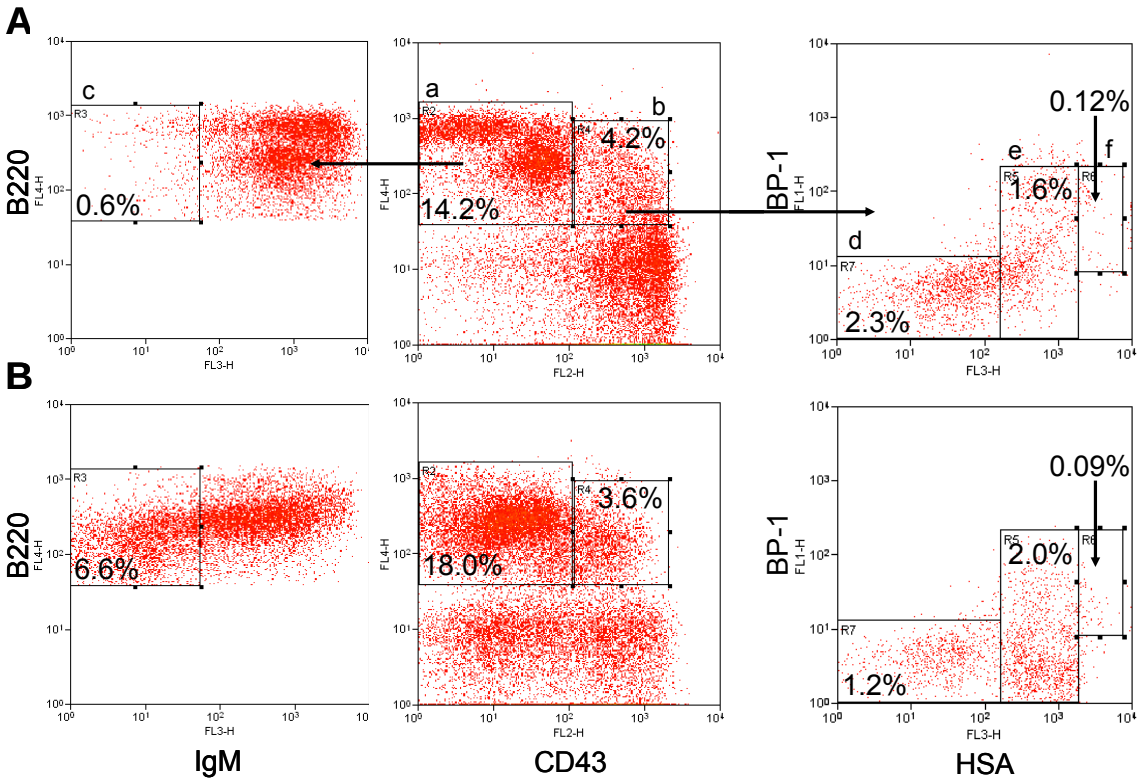

Figure 2.3 Phenotypic staining of B cell precursors by flow cytometry. Bone marrow from mice treated with ZDV plus SMX-TMP for 9 days (A) are compared to bone marrow from control mice (B). Cells were gated on lymphocyte populations and stained for B220 and CD43 (middle panels). Lymphocytes in gate **a** ($B220^+/CD43^-$) in the middle panels were stained for IgM (left panels) to determine late pre-B cell percentage shown in box **c** ($B220^+/CD43^-/IgM^-$). $B220^+/CD43^+$ cells (gate **b**) were then analyzed for HSA vs. BP-1 (right panels). Pre-pro-B cells are shown in box **d** ($B220^+/CD43^+/HSA^-/BP\text{-}1^-$), pro-B cells in box **e** ($B220^+/CD43^+/HSA^{low}$), and early pre-B cells in box **f** ($B220^+/CD43^+/HSA^{high}/BP\text{-}1^+$).

Absolute cell numbers of B-lineage subtypes are shown in Figure 2.4. Differences observed were in large part due to differences in overall bone marrow cell counts, and not alterations in percentages of each cell type (as described above). There was a

significant decrease in pre-pro-B cells ($B220^+/CD43^+/BP\text{-}1^-/HSA^-$) compared to the control group after 21 days of combination dosing (Figure 2.4A). In the single drug treatment groups, decreases in number of pre-pro-B cells were seen at day 28, similar to those seen in the combination treatment mice (Figure 2.4A). The pro-B cell fraction ($B220^+/CD43^+/HSA^{low}$) displayed similar kinetics, with a significant decrease in cell number in the combination group occurring at the 21- and 28-day timepoints (Figure 2.4B). Pro-B cell numbers were also significantly decreased in the ZDV group at day 21 and the SMX-TMP group at day 28.

The early pre-B cell population ($B220^+/CD43^+/BP\text{-}1^+/HSA^+$) was approximately three times greater in number at day 7 in the ZDV plus SMX-TMP treated mice compared to the control animals (Figure 2.4C). By day 28, however, this population fell

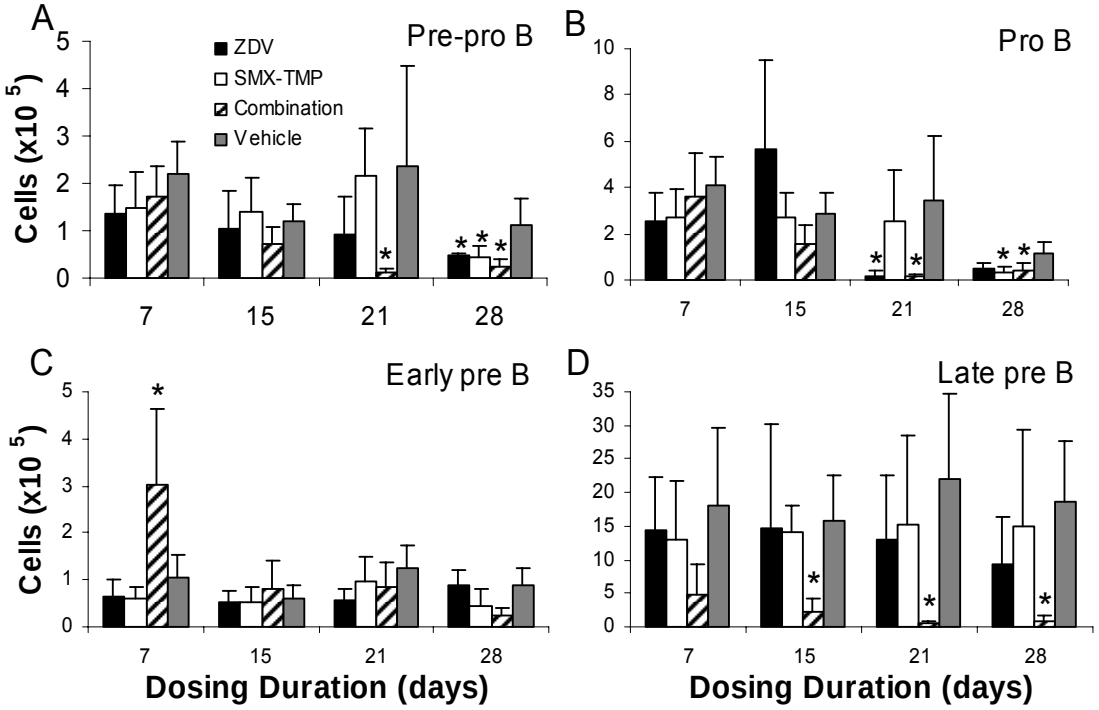

Figure 2.4 Kinetics of B lineage subsets at weekly timepoints. Mice were treated with either ZDV, SMX-TMP, ZDV plus SMX-TMP, or vehicle only control, and sacrificed at weekly time intervals. $B220^+$ B cells were phenotyped for surface marker profiles using flow cytometry as shown in Figure 3. Cell fractions were enumerated in developmental sequence, including pre-pro-B (A), pro-B (B), early pre-B (C), and late pre-B cells (D). Bars represent the mean ± SD of 4 mice per group per timepoint. Significant difference to control group (*) was defined at an alpha level of < 0.05.

significantly as compared to the control group. Interestingly, the rise in early pre-B cells corresponded to a decrease in the late pre-B cell ($B220^+/CD43^-/IgM^-$) fraction on day 7. Late pre-B cell numbers were dramatically lower on the later 3 timepoints in the combination treatment group (Figure 2.4D). The increase in cell numbers among the late pre-B cell fraction in comparison to the other B cell subtypes corresponds to the proliferative burst seen as they mature from the early pre-B cell stage to the late pre-B cell stage of development under the influence of IL-7. This proliferative burst was absent in the ZDV plus SMX-TMP group at days 15, 21, and 28 of therapy (Figure 2.4C and 2.4D).

The mode of cell death is apoptosis

To gain insight into the mechanism of bone marrow cell depletion, the percentage of cells undergoing apoptosis was determined by identifying cells that were bound to annexin V but stained negative for PI. There was a significant increase in percentage of total cells that stained annexin +/PI- in the ZDV plus SMX-TMP group at each timepoint examined (Figure 2.5A). The combination of drugs caused a significant increase in apoptotic cells in both the non-lymphocyte and B lineage populations. Statistically significant increases were observed at each timepoint for percentages of non-lymphocytes (identified via a non-lymphocyte gate) undergoing apoptosis in the combination treatment group (Figure 2.5B). Percentages of total B cells ($B220^+$) undergoing apoptosis were significantly increased at the 7-, 15-, and 28-day timepoints in the ZDV plus SMX-TMP group, with a trend toward significance at day 21 (p=0.07) as shown in Figure 2.5C.

Pro-B ($B220^+/CD43^+$) and pre-B ($B220^+/CD43^-$) cell subpopulations were examined for induction of apoptosis. Percentages of apoptotic pro-B cells were increased at the 15-, 21-, and 28-day timepoints, more than doubling in each instance in the ZDV plus SMX-TMP group as compared to the group receiving vehicle (Figure 2.5D). The percentage of pre-B cells undergoing apoptosis was significantly increased at days 7, 15, and 28 in the combination treatment group, again at more than twice the apoptosis rate as the control group (Figure 2.5E). There were no differences in percentage of B-

lineage cells undergoing apoptosis in either of the single drug treatment groups as compared to the control group (Figure 2.5). Additionally, we have also demonstrated this effect from the drug combination in FVB/N mice, to confirm that the toxicity is not strain-specific to BALB/c mice. This data is shown in Chapter 3 (Figure 3.8).

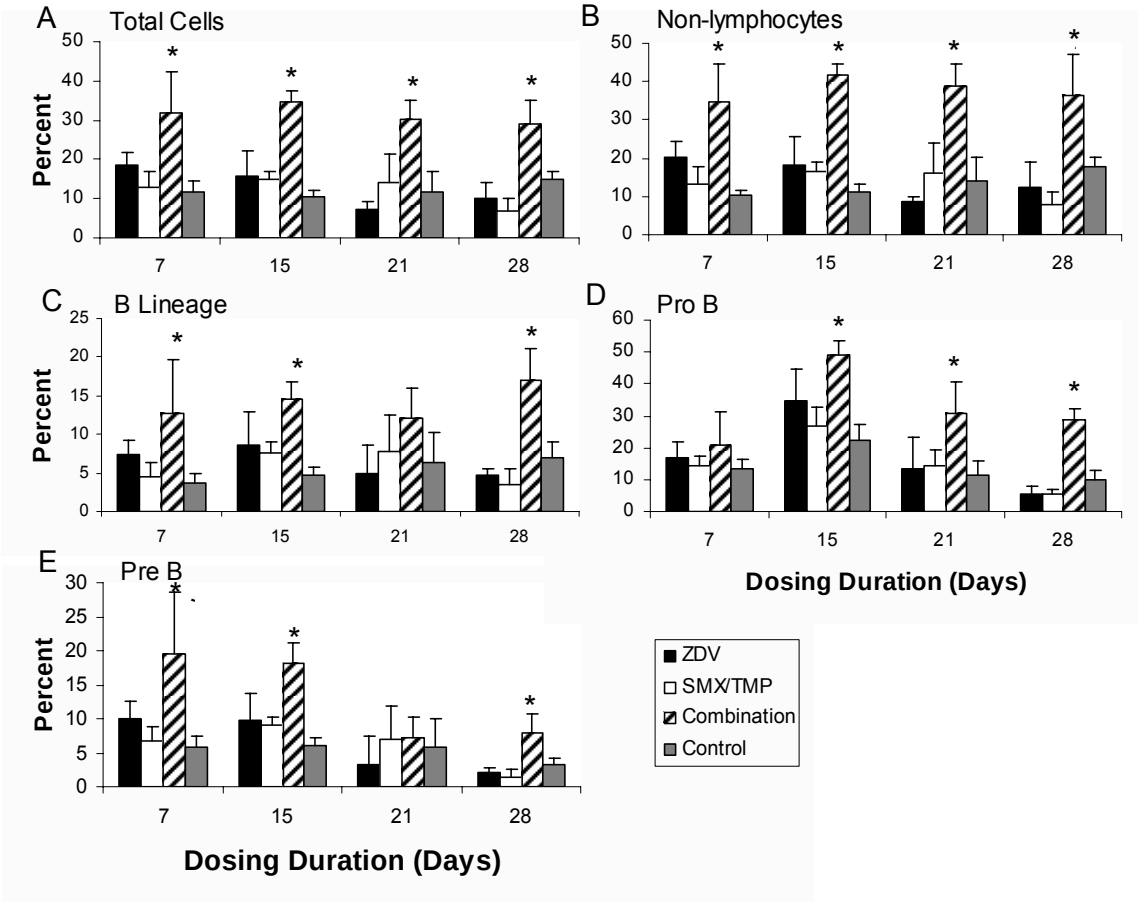

Figure 2.5 Percentages of apoptotic cells at weekly timepoints of drug dosing. Mice dosed with ZDV, SMX-TMP, ZDV plus SMX-TMP, or vehicle only control were sacrificed at weekly timepoints and the bone marrow aspirates were assayed for cells undergoing apoptosis. Cells that labeled annexin-V positive, PI negative were deemed apoptotic. Percentages of total cells (A), non-lymphocytes (B), B lymphocytes (C), pro-B cells (D), and pre-B cells (E) are shown. Data represents the mean ± SD and are representative of 3 separate experiments. Significant differences (*) from control group were determined at an alpha level of <0.05.

Long-term, low-dose exposure did not affect the bone marrow

To determine the long-term affect of ZDV plus SMX-TMP on the bone marrow, mice were dosed with ZDV, SMX-TMP, the combination of both, or vehicle only control as described previously. Dosing was altered for this experiment however, in that the doses were reduced 8-fold, to ZDV 30mg/kg, SMX 105mg/kg, and TMP 20mg/kg, and the dosing duration was extended to 55 days. These doses were chosen because of preliminary data that demonstrated a low level of bone marrow toxicity at these quantities over a dosing period of 14 days. Figures 2.6A and 2.6B show that total cells

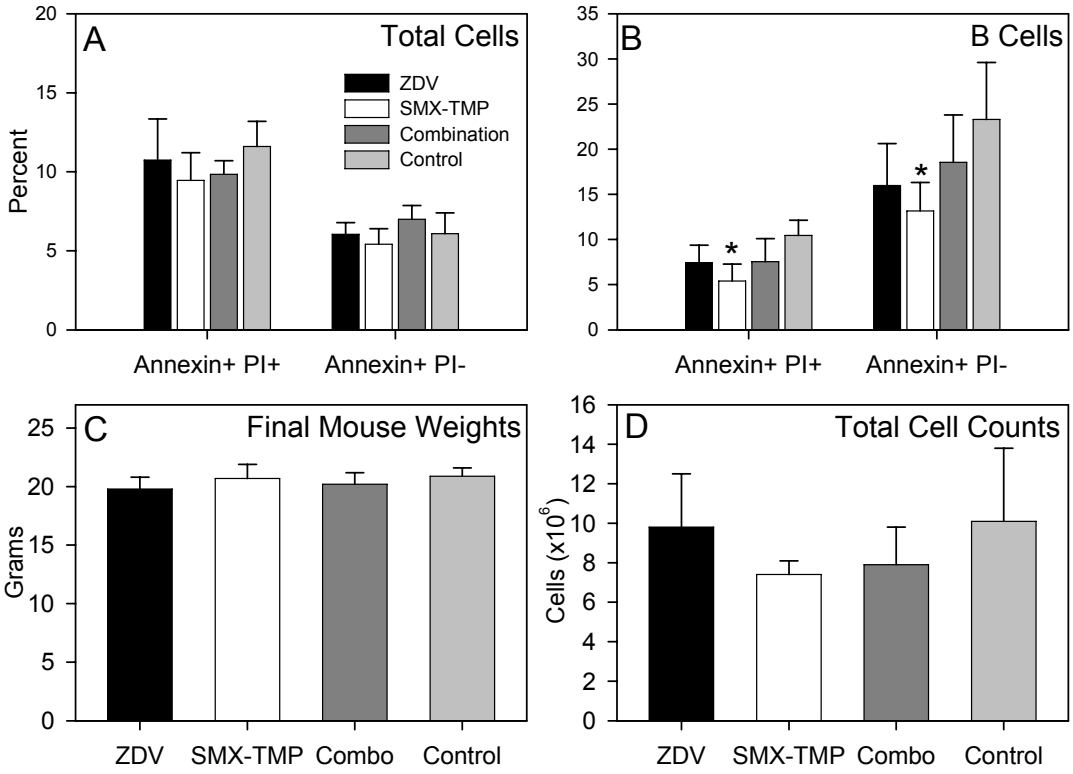

Figure 2.6 Long-term dosing effect on bone marrow total and B cells. Mice were dosed with ZDV, SMX-TMP, the combination of both, or vehicle only control as described in Materials and Methods. Dose was reduced however to ZDV 30mg/kg, SMX 105mg/kg, and TMP 20mg/kg, and the dosing duration was extended to 55 days. Panels A and B depict percentages of total cells (A) and B220+ B cells (B) harvested that were dead (annexin-V positive, PI positive) or apoptotic (annexin-V positive, PI negative). Panel C represents mean final mouse weights on day 55 of dosing. Panel D shows the total cell counts in the bone marrow at the time of harvest. Data represents the mean ± SD and are representative of 1 experiment only. Significant differences (*) from control group were determined at an alpha level of <0.05.

(A) and $B220^+$ B cells (B) were not affected after exposing the mice to low levels of drug for 55 days. Dead (annexin-V positive, PI positive) and apoptotic (annexin-V positive, PI negative) cell percentages were unaffected in the combination dosing group compared to the control group. Interestingly, dead and apoptotic B cell percentages in the SMX-TMP group were significantly reduced. Panel C represents the mean final mouse weights on day 55 of dosing, which were not affected by SMX-TMP or ZDV. Panel D shows the total cell counts in the bone marrow at the time of harvest, which also displayed no statistically-significant differences in the treatment groups compared to control.

The toxicity to B lineage subpopulations is cell-cycle specific

We have demonstrated that the transition from the early pre-B to the late pre-B cell stage appears to be affected by the drug combination, as evidenced by an accumulation of early pre-B cells followed by depletion of late pre-B cells at day 7 of drug exposure. To determine whether this was due to cell cycle arrest, mice from the four treatment groups were sacrificed after 6 and 9 days of dosing for bone marrow harvest and cell cycle analysis. Bone marrow was pooled from each group, and sorted by flow cytometry into pre-pro-B, pro-B, early pre-B, and late pre-B cell subsets. Cells were fixed and stained with PI for cell cycle analysis on the sorted samples. Samples were pooled to acquire enough events for analysis after sorting because some subtypes exist at very small percentages of the total bone marrow.

Representative cell cycle histograms are shown in Figure 2.7 to illustrate the marked accumulation of cells in the S and G2/M phases of the cell cycle as a result of dual drug treatment. Mice treated with ZDV plus SMX-TMP displayed an increased proportion of early pre-B cells in S phase and G2/M phases compared to the control mice after 6 and 9 days of treatment (Fig 2.7A-C). Panels D through F show late pre-B cells, which had an overall proliferation rate that is lower than that of early pre-B cells. Combination drug dosing did not alter the proportion of S phase late pre-B cells to a large degree, however there was an upward trend compared to the control group (Figure 2.7D-F).

The fraction of cells in S phase and G2/M phases for all groups are shown in Figure 2.8. After 6 days of dosing, the proportion of pre-pro-B, pro-B, and early pre-B cells in

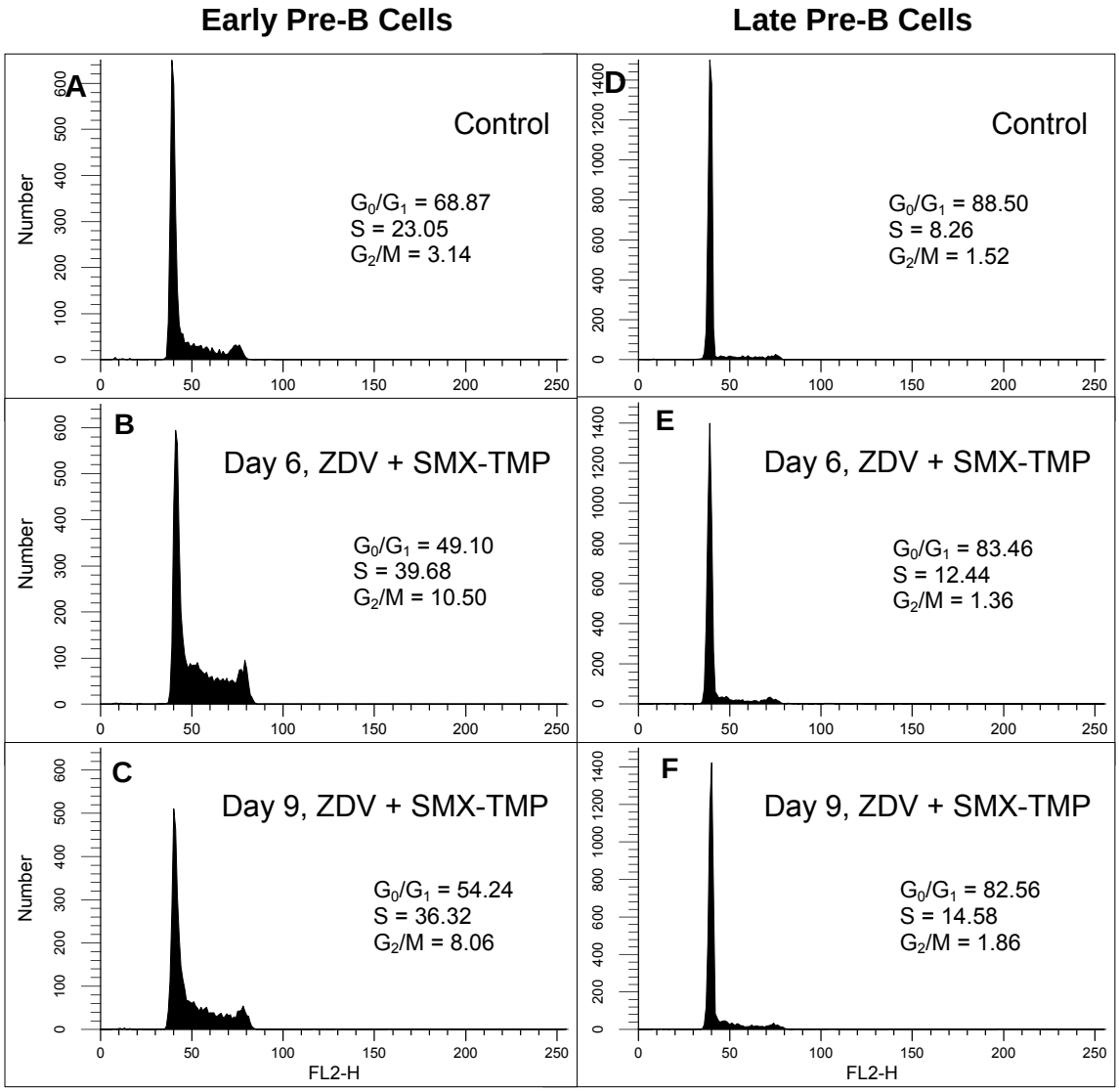

Figure 2.7 Bone marrow B lymphocyte cell cycle histograms. Bone marrow samples were analyzed for cell cycle profile by measuring PI intercalation into DNA (expressed as fluorescence intensity) on day 6 and day 9 of dosing with ZDV, SMX-TMP, ZDV plus SMX-TMP, or vehicle only. $B220^{+}$ cells from bone marrow were phenotyped by surface markers and sorted via flow cytometry prior to cell cycle analysis. The panels on the left depict the cell cycle profiles in the early pre-B cell populations from mice treated with the combination of ZDV and SMX-TMP on day 6 (B), and day 9 (C), as compared to control mice (A). The panels on the right depict late pre-B cells in the control group (D) and the ZDV plus SMX-TMP group at day 6 (E) and day 9 (F) of dosing. The proportions of cells in the different phases of the cell cycle are shown on each panel.

the S and G2/M phases were higher in the combination drug treatment group than in the other groups (panels A and B). This proliferative burst is exaggerated on day 6 of dosing in the combination group. However, by day 9, the percentage of cells in S phase and G2/M phases show no obvious differences in any of the B lineage subsets (panels C and D).

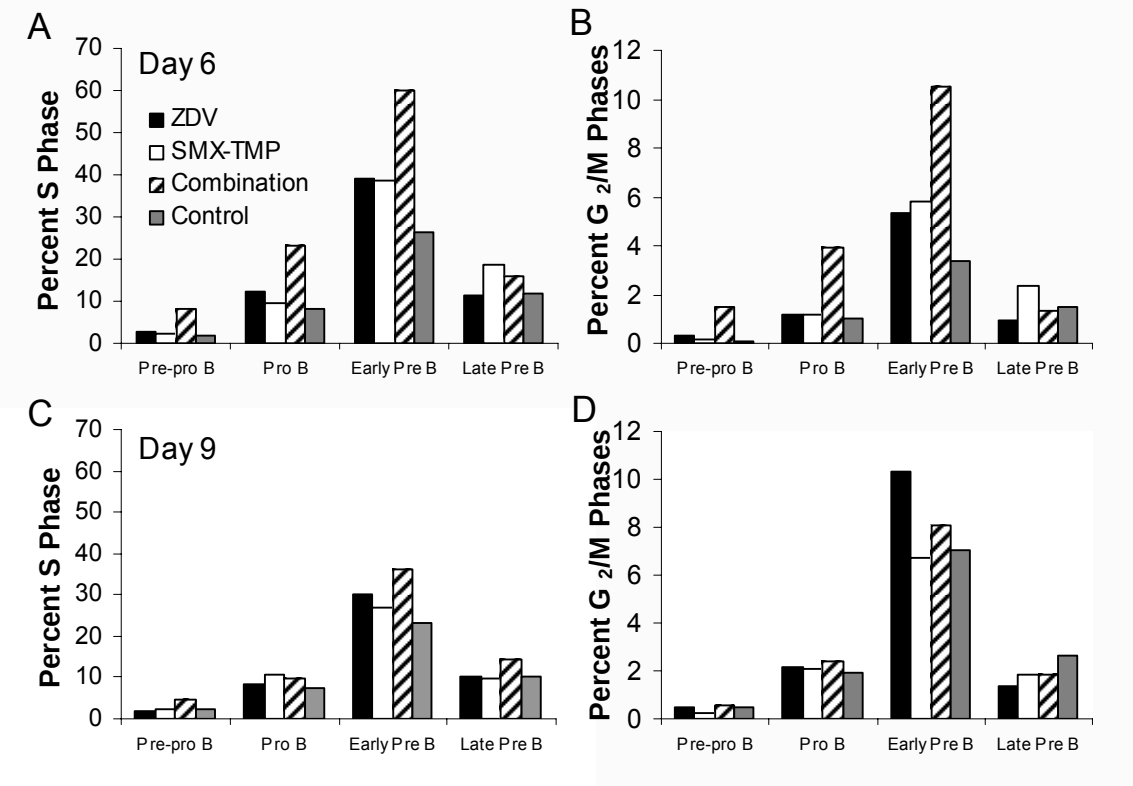

Figure 2.8 Cell cycle analysis. Cell cycle analysis experiments were performed by sorting B lineage subpopulations into pre-pro-B, pro-B, early pre-B, and late pre-B cell fractions by FACS as per Figure 5. Bone marrow from mice treated with ZDV, SMX-TMP, ZDV plus SMX-TMP, or vehicle was pooled together (3 mice per group) and sorted after 6 and 9 days of dosing. Cell cycle analysis was performed using PI intercalation and FACS. The percentage of each subpopulation in each stage of the cell cycle is reported. Panels A and B depict percentages of B lineage cells from mice treated for 6 days that are in S phase and G2/M phases, respectively. Panels C and D show the percentage of cells in S phase and G2/M phases from mice treated with the drugs for 9 days. Data are representative of 2 separate experiments.

D. CONCLUSIONS

We have demonstrated the toxic effects of the combination of ZDV and SMX-TMP on B cell development in a mouse model. Bone marrow cells in mice treated with the drug combination had a significantly higher incidence of apoptosis and the combination of drugs appears to affect the proliferative burst as B lineage cells multiply in the pre-B cell stage of development. Interestingly, we consistently found a temporal relationship between drug administration and stage of which B cell development was compromised.

We observed a significant increase in early pre-B cells at the IL-7-dependent proliferative burst at day 7 of drug treatment. However, there was a marked decrease in the numbers of cells in the late pre-B cell fraction, suggesting that ZDV plus SMX-TMP treatment blocked transition into this stage. The cell cycle data presented in Figure 2.7 shows an increased percentage of cells in the S and G2/M phases in the combination group, which could be indicative of either cell cycle arrest or increased proliferation. Taken together with the data demonstrating cellular depletion and apoptosis, we conclude that it is indicative of arrest.

In subsequent timepoints, this increased pre-B cell population is abolished, and cells in the earlier stages of development (pro-B) are decreased. It appears that over time, the toxicity of ZDV plus SMX-TMP causes fewer cells to reach the pre-B cell stage resulting in a depletion at this stage. Of note, after dosing for 28 days, proportions of pre-pro-B and pro-B cells were significantly reduced in each single drug treatment group; however, the total bone marrow B lymphocyte population in these mice was not significantly affected suggesting that the presence of the drugs in combination is required to block the IL-7 dependent pre-B cell expansion. Our data demonstrate that the cell type most affected is that which is undergoing the most cell division; this is consistent with the known propensity of ZDV and SMX-TMP to affect DNA replication during the S phase.

To further these investigations, we have expanded these studies in two ways. First, we describe the characteristics of this toxic effect in a series of *in vitro* experiments, as we analyze the apoptotic mechanism in these cells that are affected by the drugs. Secondly, we investigate in mice the affect of this drug-drug interaction on the host's

ability to respond to an infectious agent. These studies will ultimately lead to the human trial that exposes the clinical significance of this toxicity, which will be presented in Chapter 5.

CHAPTER 3: Mechanistic investigation of toxicity to B lymphocytes due to ZDV plus SMX-TMP exposure

A. OVERVIEW

In the previous chapter, we have characterized the effects of combination exposure to ZDV and SMX-TMP in mice. Because this toxicity affects cells that originate and mature in the bone marrow, we have focused our studies to this tissue to demonstrate that cells are being induced to undergo a higher rate of apoptosis when exposed to both drugs. B-lineage cells are primarily affected at the proliferative burst when transitioning from the early pre-B cell stage to the late pre-B cell phenotype; however, in addition, fewer progenitors are reaching this stage of development. In this chapter we now report a series of *in vitro* experiments designed to further characterize the toxicity of ZDV plus SMX-TMP exposure, along with additional *in vivo* assessments to investigate the mechanism of enhanced apoptosis in B lymphocytes.

While there is little in the literature addressing the toxicity of these agents in combination, the cytotoxic effects of both SMX-TMP and ZDV individually have been extensively studied. Several groups have shown that ZDV affects lymphocytes in their early stages of development in the bone marrow (107-109). The monophosphorylated form is responsible for its toxicity by inhibiting thymidylate kinase and lowering intracellular thymidine pools, as discussed in Chapter 1 (107). This toxicity is associated with an inhibition of hematopoietic progenitors in murine and human bone marrow (108, 109). ZDV induces apoptosis in immune cell populations by this inhibition of DNA synthesis, having the greatest impact on cell types that are actively cycling (111, 112). ZDV monophosphate also induces mitochondrial dysfunction in hematological cells due to inhibition of mitochondrial DNA polymerase gamma (113-116). This mechanism of toxicity also plays a role in apoptosis induction, as it is thought that ZDV makes cells more susceptible to apoptosis by inducing mitochondrial membrane hyperpolarization (112, 117).

Effects of SMX-TMP on bone marrow cell populations have been well studied. The toxicity has been attributed to the oxidative metabolites of SMX, sulfamethoxazole-hydroxylamine (SMX-HA) and nitroso-sulfamethoxazole (SMX-NO), based on *in vitro* data (152). Incubation of neutrophils and lymphocytes with the parent compound SMX caused little or no toxicity, while cytotoxic effects were demonstrated with SMX-NO and SMX-HA exposure, including cellular haptenation, direct cellular cytotoxicity, and, of importance to this dissertation, apoptosis induction (152). The cellular haptenation of SMX-HA has been shown to induce a population of SMX-HA-specific T cell clones that are implicated in SMX hypersensitivity (200). Anti-SMX antibodies have also been found in the serum of HIV-infected patients being treated with the drug (201). These data are indicative of an immune pathogenesis for the toxicity associated with the drug, along with direct cytotoxic effects observed with the metabolites.

A higher than normal incidence of adverse reactions is associated with the use of SMX-TMP in patients with AIDS (149-151). Virus-induced GSH depletion has become the leading hypothesis for the mechanism of this phenomenon. Patients with HIV infection have depleted intracellular GSH concentrations, a molecule responsible for the conversion of SMX-HA and SMX-NO back to the parent compound , which is then metabolized to non-toxic species and eliminated (153, 154, Cribb #89, 156). Investigators have linked this depletion of GSH by the virus to SMX-TMP intolerance in HIV-infected patients (153, 154). Naisbitt et. al. confirmed this hypothesis by demonstrating *in vitro* that the addition of GSH to cultured lymphocytes decreases SMX-HA- and SMX-NO-induced cellular toxicity (202).

Additionally, *in vitro* studies have shown that GSH inhibits SMX-NO haptenation to lymphocytes and neutrophils, and the $CD4^+$ T cell response to SMX-HA haptenation in this setting is also decreased (152, 200). Cysteine, another molecule capable of reducing these metabolites has been demonstrated to be protective of these effects as well (152). Although GSH depletion has not been linked to an increase in SMX metabolite concentrations in a clinical setting, this could explain the increased rate of toxicity seen with the use of SMX-TMP in patients with AIDS. Figure 3.1 represents the intracellular metabolic pathways of SMX, and the roles of oxidation and reduction that lead to its elimination. The parent is oxidized to SMX-HA by intracellular cytochrome

P450 isoenzyme 2C9 (CYP2C9), which is further oxidized spontaneously to SMX-NO. GSH (as well as other reducing agents) detoxify the compound back to the parent SMX, which can be glucuronidated by the liver into hydrophilic species that are eliminated (156, 203).

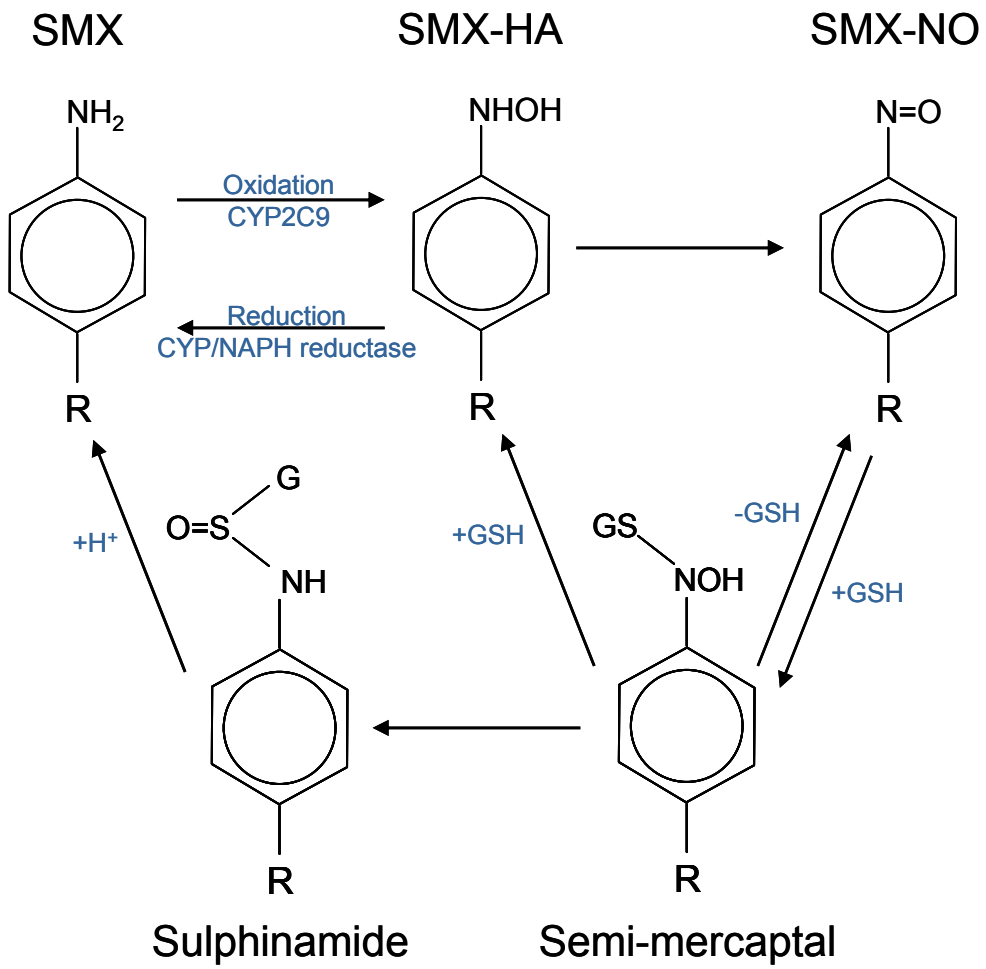

Figure 3.1 Intracellular metabolism of SMX. SMX is oxidized to the bioactive SMX-HA by CYP2C9, and oxidized further spontaneously to SMX-NO. GSH, through a series of reduction steps, converts the molecule back to the parent compound (or via CYP/NAPH reductase) to be metabolized in the liver to glucuronidated intermediates and eliminated. Adapted from Gill et al, 1996 (204). R=SO_2-NH-C_3HNO-CH_3

One hypothesis we explored is that ZDV affects the disposition of SMX and its metabolites, thereby increasing the apoptosis rate in bone marrow B cells. One possible explanation for this alteration could lie in the interesting body of literature describing the up-regulation of the multi-drug resistant protein 4 (Mrp4) by nucleoside

reverse transcriptase inhibitors (205, 206). ZDV is also a known substrate of this transporter, and has also been recently shown to induce its up-regulation (207). Mrp4 is known to be able to transport GSH from inside cells to the extracellular space, causing decreases in intracellular GSH pools (208). Since GSH detoxifies SMX metabolites by reducing them back to the parent drug, up-regulation of Mrp4 by ZDV could lead to a buildup of toxic SMX metabolites. Alternatively, since Mrp4 also transports GSH-substrate complexes (including GSH-SMX-HA), another potential hypothesis is that by competitive inhibition, ZDV (also a substrate of Mrp4) decreases the amount of GSH-SMX-HA complexes that are effluxed, thereby increasing intracellular concentrations of the toxic metabolite.

Clinical investigations into the significance of this drug interaction are difficult, due to the multiple additional factors that could be affecting immune response in HIV-infected patients. Therefore, in addition to exploring this toxicity in an animal model, we investigated the toxicity of this combination of compounds on mouse bone marrow in an *in vitro* culture system. By doing so, many questions concerning this drug interaction could be addressed, including dose dependency, drug disposition, and mechanism of apoptosis induction. Our hypotheses were three-fold: first, that cytotoxicity caused by ZDV plus SMX-TMP is concentration-dependent, synergistic, and related to oxidative stress; second, that apoptosis induction proceeds through signaling pathway that utilized caspases; and third, that the disposition of SMX is altered in mice as a result of concurrent ZDV treatment.

B. MATERIALS AND METHODS

Materials

Many materials used in these experiments were obtained as indicated in previous chapters. In addition, IL-7, dimethylsulfoxide (DMSO), 2-mercaptoethanol (2-ME), trypan blue, etoposide, caffeine, acetonitrile, acetic acid, and triethylamine were obtained from Sigma-Aldrich (St. Louis, MO). SMX-HA and SMX-NO were synthesized and obtained from Dalton Chemical Laboratories (Toronto, Ontario, Canada). The pan-

caspase inhibitor Z-Val-Ala-DL-Asp-fluoromethylketone (Z-FAD-FMK) was purchased from Alexis Biochemicals (Lausen, Switzerland).

BM isolation

Four- to six-week old normal BALB/c mice were obtained from NCI (Raleigh, NC) and isolated for at least 7 days before manipulation. Mice were housed in the Veterans Administration (VA) Veterinary Medical Unit in sterile cages with a 12 hour light/dark photocycle and food and water both freely available. This study and all of its procedures were approved by the VA Institutional Animal Care and Use Committee. Mice were sacrificed using a carbon dioxide chamber, and bone marrow was promptly isolated from femur and tibia bones under sterile conditions using 25-gauge needles into media containing RPMI-1640, 2-ME ($1x10^{-5}$ M), and 5% FCS.

Cell culture

After red cell lysis, cells were placed into 24-well culture plates at a concentration of $1x10^6$ cells/ml per well. B lineage cell proliferation was stimulated by the addition of IL-7 at a concentration of 25 units/ml. SMX-NO, SMX-HA, and ZDV were then dissolved using DMSO (resultant DMSO amount never exceeding 1% in any culture well) and placed into cell culture at increasing concentrations, so that concentration-related toxicities could be analyzed. All cultures were incubated at 37^0C and 5% CO_2. Variations in culture conditions, incubation times, and additives were performed in respective experiments.

Bone marrow phenotyping

Cells were analyzed for phenotype by flow cytometry by using a FACSCaliber Flow Cytometer (BD Biosciences, Mountain View, CA) and the WinList software package (Verity Software House, Topsham, ME). BM cells were incubated with 3 separate panels of fluorescently-labeled antibodies to phenotype B lineage cell types using IgM, CD43, B220, BP-1, and HSA as described in Chapter 2. Other experiments only required one surface marker labeling, either B220 or CD19, to classify B cells more

generally. Cells were washed before and after staining with PBS containing 0.1% BSA and 0.02% sodium azide.

Apoptosis assays

Bone marrow cells were analyzed via flow cytometry for apoptosis using the Annexin V-FITC/PI assay kit, utilizing the manufacturer's instructions (BD Pharmingen, San Diego, CA). Briefly, cells were washed and resuspended in annexin binding buffer and incubated in the presence of annexin-V-FITC and PI for 20 minutes at room temperature. Cells were analyzed by flow cytometry within 1 hour.

Cells were also analyzed for apoptosis with the "Tunel" assay using the APO-BRDU™ Kit (BD Pharmingen, San Diego, CA). Treated cells were fixed in 4% paraformaldehyde for 1 hour. Terminal deoxynucleotidyltransferase (TdT) enzyme was used to catalyze the addition of bromolated deoxyuridine triphosphate (BrdU) to the 3'-hydroxyl termini of DNA for 60 minutes at 37^0C. Cells were washed and stained with anti-BrdU antibody labeled with FITC, along with PI, for 30 minutes at room temperature. Apoptosis and cell cycle were analyzed simultaneously by flow cytometry within 3 hours.

Dose-effect analysis

To determine whether the *in vitro* interaction between ZDV and SMX-HA is additive or synergistic, the combination index method was used (209). The concentration at which 50% of the effect is reached (IC_{50}) and the slope parameter (m) for each agent alone and in combination (at a ratio of 1:1) were determined from the median-effect plot, a linear relationship plotting log(D) versus log(f_a/f_u) based on Chou's median-effect equation:

$$f_a/f_u = (D/D_m)^m$$

where D is the dose (concentration) of the drug, D_m is the IC_{50} as determined from the x-intercept of the median-effect plot, f_a is the fraction of cells affected, f_u is the fraction of cells unaffected (f_u=1-f_a), and m is an exponent signifying the steepness for the sigmoid

dose-effect curve. A combination index (CI) was then calculated to assess synergism, additivity, or antagonism according to the following equation:

$$CI = (D)_1/(D_x)_1 + (D)_2/(D_x)_2 + (D)_1(D)_2/(D_x)_1(D_x)_2$$

where $(D)_1$ and $(D)_2$ are the concentrations of ZDV and SMX-HA which *combined* produce x% cytotoxicity, and $(D_x)_1$ and $(D_x)_2$ are the concentrations of each drug which *alone* produce x% cytotoxicity. The equation assumes independent mechanisms of drug action between the agents. CI=1 indicates an additive interaction, CI<1 indicates synergy between the two drugs, and CI>1 indicates antagonism (209).

Apoptosis inhibition

The pan-caspase inhibitor Z-VAD-FMK was utilized to inhibit apoptosis associated with ZDV plus SMX-TMP exposure in cultured B lymphocytes. Increasing concentrations of ZDV (72-hour exposure) and SMX-HA (1- to 2-hour exposure) were used to induce apoptosis, with Z-VAD-FMK 20μM added 15 minutes prior to SMX-HA in an attempt to block apoptotic mechanisms that utilize caspases. Etoposide was used as a positive control to induce mitochondrial pathway apoptosis that is caspase-dependent, through the inhibition of topoisomerase II, which causes DNA strand breakage and arrest in late S or early G2 stages of the cell cycle. Cells were incubated with etoposide at an optimal concentration of 20μg/ml for 4 hours with and without Z-VAD-FMK.

RNase protection assay

RNA was isolated from cells cultured in the presence of 10μM ZDV (72 hours) and/or 10μM SMX-HA (8 hours) using TRIzol® reagent (Invitrogen, Carlsbad, CA). RNase protection assay was performed using the BD Riboquant™ RPA kit (BD Pharmingen, San Diego, CA) using the mAPO Multiprobe Template (BD Pharmingen) according to the manufacturer's instruction. Briefly, the RNA probe was synthesized using T7 RNA polymerase in the presence of ATP, GTP, UTP and CTP supplemented with [α-^{32}P]UTP. Approximately 3.6x10^5 cpm of ^{32}P-labeled probe was hybridized to RNA pools

from each sample at 56^{0}C overnight, followed by digestion with RNase T1/A for 15 minutes at 37^{0}C. The protected RNA fragments were precipitated and then separated on a 4.75% acrylamide gel, and imaged by autoradiography. Band density for each mRNA encoding for caspases-8, -3, -6, -11, -2, -7, and -1 were calculated and compared to band density from the 2 housekeeping gene products, L32 and GAPDH.

HPLC

Serum SMX concentrations were determined 18 hours after drug dosing by HPLC as previously described (210). Briefly, 50µl of each serum sample was mixed with caffeine (20µg/ml) as an internal standard. The drugs were extracted with 400µl acetonitrile, vortexed, and purified by centrifugation for 10 minutes. The supernatants were then collected and evaporated under nitrogen gas, and resuspended in 50µl of mobile phase containing a v/v ratio of 80:20:1:0.5 deionized water, acetonitrile, acetic acid, and triethylamine. Using a Shimadzu HPLC system (Kyoto, Japan), 10µl of sample was injected onto a Nova-pak C18 10cm x 5mm Z module solid phase column (Waters Corporation, Milford, MA) at a flow rate of 1ml/min. UV absorbance detection at 254nm was performed with a SMX retention time of 12.1 minutes and an internal standard retention time of 3.5 minutes. The accuracy of quality control samples based on percent difference ranged from 2.3 to 18.1 percent and the overall coefficient of variance was 0.056. The standard curve peak area ratio SMX to internal standard was linear over a range of 5µg/ml to 1000µg/ml (r^2 = 0.9866).

Mrp1 mutation experiments

Mrp1 Targeted Mutation Mice were purchased from Taconic (Germantown, NY) along with gender-and age-matched FVB/N background controls. The *mrp1* gene encodes for the ATP-binding cassette, subfamily C, member 1A protein, commonly know as the multidrug resistance protein-1 (Mrp1). This mutation renders mice deficient in functional Mrp1. This protein is responsible for the cellular excretion of many drugs, GSH, and GSH-drug complexes (211). Deficiency in this protein causes a significant decrease in GSH and GSH-conjugated substrate efflux, and increases cell sensitivity to many chemotherapeutic agents (211). These Mrp1 functional knockout mice (Mrp1$^{-/-}$)

and background-matched controls (FVB/N) were dosed with ZDV plus SMX-TMP or vehicle control via oral gavage for 14 days as described in detail in Chapter 2. Mice were humanely killed and bone marrow was isolated as described above, and analyzed for apoptosis, and for B-lineage cell phenotype populations as outlined in Chapter 2. Bone marrow cells from drug-naïve mice were also placed into culture as previously described.

Statistical analysis

All cell numbers and percentages were compared using one-way ANOVA followed by the Student-Neuman-Keul test for ad hoc pair-wise comparisons evaluating each treatment group compared to its corresponding control, using commercially available software (Sigmastat, SPSS, Chicago, IL). Data that failed normality testing was compared using the Kruskal-Wallis One Way Analysis of Variance on Ranks method (Figure 3.8B). Results were determined to be statistically significant when a *p*-value < 0.05 was obtained. Data are expressed as the mean +/- standard deviation.

C. RESULTS

Concentration-dependent cytotoxicity increases with increasing SMX metabolite concentrations

Concentration-dependent cytotoxicity was observed in bone marrow culture after 24 hour incubation with SMX-NO and SMX-HA, with SMX-HA causing a more potent toxicity than SMX-NO (Figure 3.2). As concentrations of SMX metabolites increased in the presence of 1 and 10μM ZDV, viable percentages (annexin-V negative, PI negative) of B lymphocytes decreased (Figure 3.2A). Maximum toxicity with SMX-HA occurred at the 100μM concentration at 24 hours, and substantial toxicity was not demonstrated with SMX-NO until the 40μM concentration was reached. Percentage of apoptotic cells (annexin-V positive, PI negative) increased as concentrations of SMX metabolites increased, but at the highest concentration (500μM), the percentages of apoptotic cells were diminished, likely due to low percentages of viable cells remaining (Figure 3.2B).

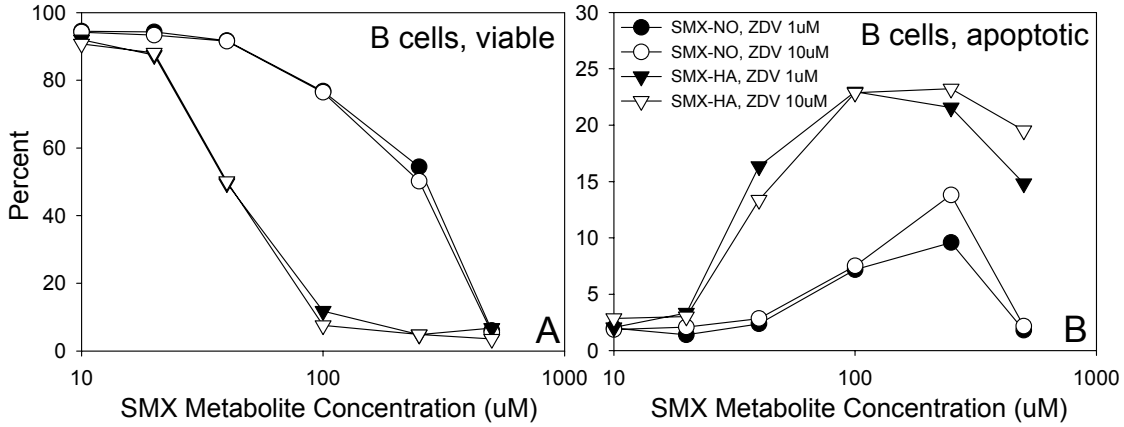

Figure 3.2 Concentration-dependent cytotoxicity in 24 culture. Mouse bone marrow was isolated and cultured at $1x10^6$ cells per well in 24-well culture tissue culture plates with IL-7 at 25U/ml to stimulate B cell proliferation as detailed in Materials and Methods. ZDV at 1 and 10μM concentrations, and SMX-HA or SMX-NO at concentrations between 10 and 500μM were added to corresponding wells, and the cells were incubated for 24 hours. Cells were harvested, stained with B220, annexin-V, and PI as described, and analyzed by flow cytometry. Panel A shows percentage of cells that were viable (annexin-V negative, PI negative) at each concentration combination, and panel B depicts percentage of cells that were apoptotic (annexin-V positive, PI negative). Data is representative of multiple trials.

Importantly, the presence of ZDV at concentrations of 1 and 10μM did not contribute to the toxicity with 24 hours of incubation, as the viability and apoptosis curves at different ZDV concentrations were virtually identical.

Absence of the reducing agent 2-ME, and the addition of TMP to culture, increased cytotoxicity

Because the toxic metabolites of SMX are oxidative species, and it has been shown that reducing agents limit their toxicity, a series of experiments was performed analyzing the contribution of 2-ME, a powerful reduction species present in our culture system, to the overall toxicity of ZDV and SMX metabolites to B cells. Figure 3.3A shows that the toxicity to B lymphocytes is increased when 2-ME is removed from cell culture in the presence of ZDV and SMX-NO or SMX-HA. When comparing cell viability to panel A in

Figure 4.2, the toxicity is decreased from approximately 90% at lower SMX metabolite concentrations, to approximately 40 to 60% in the absence of 2-ME.

Figure 3.3B depicts the cytotoxicity resultant from the addition of TMP to the culture system along with ZDV and SMX metabolites (again in the absence of 2-ME). Viable cell percentages are shown, and the addition of TMP increased cytotoxicity among B cells in culture, reducing viability to approximately 20-30% at the lower SMX-HA concentrations.

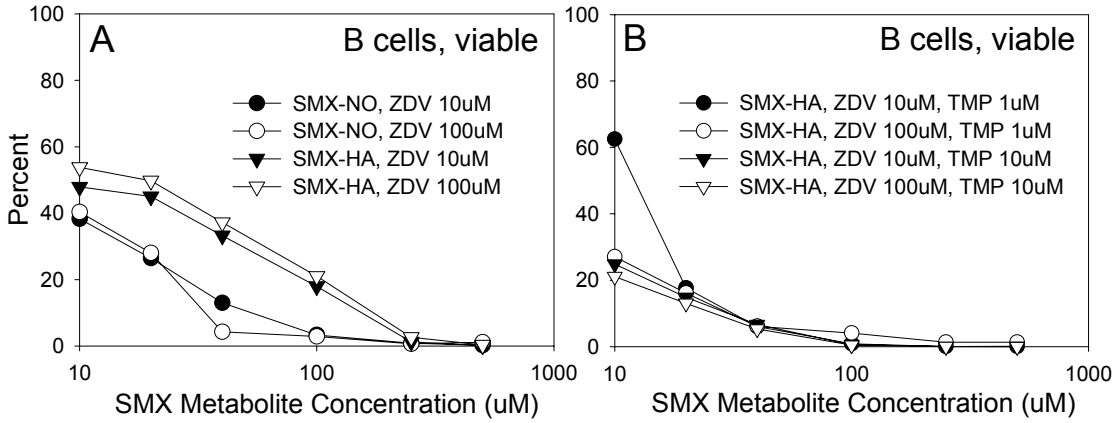

Figure 3.3 Absence of 2-ME, addition of TMP increase toxic effects. Mouse bone marrow was isolated and cultured at $1x10^6$ cells per well in 24-well culture tissue culture plates with IL-7 at 25U/ml to stimulate B cell proliferation as detailed in Materials and Methods, except in these experiments, 2-ME was omitted from the culture medium. ZDV at 10 and 100μM concentrations, TMP at 1 and 10μM (panel B), and SMX-HA or SMX-NO at concentrations between 10 and 500μM were added to corresponding wells, and the cells were incubated for 24 hours. Cells were harvested, stained with B220, annexin-V, and PI as described, and analyzed by flow cytometry. Data depicts percentage of B cells viable (annexin-v negative, PI negative) (A) with SMX metabolite and ZDV exposure, and (B) when TMP is also added along with SMX-HA and ZDV. Graphs are representative of one trial only.

ZDV contributes to cytotoxicity when exposure is lengthened to 72 hours

Mouse bone marrow was again cultured along with IL-7 and 2-ME, with the addition of ZDV and SMX-HA to the culture medium. In this set of experiments, ZDV exposure (10 and 100μM) was lengthened to 72 hours. SMX-HA, at increasing concentrations, was added to the cells for the final 18 hours of incubation time. Upon harvest and

analysis by trypan blue staining and flow cytometry, cytotoxicity increased with increasing ZDV concentrations. In Figure 3.4, panels A and B depict total cell and B cell viable percentages, respectively, over increasing SMX-HA concentrations for ZDV 0, 10, and 100μM series. As ZDV concentration increased, cytotoxicity increased. Panel C shows the total number of cells that were viable that correspond to the percentages in Figure 3.4A. In panel D, the percentages of B cells that were apoptotic are shown as a

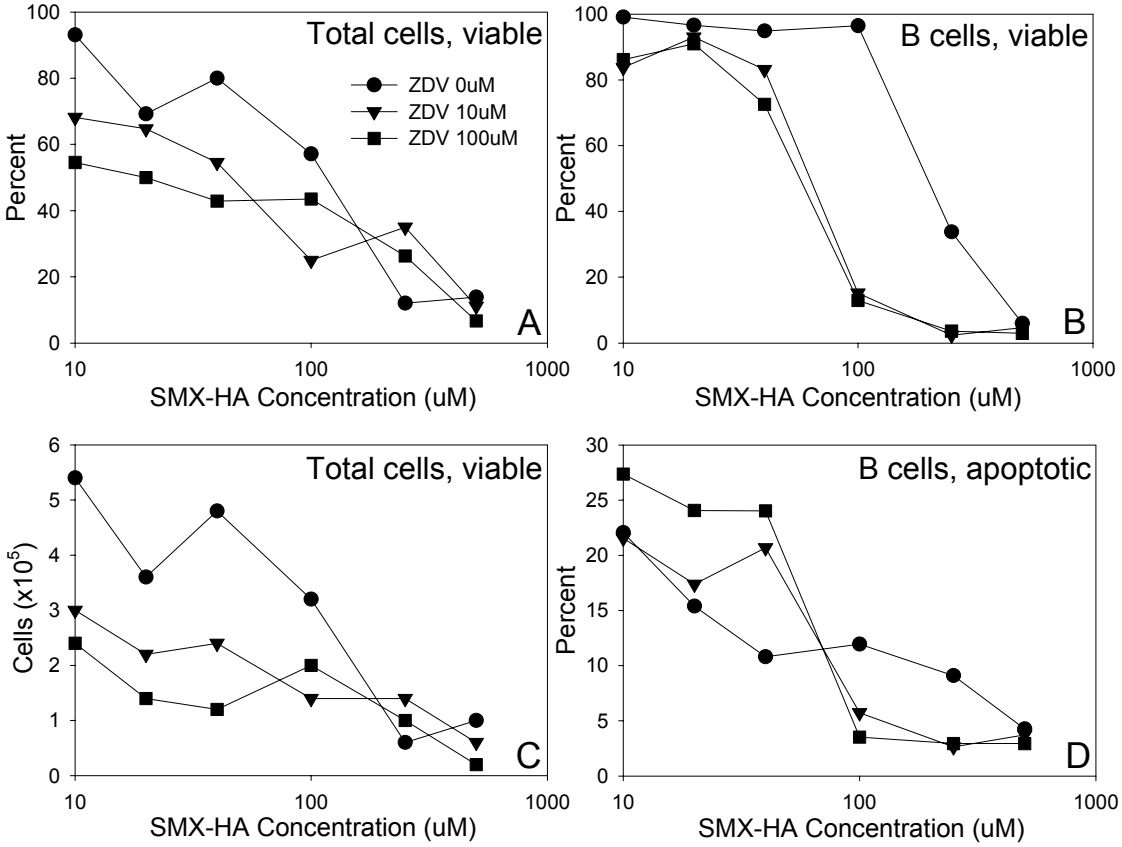

Figure 3.4 ZDV cytotoxicity with 72 hours incubation. Mouse bone marrow was isolated and cultured at $1x10^6$ cells per well in 24-well culture tissue culture plates with IL-7 at 25U/ml to stimulate B cell proliferation as detailed in Materials and Methods. ZDV at 0, 10, and 100μM concentrations was incubated with the cells for 72 hours, and SMX-HA was added to the appropriate wells at concentrations between 10 and 500μM for the final 18 hours of incubation. Cells were harvested, stained with B220, annexin-V, and PI as described, and analyzed by flow cytometry. Viability was also determined for the total cell population by trypan blue staining. Data depicts percentages of (A) total cells and (B) B cells viable after drug exposure. Panel C represents the total number of viable cells in culture, and panel D represents the percentage of B cells that were apoptotic (annexin-V positive, PI negative). Data are representative of multiple trials.

function of increasing SMX-HA concentration. The percentages of apoptotic cells fall with increasing concentrations of SMX-HA because most cells are already dead at the higher concentrations.

Cytotoxicity *in vitro* is synergistic

When culture conditions were determined to produce an induction of cytotoxicity with each drug and in combination (see above), we analyzed the data generated to assess synergy. The median-effect combination index method was used to calculate CI values. CI=1 was defined by Chou and Talalay as signifying an additive effect. CI<1 indicates synergy between 2 agents, and CI>1 indicates antagonism. CI values were calculated for dose effect levels based on levels of cell death of 25, 50, and 75%. Parameters used to calculate CI were derived from dose-response curves generated for ZDV alone, SMX-HA alone, and the combination of both drugs used at a ratio of 1:1. Cells were cultured in the presence of IL-7 at $1x10^6$ cells/ml per well as described and over incubation times for ZDV and SMX-HA of 72 hours and 24 hours, respectively. Concentrations ranged from 1 to 100μM for ZDV, and from 10 to 100μM for SMX-HA. Table 3.1 shows the IC values at the various levels of cell death, along with the

Table 3.1 Combination index values for synergy.

Agent	CI value cell death induction, $IC_{(x)}$			Parameters		
	IC_{25}	IC_{50}	IC_{75}	D_m(uM)	m	r
ZDV				61.1	0.56	0.91
SMX-HA				51.9	0.48	0.93
Combination	0.16	0.31	0.63	8.17	0.39	1.00
Interaction	synergy	synergy	synergy			

Combination index values calculated at various levels of cytotoxicity of total bone marrow cells treated with the combination of ZDV and SMX-HA. CI=1 indicates additivity, CI<1 indicates synergy, and CI>1 indicates antagonism. $IC_{(x)}$=concentration at which cell death is induced by x%. D_m=median-effect dose (IC_{50}), m=slope parameter, and r=correlation coefficient of median-effect plot. Data is representative of multiple experiments.

parameters from the median-effect plots. The cytotoxic effect of the 2 drugs in combination is synergistic to bone marrow cells *in vitro*.

Most apoptotic cells arise from the S/G2/M phases

To further explore how cell cycle affects relate to apoptosis with ZDV plus SMX-TMP exposure, we designed a series of experiments to investigate from which stages of the cell cycle cells were becoming apoptotic. Mouse bone marrow cells were either incubated for 20 hours with 1mM hydrocortisone, or with ZDV 10μM for 72 hours with SMX-HA 20μM added for the final 24 hours. These doses were chosen based upon the data presented in Figure 3.4, due to the high percentage of apoptotic cells at this dosing combination.

Cells were analyzed for apoptosis via the Tunel assay while simultaneously stained with PI. The data is displayed in Figure 3.5. Panels A and B are representative dot plots for cells exposed to hydrocortisone (A) and ZDV plus SMX-HA (B). Regions indicate cells in the G0/G1 interval of the corresponding cell cycle histograms. It is evident that the majority of cells that are apoptotic (BrdU-FITC positive) arise from the S/G2/M phases as a result of ZDV plus SMX-HA exposure (panel B). Comparatively, hydrocortisone treatment causes cells to undergo apoptosis in a cell-cycle non-specific manner, as the apoptotic cell proportions are similar to overall cell cycle proportions (panel A). Panel D shows the percentages of total cells that were in G0/G1 phases, in S phase, and the percentage of total cells that were simultaneously in S/G2/M phases and apoptotic. This data demonstrates that ZDV plus SMX-TMP exposure is causing cells to initiate the apoptotic process from these phases, and that cells are sequestered in the S phase, with a simultaneous depletion of cells reaching G0/G1. Statistically-significant differences were not reached because only 2 wells were used per experiment.

Addition of a pan-caspase inhibitor did not alter apoptosis induction

Mouse bone marrow was again cultured as above, along with ZDV at 100μM for 72 hours, with the addition of SMX-HA for the final 1 or 2 hours of incubation. The pan-caspase inhibitor Z-VAD-FMK at a concentration of 20μM was added to the appropriate

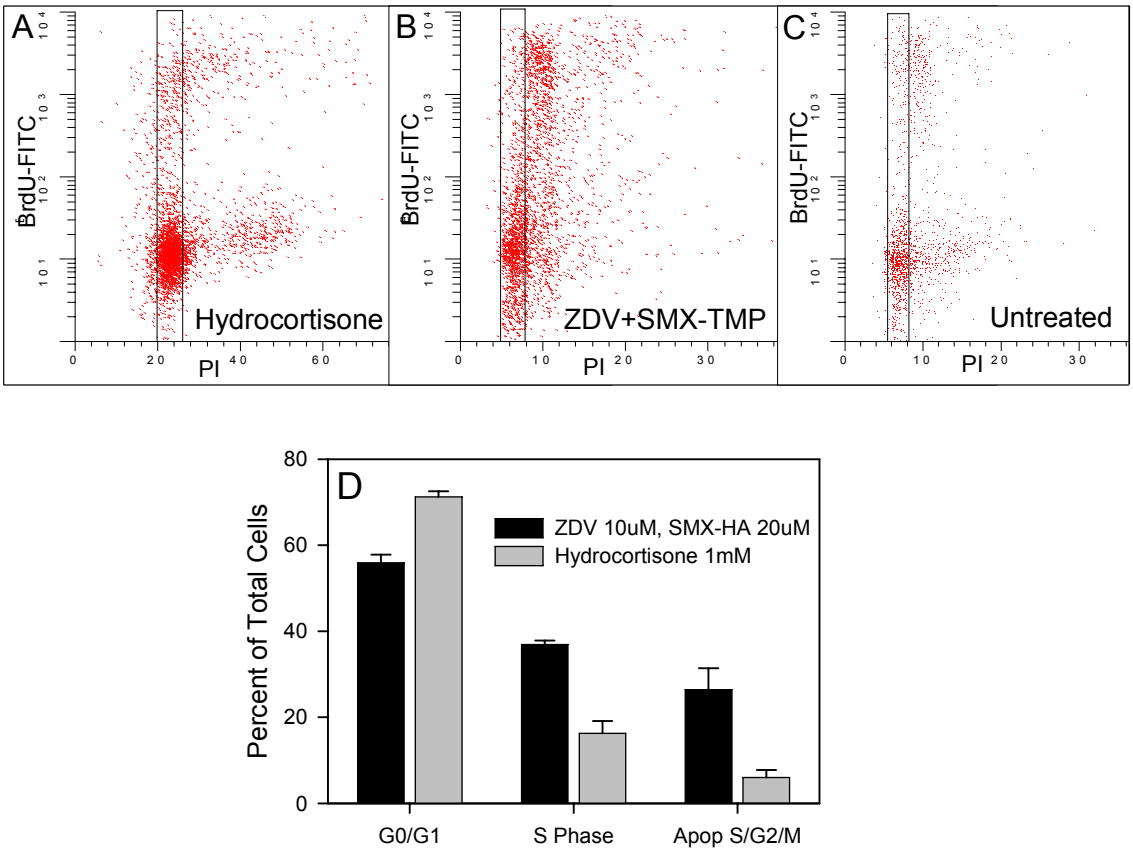

Figure 3.5 Relationship between apoptosis and cell cycle. Bone marrow cells were obtained from normal BALB/c mice and placed into culture with IL-7 at $1x10^6$ cells/ml per well as described in Materials and Methods. Cells were either incubated for 20 hours with 1mM hydrocortisone, or with ZDV 10μM for 72 hours plus SMX-HA 20μM for the final 24 hours. Cells were harvested and analyzed via the Tunel assay while simultaneously stained with PI. Panels A and B display flow cytometry output from representative dot plots for cells exposed to hydrocortisone (A) and ZDV plus SMX-HA (B). Regions indicate cells in the G0/G1 interval of the corresponding cell cycle histograms. Panel C shows the percentage of total cells that were in G0/G1 phases, in S phase, and the percentage of total cells that were concurrently in S/G2/M phases and apoptotic. Data represents mean percentages for 2 wells per group, and are representative of multiple repetitions. Differences were not statistically significant for $p < 0.05$.

wells 15 minutes before the SMX-HA. Figure 3.6 shows that as SMX-HA concentrations increase, apoptosis increases. Z-VAD-FMK did not significantly decrease this apoptotic effect at any concentration, or at either timepoint. The etoposide-exposed cells served as a positive control, showing that Z-VAD-FMK

significantly decreased percentage of apoptotic cells (annexin-V positive, PI negative) and returned it to baseline.

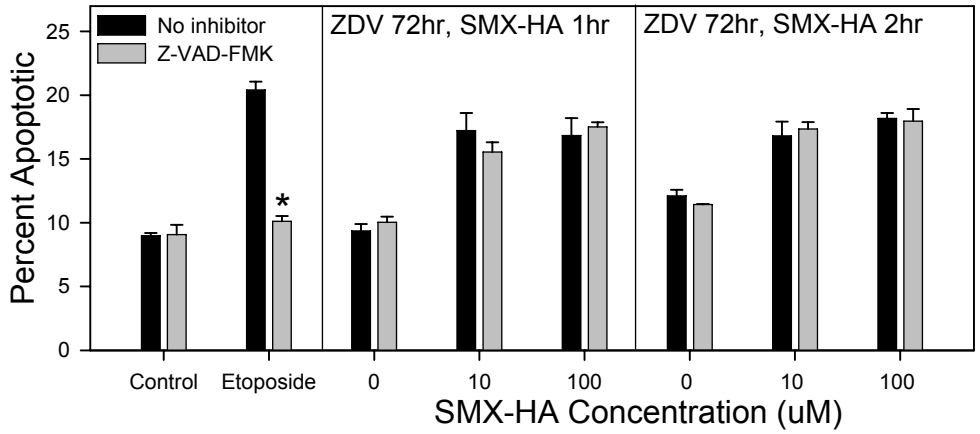

Figure 3.6 Caspase inhibition and apoptosis. Mouse bone marrow was isolated and cultured at $1x10^6$ cells per well in 24-well culture tissue culture plates with IL-7 at 25U/ml to stimulate B cell proliferation as detailed in Materials and Methods. ZDV at 100μM was incubated with the cells for 72 hours, and SMX-HA was added to the appropriate wells at 10 and 100μM concentrations for the final 1 or 2 hours of incubation, as indicated. The pan-caspase inhibitor Z-VAD-FMK at 20μM was added to half of the wells 15 minutes prior to the addition of SMX-HA. Cells were harvested and stained for apoptosis with annexin-V and PI as described, and analyzed by flow cytometry. Cells were gated on lymphocytes and the percentages apoptotic (annexin-V positive, PI negative) are reported. Etoposide 20ug/ml was used as a positive control to induce apoptosis (4 hour incubation). Each bar represents triplicate wells. A statistically-significant reduction in apoptosis (*) by the addition of Z-VAD-FMK was defined at $p < 0.05$.

mRNA of initiator and effector caspases is not up-regulated in the presence of combination drug exposure

Bone marrow isolated from normal mice was once again placed into culture as described above for 72 hours with 10μM ZDV added to 50% of the wells. For the final 8 hours, SMX-HA was added at a concentration of 10μM to the appropriate wells to generate cells that were exposed to ZDV, SMX-HA, both drugs, or neither. At the end of the incubation, cells were harvested and RNA was isolated with TRIzol Reagent. RPA was performed as described to ascertain relative message of genes encoding

signaling and effector caspases. Data comparing the mRNA expression to the housekeeping genes L32 and GAPDH are presented in Figure 3.7. Combination exposure did not increase the relative expression of any caspases tested. The cells that were exposed only to SMX-HA had moderate increases in relative message levels of caspase-8, caspase-3, and caspase-2. This experiment has not been repeated and the results should be viewed as preliminary.

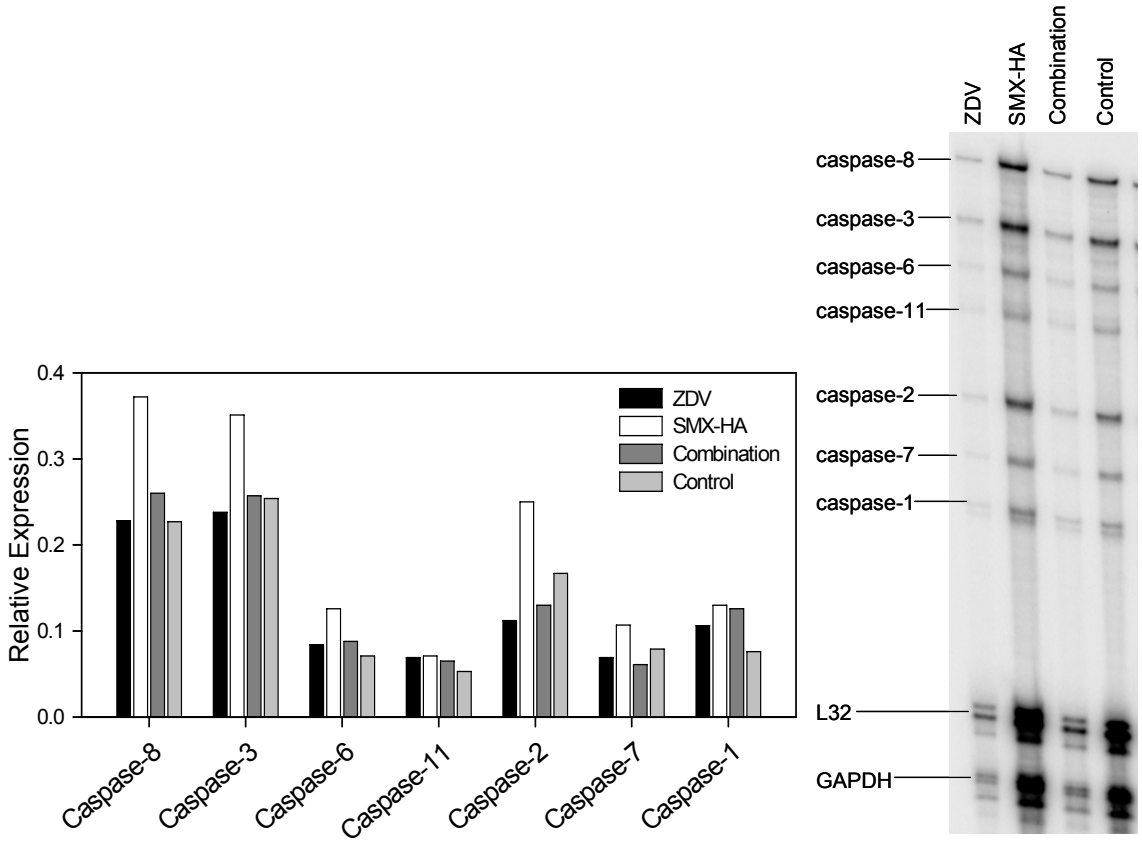

Figure 3.7 Message expression for signaling and effector caspases. Bone marrow isolated from normal mice was cultured as described for 72 hours with 10μM ZDV added to 50% of the wells. For the final 8 hours, SMX-HA was added at a concentration of 10μM to the appropriate wells to generate cells that were exposed to ZDV, SMX-HA, both drugs, or neither (control). RNA was isolated with TRIzol Reagent. RPA was performed as described using the mAPO Multiprobe template to ascertain relative expression of genes encoding caspase-8, caspase-3, caspase-6, caspase-11, caspase-2, caspase-7, and caspase-1. Expression of mRNA relative to the housekeeping genes L32 and GAPDH were plotted. Data is representative of a single experiment. received ZDV plus SMX-TMP versus mice that received only SMX-TMP.

SMX steady-state serum concentrations were increased with ZDV exposure

To investigate whether there was a systemic pharmacokinetic effect on drug disposition, SMX serum concentrations were compared between mice that

Mean SMX serum concentrations for these groups of mice are shown in Figure 3.7A. Samples are indicative of drug concentrations 18 hours after the 28th daily doses of SMX-TMP and ZDV. Mice were dosed as described in detail in Chapter 2.

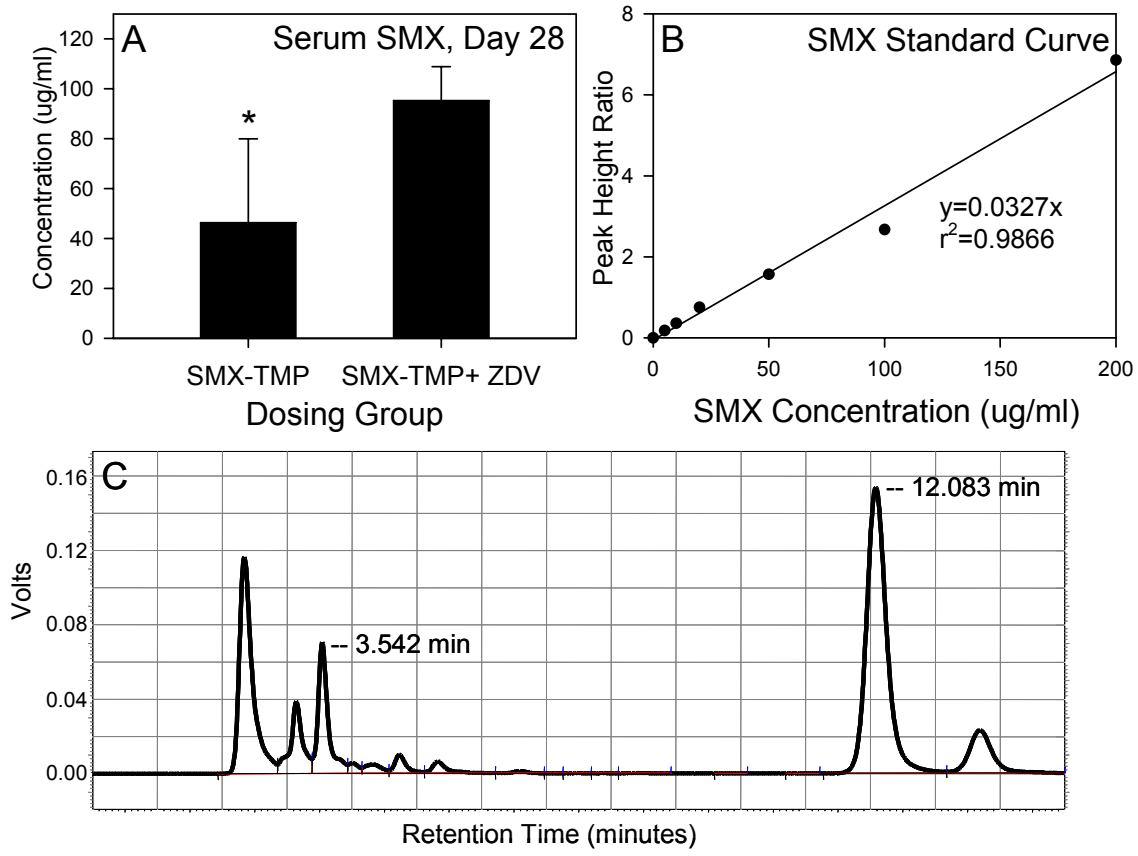

Figure 3.8 SMX serum concentrations. SMX serum concentrations increased in mice when also exposed to ZDV. Normal BALB/c mice were dosed for 28 days with SMX-TMP (840mg/kg SMX and 160mg/kg TMP) with or without ZDV (240mg/kg) daily via oral gavage. Mice were humanely killed after 28-days dosing, 18 hours after the final dose of each drug, and serum was collected. SMX concentration was determined by HPLC as detailed in Materials and Methods (panel A). Panel B shows the standard curve generated using the peak height ratio with the internal standard. Panel C is a representative chromatogram from a mouse in the SMX-TMP group, showing the internal standard peak (3.542 minute retention time) and the SMX peak (12.083 minute retention time). Significant difference to control group (*) was defined at an alpha level of < 0.05. Data represents 5 mice per treatment group, and representative of 2 separate experiments.

The mean SMX concentration in the combination treatment group was 95.4 ± 13.5 μg/ml, which was significantly higher than the mean SMX concentration in the SMX only group (46.4 ± 33.5 μg/ml). Figure 3.8B illustrates the standard concentrations curve used to calculate sample concentrations, with an r^2 value relating SMX concentration to peak height ratio of SMX to the internal standard of 0.9866. Panel C of Figure 3.8 is a representative chromatogram showing the internal standard peak (3.542 minute retention) and SMX peak (12.083 minute retention).

Mrp1$^{-/-}$ mice

One hypothesis to explain the altered disposition of SMX by ZDV concerns the up-regulation of Mrp4 by ZDV (discussed above). Because of the availability of Mrp1$^{-/-}$ mice, and because Mrp1 has the same function of GSH and GSH-substrate efflux as does Mrp4, we decided to test whether the absence of Mrp1 had any effect on SMX toxicity. Figure 3.9A represents data collected after bone marrow cells from Mrp1$^{-/-}$ and FVB/N background control mice were incubated in the presence of SMX-HA for 24 hours. Although no statistics could be performed, there was a slight decrease in the percentage of viable cells in the Mrp1$^{-/-}$ animals versus the control mice, as well as a slight increase in percentage of dead cells at each concentration combination. The percentages of apoptotic cells were virtually identical between the two strains (Figure 3.9A).

We then dosed mice of both phenotypes as described above with either the combination of ZDV and SMX-TMP, or neither drug for a period of 14 days. Figure 3.8B depicts percentages of dead B220$^+$ B cells and apoptotic B220$^+$ B cells harvested from the bone marrow of Mrp1$^{-/-}$ and background control mice. Of importance, only 2 of the 5 Mrp1$^{-/-}$ mice dosed with ZDV plus SMX-TMP survived until time of sacrifice. The percentages of dead cells (annexin-V positive, PI positive) and apoptotic cells (annexin-V positive, PI negative) in the combination treatment mice were only significantly increased in the background control mice. The Mrp1$^{-/-}$ mice show a trend toward an increase in dead and apoptotic B cell percentages, but the data is not statistically significant.

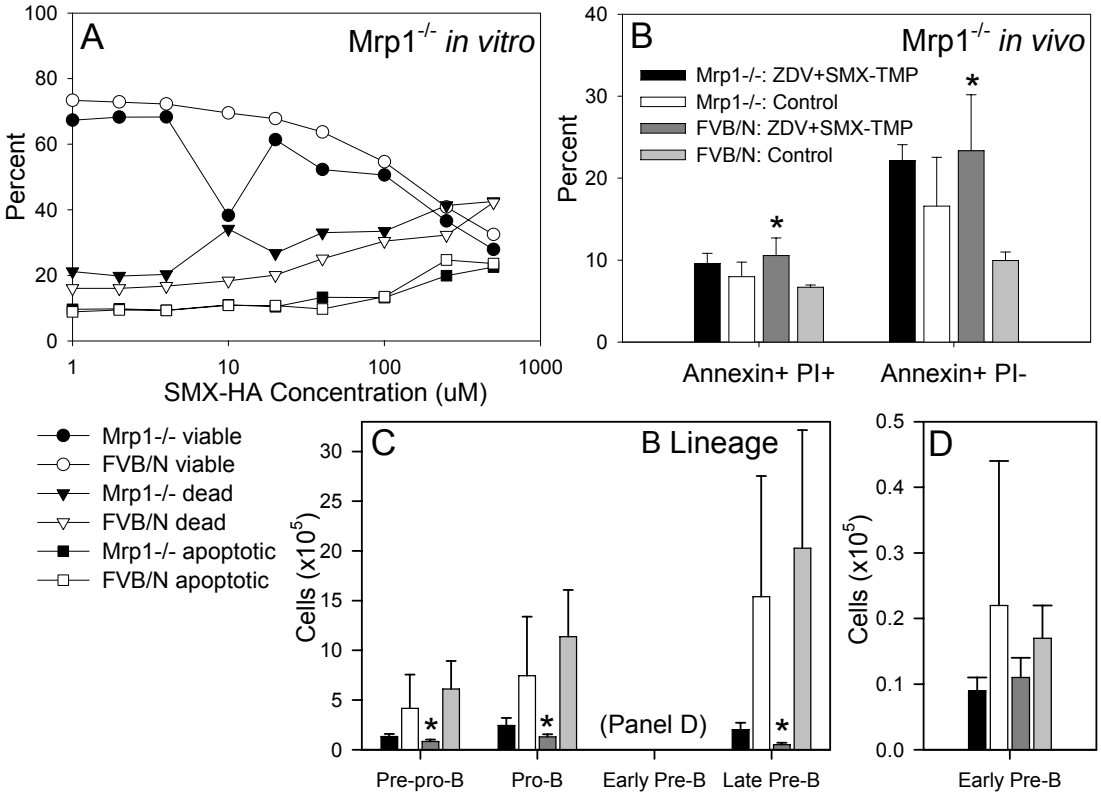

Figure 3.9 Mrp1$^{-/-}$ mice display similar toxicity as background controls. Mouse bone marrow was isolated from Mrp1$^{-/-}$ and background matched FVB/N mice as described. Cells were cultured at 1x10^6 cells per well in 24-well culture tissue culture plates with IL-7 at 25U/ml to stimulate B cell proliferation as detailed in Materials and Methods. SMX-HA was incubated with the cells for 24 hours, and cells were harvested and stained for CD19, annexin-V, and PI and analyzed for apoptosis via flow cytometry. Panel A shows percentages of bone marrow B cells that are either viable (annexin-V negative, PI negative), dead (annexin-V positive, PI positive), or apoptotic (annexin-V positive, PI negative) for each mouse strain for increasing SMX-HA concentrations. In addition, Mrp1$^{-/-}$ and FVB/N mice were dosed *in vivo* for 14 days with either ZDV plus SMX-TMP or control vehicle daily via oral gavage, and the bone marrow was harvested. Panel B shows the percentage of cells in the bone marrow that were either dead (annexin-V positive, PI positive) or apoptotic (annexin-V positive, PI negative). Panel C illustrates the numbers of B-lineage cells after 14 days of dosing discerned by flow cytometry in both mouse strains and both treatment groups, including pre-pro-B, pro-B, and late pre-B cells. The early pre-B cell subtype populations are expressed on panel D due to the smaller scale needed. Differences of statistical significance (*) from control were defined at a *p*-value of < 0.05. Data in panels B-D are mean ± SD, representative of one experiment only, with 2-5 mice per group.

Upon examination of B-lineage subtypes in the bone marrow, pre-pro-B, pro-B, and late pre-B cell numbers were similarly depleted in both mouse strains by combination drug treatment (Figure 3.9C). Differences were statistically significant in the FVB/N background control mice, but not in the Mrp1$^{-/-}$ strains, due to the fact that only 2 mice lived to the time of sacrifice in the combination therapy group of the Mrp1$^{-/-}$ mice. Early pre-B cell numbers, although depleted to a degree in the combination-treated groups in both mouse strains, did not reach statistically-significant differences (Figure 3.9D). These results should be considered preliminary since these *in vivo* experiments have not been repeated.

D. CONCLUSIONS

While this chapter contains much data that is preliminary in nature, many aspects of the combination toxicity concerning ZDV and SMX-TMP have been addressed. These data have laid a foundation for further investigation into the mechanism of this toxicity.

ZDV and SMX metabolites both cause concentration-dependent toxicity to IL-7 dependent B cell populations in our *in vitro* model. We confirmed the fact that SMX-HA is more toxic than SMX-NO here in B cells, as has been shown in the literature to be the case in lymphocytes and neutrophils (152). We were unable to demonstrate contributions of ZDV to the toxicity with 24 hours exposure; its effects were contributory only when exposure time was extended to 72 hours. Synergy was then demonstrated at doses ranging from IC_{25} to IC_{75}. Future work to determine synergy *in vivo* would be contributory to this study. The steady-state concentrations obtained for SMX in patients also receiving ZDV increased to over the IC_{50} of SMX from the *in vitro* data. The significance of this is yet to be determined.

It is known that the toxicity of the oxidative metabolites of SMX can be diminished by the presence of reducing agents, such as GSH. Here, we have shown that the combination toxicity is also decreased by the presence of 2-ME in the culture medium. When it was removed, cell viability was much lower as a result of drug exposure at

corresponding concentrations of ZDV and SMX metabolites. The removal of 2-ME is expected to lower the baseline viability rate in any culture system.

Apoptosis is also confirmed in this chapter by a second method of measurement, the Tunel assay. Figure 3.5 demonstrates that cells are selectively entering the apoptotic state from the S/G2/M phases of the cell cycle. This confirms the data from our *in vivo* trials indicating that cells are being sequestered in these proliferative phases in the early pre-B cell population. The evidence that cells are entering apoptosis from selected phases strengthens the argument that this is a cell-cycle specific effect.

Apoptosis can be caused by the presence or absence of a variety of stimuli, but most often the intracellular signaling pathways utilize caspases to carry out the apoptotic process. Whether the initiation is mediated through death receptors on the cell surface, or through the mitochondrial pathways, several caspases are activated to signal an apoptotic death. It appears that B cells in our culture system are undergoing a caspase-independent apoptosis as a result of ZDV plus SMX-HA treatment. Refer to Chapter 6 for an in-depth discussion.

The addition of the pan-caspase inhibitor Z-VAD-FMK did not diminish the percentage of cells in the apoptotic phase as a result of combination drug exposure. This is shown in Figure 3.6 for cells incubated with ZDV 100μM for 72 hours and SMX-HA at 10 and 100μM for the final 1 or 2 hours. This short incubation was the optimal time to test, as apoptosis occurs quickly upon SMX-HA exposure when cells have been in the presence of ZDV for an extended period. Of note, the aldehyde-based caspase-3 inhibitor Ac-Asp-Met-Gln-Asp-CHO (Ac-DMQD-CHO) was also used in many experiments in an attempt to inhibit apoptosis as a result of drug exposure. Although it was never effective in diminishing the apoptotic effect, an appropriate positive control was never established, so the data was not presented.

This caspase-independent mechanism of apoptosis is also supported by the RPA data presented in Figure 3.7. Combination drug exposure did not alter the relative message levels of any caspases tested. Although message was slightly increased in the SMX-HA exposure group of caspases 8, 3, and 2, we cannot draw any conclusions from this data, because of a lack of confirmatory trials. See Chapter 1 for a detailed discussion of apoptosis.

The steady-state SMX concentration in the serum is increased in mice receiving concurrent ZDV treatment. The 28-day data shown in Figure 3.8 was also confirmed by data generated after 21 days of dosing. This is a significant piece of information with regards to the mechanism of combined toxicity. This is a foundation for further study. The SMX concentration was increased from approximately 50µg/ml to 100µg/ml. This corresponds to a molar increase from approximately 200µM to a level of 400µM. When comparing these ranges to our *in vitro* studies, this increase is within the concentration range tested, that showed a dose-dependent increase in toxicity. However, both concentrations are in the range in which toxicity was at its maximum. How this corresponds to concentrations obtained in the bone marrow is unknown.

If GSH efflux is involved in this drug-drug interaction, the *in vitro* data obtained using $Mrp1^{-/-}$ mice support the hypothesis that ZDV competitively inhibits the transport of SMX-HA-GSH complexes, thereby increasing the SMX-HA concentrations inside the cells. This would increase the sensitivity of bone marrow cells from the $Mrp1^{-/-}$ mice, which was seen slightly in Figure 3.9A. While there is a slight increase in toxicity *in vitro*, the *in vivo* dosing data in Figure 3.9 shows that the absence of Mrp1 may be protective. This, despite the fact that 3 of the 5 $Mrp1^{-/-}$ mice dosed with ZDV plus SMX-TMP died. The cause of death in the mice that died is unknown. These results do not take into account other mechanisms of GSH and GSH-substrate efflux that could be compensating for the lack of transport from Mrp1. Clearly, further study is needed to determine the role of Mrp transporters in this context.

Because we find the toxicity of this combination to be concentration (or dose) - dependent, this data raises the concern of the potential clinical significance of this interaction. It is difficult to determine allometrically the proper dose to give to mice to mimic human drug exposure, especially to generate comparable exposure to sites that have unknown drug concentrations, such as the bone marrow. The next step taken was to investigate the effect of combination drug exposure on the immune response in mice challenged with an infectious agent, which will be presented in Chapter 4.

CHAPTER 4: Impact on host response

A. OVERVIEW

The previous chapters demonstrate that ZDV plus SMX-TMP exposure decreases immune cell populations in the bone marrow of normal mice due to apoptosis induction. Our next goal was to investigate whether the effects of this drug toxicity have an impact on host response. To determine this, BALB/c mice were exposed to each drug separately or in combination as described. On day 4 after dosing completion, mice were infected intratracheally with *Pneumocystis murina*. This infection model was utilized to investigate cellular and humoral immune responses in these mice as a result of combination drug exposure.

PCP continues to be one of the most common AIDS defining illnesses (212, 213). The Centers for Disease Control and Prevention recommend clinicians to prophylax for PCP when HIV-infected individuals have $CD4^+$ T lymphocyte counts of less than 200 cells/μl (214). The drug of choice for the prophylaxis and treatment of this fungal infection is SMX-TMP, which has been shown to improve survival rates among patients with HIV (214). SMX and TMP are used in combination to potentiate their inhibition of folate synthesis and increase activity against *Pneumocystis*, as well as many susceptible bacteria.

Components of adaptive immune function that are necessary in the clearance of *Pneumocystis murina* from mice have been thoroughly studied. Mice that lack functional $CD4^+$ T cells have an inability to mount an effective response to *Pneumocystis* (215, 216). In addition, mice that lack functional B lymphocytes have been shown to also be highly susceptible to *Pneumocystis* infection (217-219). Because B cells are depleted from the bone marrow of mice that receive ZDV and SMX-TMP, we used this infection model to assess the impact of drug toxicity upon host response to an opportunistic pathogen.

Our hypothesis was that exposure to ZDV plus SMX-TMP would alter the humoral immune response to pulmonary *Pneumocystis* infection in normal mice, and the

clearance of *Pneumocystis* would be delayed. The aims of this chapter were 1) to evaluate the cellular host response to *Pneumocystis* in the lungs and draining lymph nodes, 2) to compare *Pneumocystis*-specific antibody responses between groups, and 3) to evaluate *Pneumocystis* clearance profiles among drug dosing groups. An additional aim in this series of experiments was to characterize the recovery of B-lineage populations in the bone marrow after drug discontinuation.

Immune cell populations (in lung digest and bronchial alveolar lavage fluid (BALF), and tracheobronchial lymph nodes (TBLN)), lung *Pneumocystis* burden, and serum *Pneumocystis*-specific antibody titers were determined at post-infection timepoints. The result of combination drug exposure was primarily manifested in the B cell response in the TBLN, resulting in a lower *Pneumocystis*-specific antibody titer in the serum. The overall effect did not significantly change *Pneumocystis* clearance, although there was a trend of a delayed clearance in the combination treated animals.

B. MATERIALS AND METHODS

Mice and experimental design

Four- to six-week old BALB/c mice were obtained from NCI (Indianapolis, IN) and quarantined for at least 7 days before manipulation. C.B-17 severe combined immunodeficient mice (SCID), originally from Taconic (Germantown, NY), were bred in our facility and used to maintain a source of *Pneumocystis*. Mice were housed in the Veterans Administration Veterinary Medical Unit under pathogen free conditions with a 12 hour light/dark photocycle and food and water both freely available. All experiments and procedures were approved by the Veterans Administration Institutional Animal Care and Use Committee.

ZDV (3'-azido-3-deoxythymidine), TMP (2,4-diamino-5-[3,4,5-trimethoxy-benzyl]pyrimidine), SMX (4-amino-N-[5-methyl-3-isoxazolyl]benzenesulfonamide) were purchased from Sigma-Aldrich (St. Louis, MO). Drug doses were prepared daily by weighing each powder form into polypropylene tubes, SMX and TMP together, and ZDV separately, and suspending each in its appropriate vehicle: ZDV dissolved into sterile-

filtered deionized water to a concentration of 50mg/ml, SMX and TMP suspended in 0.5% methylcellulose at concentrations of 106mg/ml and 8mg/ml, respectively. Mice were randomized into four treatment groups, either receiving ZDV or SMX-TMP alone, in combination, or vehicle only (control), at the following doses based on an approximate mean mouse weight of 20 grams: ZDV 240mg/kg (5mg per mouse), SMX 840mg/kg (16mg per mouse), and TMP 160mg/kg (1.2mg per mouse). Each mouse received two doses daily, either with drug or vehicle. Doses were given via oral gavage with an 18-gauge blunt-tipped dosing needle.

Pneumocystis infection

Lungs from *Pneumocystis*-infected immunodeficient mice were excised and pushed through steel mesh in Hank's Balanced Salt Solution (HBSS). Aliquots were spun onto glass slides, fixed in methanol, and stained with Diff-Quik (Dade Behring Incorporated, Newark, DE). *Pneumocystis* was enumerated microscopically as described below (215, 220, 221). Mice were infected intratracheally under halothane anesthesia with 10^7 *Pneumocystis* organisms 4 days after discontinuation of drug dosing. Mice were then humanely killed at various timepoints post-infection for analysis.

Tissue processing and *Pneumocystis* enumeration

Lungs were lavaged by tracheal cannulation under deep halothane anesthesia with 5 washes performed with 1ml HBSS containing 3mM ethylenediaminetetraacetic acid (EDTA). Lungs were minced and digested by incubation with 50 U/ml DNase and 1mg/ml collagenase A and pushed through mesh to form single cell suspensions. TBLN were excised into HBSS and pushed through mesh to create single cell suspensions. Bone marrow was flushed from femurs and tibias into RPMI-1640 plus 5% fetal calf serum, and single cell suspensions were obtained via passage through a 25-gauge needle. Red blood cells in all samples were lysed with hypotonic buffer consisting of 8.24g/l ammonium chloride, 1g/l potassium bicarbonate, and 37.2mg/l EDTA. Cells were then washed, enumerated, and transferred into 5ml round-bottom polystyrene tubes for phenotyping via flow cytometry. Lung digest aliquots were diluted to 1:20 and 100μl was spun into a 28.3 mm^2 area on glass slides using a cytocentrifuge,

then fixed with methanol and stained with Diff-Quick staining solutions. *Pneumocystis* nuclei were enumerated microscopically by counting the number of nuclei per 20-50 oil emersion fields. This number was used to calculate the total number of nuclei per lung (215, 220, 221). Slides from the mice were counted in a randomized, blinded fashion. The limit of detection of Pneumocystis was $\log_{10}$ 3.23.

Cell phenotyping

Splenocytes, BALF cells, and lung digest cells were incubated with the appropriate concentrations of fluorescently-labeled monoclonal antibodies (mAb) specific to murine T cells (CD4, CD8, CD44, and CD62L) and B cells (CD19, CD80 and CD86). Activated $CD4^+$ and $CD8^+$ T cells were defined as the $CD44^{hi}/CD62L^{lo}$ phenotype, and B cells were considered activated if either CD80 or CD86 was up-regulated. Bone marrow cells were incubated with 2 separate panels of fluorescently-labeled mAb for phenotyping B lineage cells. Antibodies were purchased from BD Biosciences Pharmingen, San Diego, CA or eBiosciences San Diego, CA. These panels were 1) IgM, CD43, and B220; and 2) CD43, B220, BP-1, and heat stable antigen (HSA). Subpopulations delineated included pre-pro-B, pro-B, early pre-B, and late pre-B cells according to B lineage subgroups as described by Hardy et. al. (178). Cells were washed before and after staining with Dulbecco's Phosphate Buffered Saline containing 0.1% bovine serum albumin and 0.02% sodium azide. All cells were analyzed for phenotype by flow cytometric multiparameter analysis using a FACSCaliber Flow Cytometer (BD Biosciences, Mountain View, CA) and analyzed using WinList software package (Verity Software House, Topsham, ME). Greater than 50 thousand events were routinely examined.

Apoptosis analysis

Cells were determined to be in the process of an apoptotic cell death by using the annexin-V binding protocol with propidium iodide (PI) exclusion kit according to the manufacturers instructions (BD Biosciences Pharmingen). Samples were analyzed by flow cytometry as above, and cells that fluoresced annexin-V positive/PI negative were considered apoptotic.

Pneumocystis-specific enzyme linked immunosorbent assay (ELISA)

Specific antibodies to *Pneumocystis* antigens were measured in the serum of mice at each timepoint as previously described (221). Blood was collected from the abdominal aorta, and sera were isolated by centrifugation and frozen at -80^{0}C until time of analysis. 96-well microtiter plates were coated with sonicated *Pneumocystis* (10µg/ml) for 2 hours, and coated plates were blocked with 5% dry milk in HBSS supplemented with 0.05% Tween 20 for 1 hour. Test sera were diluted serially from 1:50 to 1:1600 and incubated in the plates overnight at 4^{0}C. Plates were extensively washed, and bound antibodies were detected by using anti-IgG and anti-IgM secondary antibodies conjugated to alkaline phosphatase. After 4 hours at 37^{0}C, plates were washed and developed by using p-nitrophenylphosphate (1 mg/ml) in diethanolamine buffer and read at 405nm. The endpoint dilutions at which the optical density at 405nm dropped below 0.1 are reported.

Statistical analysis

All cell numbers, *Pneumocystis* counts, and antibody titers in the drug exposure groups were compared to the control group using one-way ANOVA followed by the Student-Neuman-Keul test for ad hoc pair-wise comparisons using commercially available software (Sigmastat, SPSS, Chicago, IL). Data that failed normality testing was compared using the Kruskal-Wallis One Way Analysis of Variance on Ranks method. Results were determined to be statistically significant when a p-value < 0.05 was obtained. Data are expressed as the mean ± standard deviation.

C. RESULTS

Combination dosing increased sensitivity to *Pneumocystis* inoculation

Day to day subjective observation of the mice showed an increase in lethargy, failure to groom, hunched appearance, and an overall decrease in health in the ZDV plus SMX-TMP group as compared to the other groups, becoming marked by approximately

day 7 of dosing. During all infection experiments conducted, six out of a total of 24 mice in the combination treatment groups died after being infected with *Pneumocystis*. The median time to death was 4 days, with a range of 1 to 7 days post-infection. Out of all infection experiments completed, one of 24 mice in the control group died (1 day after inoculation), whereas all mice dosed in the single drug groups survived until time of sacrifice. Only mice that survived to the scheduled timepoints were included in the analyses.

B cell recovery in the bone marrow was delayed after drug discontinuation

We demonstrated in previous chapters that ZDV plus SMX-TMP ablates B lineage cell populations in the bone marrow. To determine whether discontinuation of the drugs would result in recovery of bone marrow B cells, we examined total cellularity and total B cells at 10, 14, and 24 days post-dosing. Total bone marrow cellularity had recovered to control levels by day 10 post-dosing (Figure 4.1). The group of mice that received only ZDV had a mean bone marrow cellularity that was significantly higher than that of the control mice. Despite *total* bone marrow numbers being normal in the combination group, we found that B lymphocytes were still significantly lower at this first timepoint

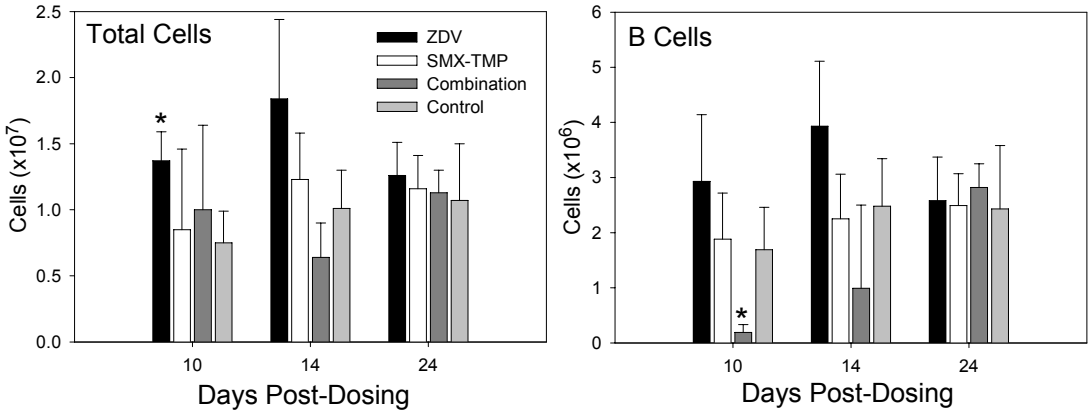

Figure 4.1 Total and B cell population recovery after dosing discontinuation. Mice were dosed with ZDV, SMX-TMP, ZDV plus SMX-TMP, or vehicle only for 21 days. Bone marrow was harvested from the femurs of mice at various timepoints after dosing was terminated. Cells were enumerated by counting, and the number of B lymphocytes was determined by staining cells with fluorescently-labeled antibody specific for B220 assessed by flow cytometry. Data represent the mean ± SD of 4 mice per group and are representative of multiple repetitions. *, $P < 0.05$ compared to vehicle only control.

(Figure 4.1). To determine which B lineage cell types were affected to the highest degree, we enumerated each of the B lineage subtypes present at each timepoint (Figure 4.2). Cell types presented in Figure 4.2A through 4.2D correspond to their order of maturity, with the number of cells recovered at each post-infection timepoint shown. Pro-B cells ($B220^{+}/CD43^{+}/HSA^{low}$) were significantly depleted at day 10 post-exposure (Figure 4.2B). Late pre-B cells ($B220^{+}/CD43^{-}/IgM^{-}$) were affected to the largest degree, with an 83% reduction in number compared to the control animals (Figure 4.2D). Day

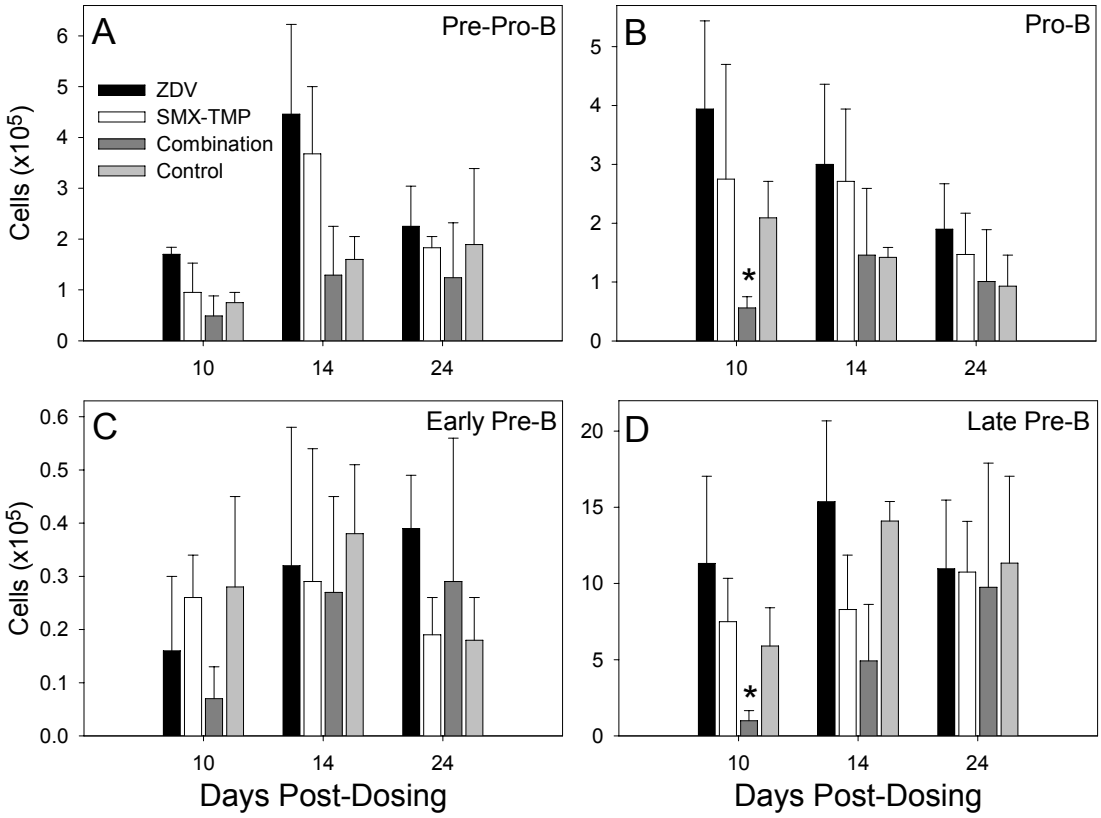

Figure 4.2 B lineage subtypes recovery after exposure termination. Mice were dosed with ZDV, SMX-TMP, ZDV plus SMX-TMP, or vehicle only for 21 days. Bone marrow was harvested from the femurs of mice at various timepoints after dosing was terminated. Cells were fluorescently stained to delineate B lymphocyte precursors and absolute number of each were determined by flow cytometry including, in their order of maturation: pre-pro-B ($B220^{+}/CD43^{+}/BP\text{-}1^{-}/HSA^{-}$), pro-B ($B220^{+}/CD43^{+}/HSA^{low}$), early pre-B ($B220^{+}/CD43^{+}/BP\text{-}1^{+}/HSA^{+}$), and late pre-B cell ($B220^{+}/CD43^{-}/IgM^{-}$) subtypes in panels A through D, respectively. Data represent the mean ± SD of 4 mice per group and are representative of multiple repetitions. *, $P < 0.05$ compared to vehicle only control.

14 data demonstrated a partial recovery in these B lineage cell types, as statistically-significant differences were no longer observed, and by day 24 the B lymphocyte populations in the bone marrow of combination treatment animals had made a full recovery.

The cellular response to *Pneumocystis* was affected by the drug combination primarily in the lung-draining lymph nodes

To assess the adaptive cellular response to *Pneumocystis* challenge during reconstitution of bone marrow B lineage cells, cell phenotypes were analyzed in the lung digest, BALF, and TBLN over time after infection. Lung lavage $CD4^+$ and $CD8^+$ T lymphocyte and lung digest $CD19^+$ B lymphocyte populations are shown in Figure 4.3. No statistically-significant differences were observed at any timepoint in the T cell populations in the BALF (Figure 4.3A-B) as a result of single drug or combination drug exposure as compared to control animals. The numbers of alveolar infiltrating T cells that displayed an activated phenotype ($CD44^{hi}/CD62L^{lo}$) likewise were not different among the treatment groups compared to control mice (Figure 4.3D-E). Pulmonary $CD19^+$ B cell and activated B cell ($CD80^+$ and/or $CD86^+$) numbers were similar among the groups at days 10 and 20 post-infection (Figure 4.3C and 4.3F). At day 6 post-infection however, total and activated B cells were significantly lower in the single drug treatment groups versus the control group, but this was not the case for the combination treatment animals. These differences were due to a wide range of total cell counts in the lung digests at day 6 post-infection, and not because of differences in percentage of these cell types.

TBLN $CD4^+$, $CD8^+$, and $CD19^+$ cell populations were significantly reduced at days 10 and 20 post-infection in the mice that received both ZDV and SMX-TMP compared to control mice (Figure 4.4A-C). Activated $CD4^+$ T cells were fewer at day 10 post-infection in the combination group, but the difference at day 20 post-infection did not reach statistical significance (Figure 4.4D). Activated $CD19^+$ B cells did not increase in response to the infectious stimulus on days 10 and 20 post-infection as they did in the

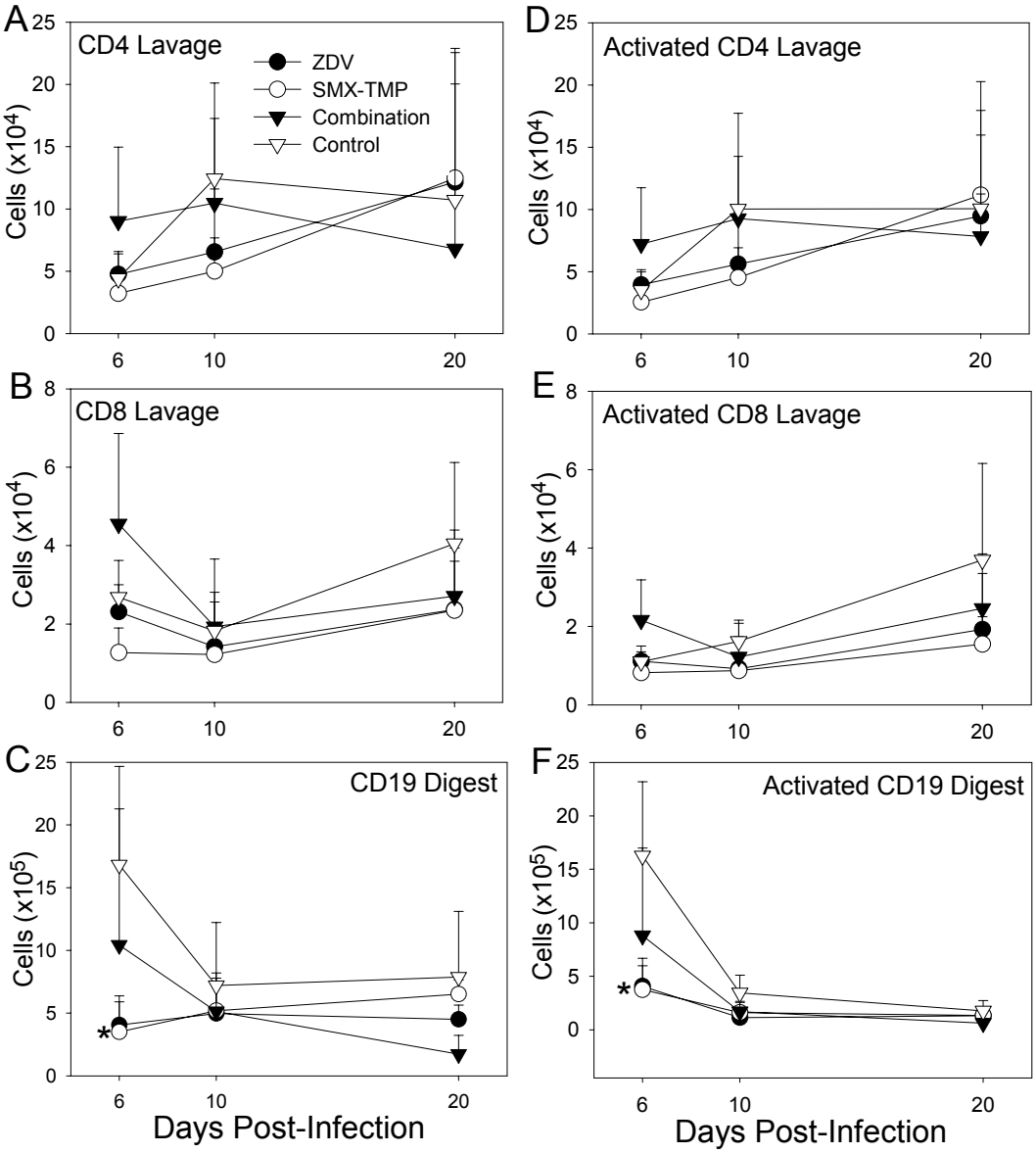

Figure 4.3 Lung digest and BALF immune cell populations. Mice were dosed with ZDV, SMX-TMP, ZDV plus SMX-TMP, or vehicle only for 21 days. After 4 days of rest to allow the drugs to clear, mice were intratracheally inoculated with $1x10^7$ *Pneumocystis* organisms isolated from a SCID colony of infected animals as detailed in Materials and Methods. $CD4^+$, $CD8^+$ T cells, and their activated phenotype ($CD44^{hi}/CD62^{lo}$), along with $CD19^+$ B cells and their activated phenotype ($CD80^+$ and/or $CD86^+$) were enumerated by flow cytometry in the BALF (T cells) and lung digest (B d with highl^y acti^{v}e antiretr^{o}viral therapy</title><secondary-title>Aids</secondary-title></titles><periodical><full-title>Aids</full-title></periodical><pages>F217-2 time in panels D through F. Data represent the mean ± SD of 4 mice per timepoint per group and are representative of 3 separate experiments. *, $p < 0.05$ as compared to the vehicle only control group.

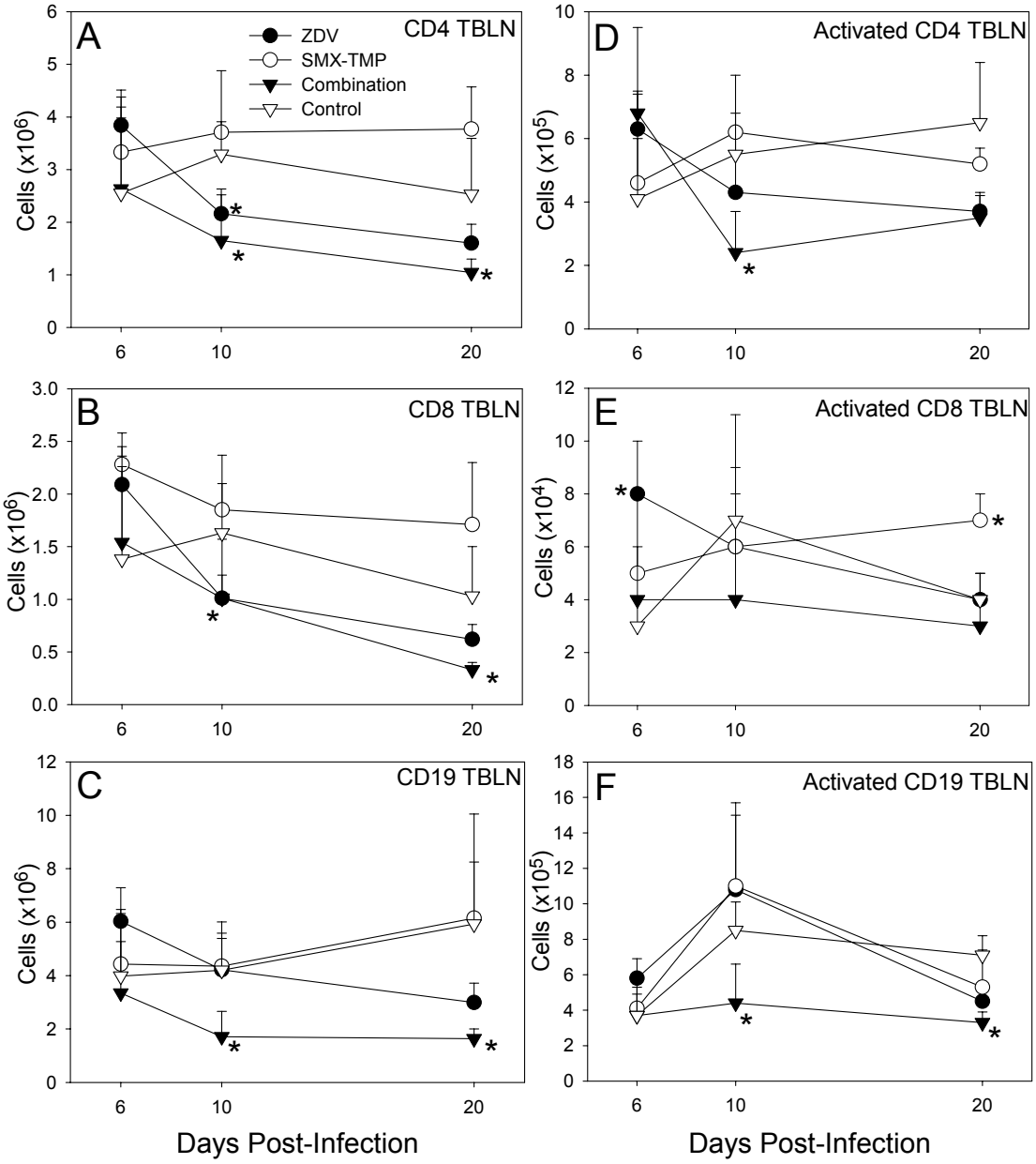

Figure 4.4 T and B cells populations in TBLN. Mice were dosed with ZDV, SMX-TMP, ZDV + SMX-TMP, or vehicle only for 21 days. After 4 days of rest to allow the drugs to clear, mice were intratracheally inoculated with $1x10^7$ *Pneumocystis* organisms isolated from a SCID colony of infected animals as detailed in Materials and Methods. $CD4^+$ T cells, $CD8^+$ T cells, $CD19^+$ B cells, and their activated phenotypes ($CD44^{hi}/CD62^{lo}$ T cells and $CD80^+$ and/or $CD86^+$ B cells) were enumerated by flow cytometry in the TBLN of mice at post-infection timepoints. $CD4^+$, $CD8^+$, and $CD19^+$ cell counts were plotted over time in panels A, B, and C, respectively. The activated phenotypes were plotted over time post-infection in panels D, E, and F. Data represent the mean ± SD of 4 mice per timepoint per group and are representative of 3 separate experiments. *, $p < 0.05$ as compared to the vehicle only control group.

other groups (Figure 4.4F). Interestingly, the mice that received only ZDV had a significantly elevated activated $CD8^+$ cell number in the TBLN at day 6 post-infection compared to control mice, and mice receiving only SMX-TMP had an increased number of activated $CD8^+$ cells at the day 20 post-infection timepoint (Figure 4.4E).

Pneumocystis clearance kinetics corresponded to decreased specific IgG titers in drug combination-treated mice

Serum *Pneumocystis* antigen-specific IgG and IgM concentrations were measured by semi-quantitative ELISA to evaluate the humoral response to pulmonary infectious challenge after dosing with ZDV plus SMX-TMP. Figure 4.5A shows that a significantly

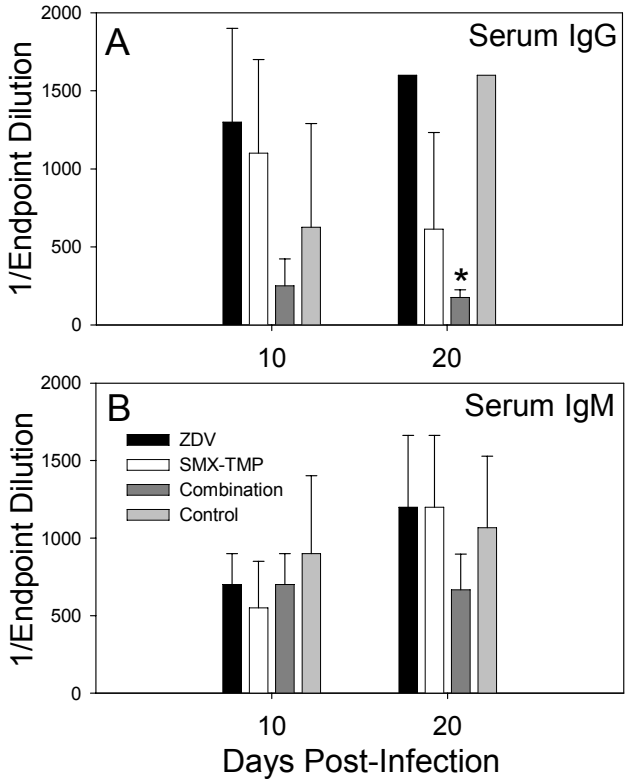

Figure 4.5 *Pneomocystis*-specific serum IgG and IgM titers. Mice were dosed with ZDV, SMX-TMP, ZDV + SMX-TMP, or vehicle only (controls) for 21 days. After 4 days of rest to allow the drugs to clear, all mice were intratracheally inoculated with $1x10^7$ *Pneumocystis* organisms isolated from a SCID colony of infected animals as detailed in Materials and Methods. At days 6, 10, and 20 post-infection PC-specific IgG (panel A) and IgM (panel B) endpoint dilution titers were determined by ELISA, with data from days 10 and 20 post-infection shown. Data represent mean ± SD reciprocal endpoint dilution for 4 mice per timepoint per group. *, $p < 0.05$ as compared to the control group.

lower *Pneumocystis*-specific IgG endpoint titer was seen in the mice that received combination exposure compared to infected control mice at day 20. Additionally, there was a trend toward a significant decrease at day 10 post-infection. Despite these decreases in IgG, the IgM titers were not significantly affected by combination treatment as compared to the single drug treatment and control animal groups (Figure 4.5B).

Decreased specific antibody levels corresponded to a trend toward a higher lung *Pneumocystis* burden on day 20 post-infection (p=0.080). Although there was no statistically significant differences in *Pneumocystis* nuclei present in the lung digest of the combination treatment animals compared to controls at any timepoint (Figure 4.6), the data at day 20 reflected a mean *Pneumocystis* burden that actually increased from that of day 10 in the combination treated mice, whereas the *Pneumocystis* counts continued to decline in each of the other groups. The group exposed to only SMX-TMP had a lung burden significantly lower than the combination treatment group (Figure 4.6).

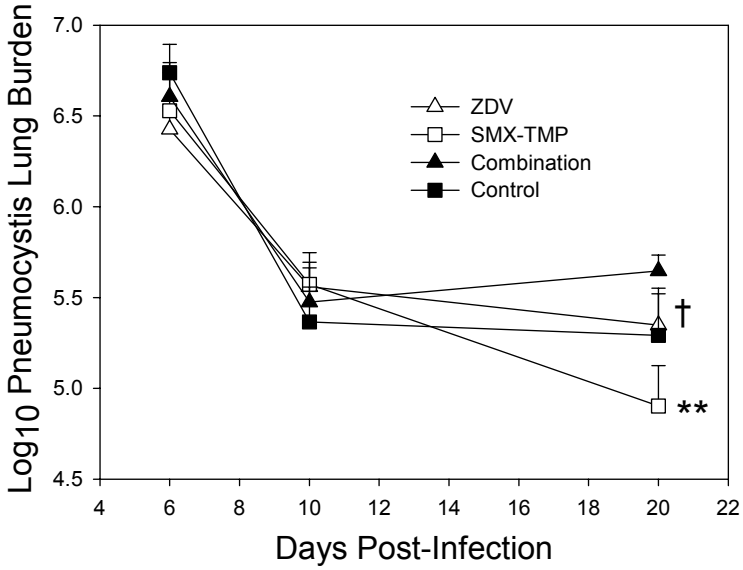

Figure 4.6 Lung *Pneumocystis* burden. Mice were dosed with each drug for 14 days as described in Materials and Methods and inoculated after 4 days of rest with $1x10^7$ *Pneumocystis* organisms intratracheally. Lung burdens of PC were then determined microscopically at days 6 through 20 post-infection. Data represent the mean ± SD *Pneumocystis* organisms per lung of 4 mice per group per timepoint. †, p = 0.08 for the combination treatment group compared to the control animals. **, $p < 0.05$ for the SMX-TMP group compared to the combination treatment group.

D. CONCLUSIONS

In this chapter we have shown that the toxicity caused by combination exposure to ZDV and SMX-TMP impacts the ability of mice to fully respond to an infectious challenge. We have demonstrated that mice treated with ZDV plus SMX-TMP prior to *Pneumocystis* infection exhibits diminished B and T lymphocyte activation in the draining lymph nodes of the lungs in response to this organism. The numbers of infiltrating lymphocytes into the site of infection were not altered to a significant degree as a result of combination drug exposure. However, clearance of pulmonary infection with *Pneumocystis* in normal mice requires the use of a combination of cellular and humoral components of adaptive immunity, therefore we additionally examined TBLN lymphocyte populations, as well as antibody response (for a review, see Chapter 6).

TBLN populations of $CD19^+$ B cells, as well as $CD4^+$ and $CD8^+$ T cells, were fewer in number after the response to *Pneumocystis* as compared to control mice at days 10 and 20 post-infection. B cells are responsible for differentiating into plasma cells that will secrete antibody against antigens associated with invading organisms. As a result of decreased cell numbers in the draining lymph nodes, *Pneumocystis*-specific serum IgG titers were significantly lower in mice that were exposed to the combination of ZDV and SMX-TMP. Previous characterization of this combination toxicity (by our group and others) revealed that peripheral T cell numbers in the spleen were unaffected (1). Here, in the context of infection, total and activated $CD4^+$ T cell frequencies were lower in the TBLN of the combination treatment animals. This could be a direct effect of the drugs, or a secondary effect stemming from the B cell depletion, which will be discussed thoroughly in Chapter 6.

Although statistical significance was not reached, the clearance of *Pneumocystis* appears to have stalled in the mice exposed to both ZDV and SMX-TMP. It would be informative to extend this experiment to examine timepoints greater than 20 days post-infection. It is unknown why the SMX-TMP only group of mice had an enhanced *Pneumocystis* clearance, as the 4 day rest period should have been ample time to clear the drugs from these mice. There was a difference in *Pneumocystis* clearance between the SMX-TMP only group, and the group that received both SMX-TMP and ZDV. Any

enhanced clearance of the organism that occurred in the SMX-TMP only group was ablated by the concurrent ZDV exposure.

Mice in the combination treatment group had a higher rate of mortality than mice from the other treatment groups. Although the cause of death of these mice is unknown, it is likely that they died as a result of the stress associated with pulmonary inoculation, and not from *Pneumocystis* infection. Time to death was 1-3 days from inoculation, and it would take much longer for an infection to develop from this slow-growing organism. ZDV plus SMX-TMP exposure seems to render the mice vulnerable to this stressor, perhaps due to an increased inflammatory response. More work is needed to determine the reason for this increase mortality rate.

Overall bone marrow cellularity was restored by day 10 post-exposure, with all subpopulations restored except for B lineage cells. Because pro-B and late pre-B cell populations were not fully recovered until after day 14 post-dosing, the altered response of B cells in the TBLN could be due to this residual bone marrow depletion in the mice receiving ZDV plus SMX-TMP.

Together, these findings suggest that the toxicity associated with the use of ZDV and SMX-TMP could adversely affect the immune response in HIV-infected patients as they respond to vaccines as well as infectious agents. As the virus weakens the immune function in these individuals, it is important to discern whether this drug-drug interaction is propagating this impairment to a clinically-significant degree. Chapter 5 investigates the clinical application of this work to address the impact of this toxicity in an HIV-infected patient population.

CHAPTER 5: Clinical impact of combination drug exposure on host response

A. OVERVIEW

While HAART has an enormous impact on reducing morbidity and mortality in HIV-infected patients by decreasing viral load, these agents are not free from toxicity. The effects of these agents on the immune function of HIV-infected individuals have been underappreciated. Researchers have defined adverse effects of HAART using *in vitro*, animal, and clinical investigations, which are reviewed extensively in Chapter 1. While we have focused thus far on defining the toxicity with combination exposure to ZDV plus SMX-TMP in mice, we now extend our study into a human population of HIV-positive subjects to determine clinical relevance of this phenomenon. The yearly influenza vaccine was used as a marker of host immunity to determine if response is altered in patients receiving ZDV plus SMX-TMP.

Influenza types A and B are the two types of influenza viruses that cause epidemic human disease (222). New influenza virus variants result from frequent antigenic change (antigenic drift) due to point mutations occurring during viral replication. The 2004-2005 influenza virus vaccine (Fluzone®) contains inactivated viral hemagglutinin antigenic determinants representative of three prototype strains: A/New Caledonia/20/99, A/Wyoming/03/2003 (an A/Fujian/411/2002-like strain) and B/Jiangsu/10/2003 (a B/Shanghai/361/2002-like strain) (222). The vaccine contains the hemagglutinins of these strains that are likely to circulate in the United States for the winter months.

HIV infection has a detrimental effect on immune responses to infectious agents or other forms of immune challenge, such as vaccination. This is due in part to the inability of B lymphocytes to mount antigen-specific antibody responses, as outlined in detail in Chapter 1 (52). Influenza vaccination of HIV-infected individuals has been extensively studied, and the current recommendation from the CDC is to vaccinate all HIV infected persons at the beginning of each influenza season (214). Investigators have shown, however, that lower percentages of HIV-infected patients will adequately respond to this

vaccine, demonstrated by the absence of protective influenza-specific antibody titers in the serum in high percentages of patients (223-225). The success of this response has been correlated directly with $CD4^+$ count, and inversely with viral load (226, 227). It is not known if the interaction between ZDV and SMX-TMP contributes to this inability to produce an appropriate antigen-specific immune response, as clinical trials have not reported which patients were receiving particular drug regimens for HAART and OI prophylaxis. Since patients who have low $CD4^+$ counts (below 200 cells/μl) are usually on SMX-TMP, the interaction between SMX-TMP and ZDV could be a contributing factor.

We therefore conducted a clinical trial to investigate the effects of this drug combination on the ability of subjects to respond to an immune challenge. The animal data presented in Chapter 4 revealed an altered antigen-specific antibody response in mice exposed to ZDV plus SMX-TMP. The yearly influenza vaccine was utilized as a marker of immune response in a group of healthy HIV-infected patients to determine whether exposure to ZDV and SMX-TMP affected humoral immune function.

We hypothesized that humoral immunity would be altered as a result of combination drug exposure. Our aims of the study were 1) to compare the antigen-specific antibody response in patients vaccinated for influenza who were receiving ZDV and SMX-TMP versus the appropriate control groups, 2) to compare peripheral blood lymphocyte populations among the groups, and 3) to examine the relationship between CD4 count and antigen-specific antibody response and how this relationship is altered with combination drug exposure. We demonstrate that disease severity-matched patients receiving both drugs have an altered antigen-specific response to influenza vaccination.

B. MATERIALS AND METHODS

Clinical Design

HIV-infected patients at the Bluegrass Care Clinic at the University of Kentucky Chandler Medical Center were screened for inclusion, and informed consent was obtained for those that met criteria and were willing to participate. HIV-positive patients

between the ages of 18 and 65 years with $CD4^+$ lymphocyte counts greater than 350 cells/μl, undetectable viral loads, and receiving a HAART regimen unchanged for greater than 2 months were placed into one of four parallel treatment groups: 1) ZDV only (300mg twice daily), 2) SMX-TMP only (one double-strength tablet daily), 3) ZDV plus SMX-TMP, or 4) control group (receiving neither drug). Patients with high $CD4^+$ counts and undetectable viral loads were included to minimize the effects of the disease state on immune function.

Patients receiving ZDV as part of HAART were placed in either group 1, or were given a 28-day course of SMX-TMP and placed in group 3. Patients not receiving ZDV as part of HAART were placed either in group 4, or given a 28-day course of SMX/TMP and placed in group 2 (Figure 5.1). Exclusion criteria consisted of the following: prior vaccination for influenza or history suggestive of influenza infection during the 2004-05 season; current treatment with SMX/TMP or treatment within the past 2 months; hypersensitivity to any component of the influenza vaccine, including eggs, egg products, or thimerosal, or hypersensitivity to sulfonamides, TMP, or ZDV; current active infection (other than HIV) or acute febrile illness within the past 30 days; known folate deficiency or known glucose-6-phosphate dehydrogenase deficiency; pregnant patients or nursing mothers; severe allergies or severe bronchial asthma; renal or hepatic failure; and poor adherence to home medication regimens as deemed by patient, study personnel, or treating physician.

Sample Collection

Baseline blood draws were obtained either on day 21 of the SMX/TMP course (groups 2 and 3) or on the day of consent (groups 1 and 4), after which patients received an intramuscular dose of the 2004 annual influenza vaccine (Fluzone®, Aventis Pharmaceuticals,Bridgewater, New Jersey). Between 20 and 24 days after vaccination, blood was again drawn to assess immune response to the vaccine. Blood was collected by venopuncture into tubes coated with EDTA to keep the blood anticoagulated. Cellular components were analyzed by flow cytometry immediately as described below. Serum was separated from the cellular component and frozen at -80^0C for later analysis of influenza-specific IgG and IgM. The study design is depicted

in Figure 5.1. Personnel analyzing patient samples were blinded to patient group number. Note that patients were not randomly assigned to groups. The Institutional Review Board approved this study and all of its procedures.

Flow cytometric analysis of peripheral lymphocytes

After serum separation, blood samples were incubated with fluorescently-labeled monoclonal antibodies specific to human cell surface markers for T cells (CD4, CD8, and CD25) and B cells (CD19, CD80, and CD86). Antibodies were purchased from either Pharmingen (San Diego, CA) or eBioscience (San Diego, CA). Activated $CD4^+$ and $CD8^+$ T cells were defined as cells staining positive for CD25, the IL-2R alpha chain

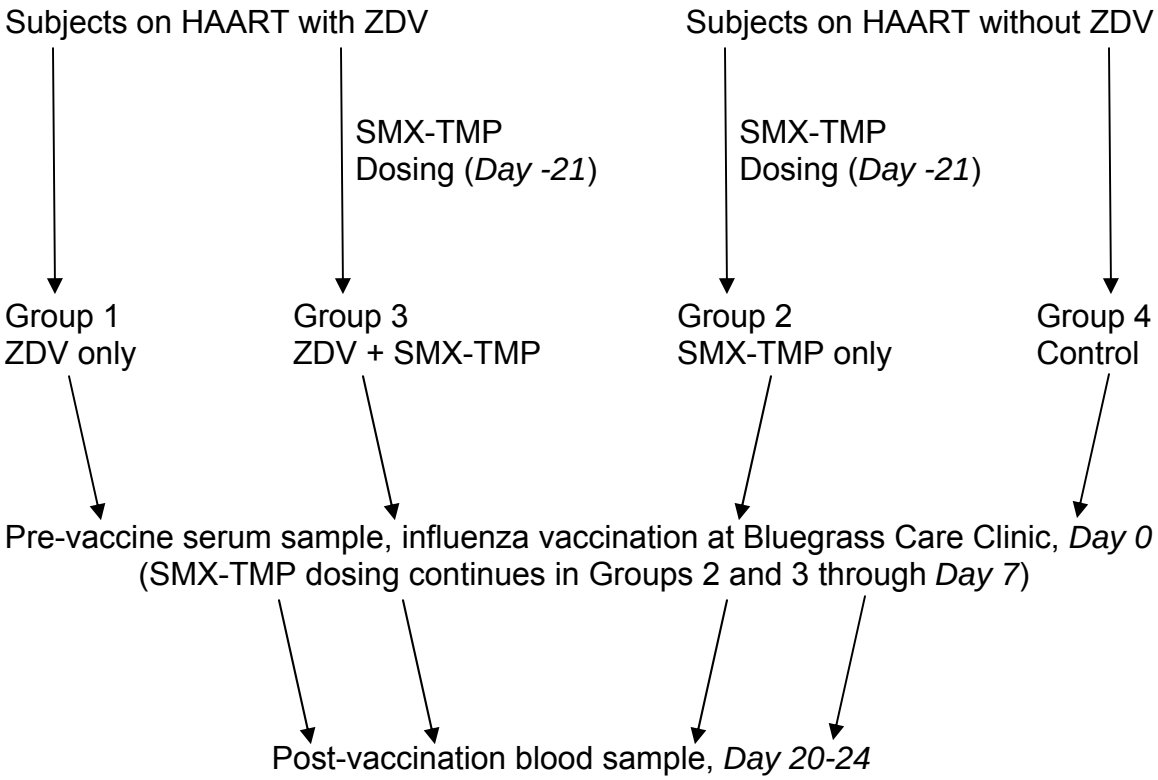

Figure 5.1 Study design. Subjects meeting inclusion/exclusion criteria who were on HAART +/- ZDV were placed into one of four groups as shown. Groups 2 and 3 were generated by dosing subjects with a 28-day course of SMX-TMP. The influenza vaccine was given on day 0, and a post-vaccination blood sample was obtained from each patient 20-24 days later.

that is up-regulated as the cells are activated. B cells were considered activated if either CD80 or CD86 was up-regulated. Both CD80 and CD86 are receptors that are up-regulated with B cell activation. A 100μl aliquot of whole blood for each sample was placed into a tube containing antibodies for either the T or B cell panels, and incubated for 15 minutes at room temperature. Erythrocytes were then lysed by the addition of 2ml of lysing solution containing ammonium chloride (0.15M), sodium bicarbonate (10mM), and tetrasodium EDTA (1mM) for 10 minutes. Cells were then washed and resuspended in PBS containing 1% paraformaledhyde for fixation. After gating on lymphocyte populations defined by cell size and granularity, surface expression of each marker was determined by flow cytometric multiparameter analysis using a FACSCaliber Flow Cytometer (BD Biosciences, Mountain View, CA) and WinList software package (Verity Software House, Topsham, ME). Greater than 50 thousand events were routinely examined.

Antibody Titer Assay

Serum samples were thawed and sent to the medical reference laboratory ARUP Laboratories (Salt Lake City, UT) for influenza A and B virus IgG and IgM antibody quantification. Amount of antibody was compared to reference values using an ELISA method. The reference range of 0.89 or less corresponds to a negative result (no significant level of antibody present), 0.90 to 1.10 represents equivocal results, indicating a questionable presence of virus-specific antibody, and values greater than or equal to 1.11 indicate the presence of influenza antibodies at an immunoprotective titer.

Statistical Analysis

Data are expressed as mean ± standard deviation for cell population percentages and antibody reference values. Differences between treatment groups and the control group were determined by analysis of variance (ANOVA) followed by the Student-Newman-Keuls post-hoc testing where appropriate. Antibody responses (positive versus negative/equivocal) between the combination drug treatment group and control group were analyzed using Fisher's Exact Test. Differences were considered statistically significant when p was < 0.05. SigmaStat statistical software (SPSS, Inc.,

Chicago, IL) was used for these analyses. Regression analyses of the relationships between antibody response and CD4 count were compared for overall coincidence by calculating the *F*-statistic to determine if a significantly better fit to the data is obtained by fitting it with two separate lines compared to fitting all of the data with one regression line. This *F*-statistic was then compared to the critical value *F* for $p < 0.025$ with the appropriate degrees of freedom to determine statistical significance. This Type I error rate was adjusted for multiple comparisons using the Bonferroni correction.

C. RESULTS

Subject demographics were homogeneous among study groups

Twenty-eight subjects were enrolled in the study, and 23 were included in the final analysis. Two subjects developed a rash on SMX-TMP and were terminated from the study, and 3 subjects did not return for post-vaccination blood sampling. The demographics of the study population are outlined in Table 5.1. Each group had between 5 and 7 individuals, with each group including one female. Mean subject age and $CD4^+$ lymphocyte counts were not significantly different among treatment groups. The average mean corpuscular volume was significantly higher for the two groups that received ZDV as compared to the control group. Macrocytosis is a known effect of ZDV, and investigators have demonstrated that it is so reliable that it can be used to monitor adherence to ZDV therapy (103, 106). All patients receiving ZDV were above the normal erythrocyte mean corpuscular volume range of 88 to 98 μl.

Antiretroviral regimens varied from 3 to 6 agents, with a median number of 3 or 4 in each group. All 23 patients were receiving an NRTI other than ZDV. Fifty-six percent were receiving an NNRTI, and only 26% were receiving a PI. One patient in each group, with the exception of the combination group, was receiving multiple PI. Subjects recorded doses of ZDV and SMX-TMP in dosing diaries as a measure of adherence to study protocol. One patient reported missing one dose of SMX-TMP, while one other patient reported missing two doses of SMX-TMP. All other patients reported 100% adherence to the study regimen of SMX-TMP, and to HAART.

Table 5.1 Patient demographics.

	Dosing Groups				ANOVA
Parameters	**ZDV**	**SMX-TMP**	**Combination**	**Control**	**p-value**
Age, mean years (range)	51.5 (46-61)	47.0 (32-59)	40.4 (26-47)	42.8 (32-54)	0.163
Gender, male/female	5/1	6/1	4/1	4/1	
CD4, cells/μl (mean ± SD)	592.2 ± 333.5	692.8 ± 528.4	597.2 ± 254.5	850.8 ± 468.7	0.442
MCV, μm^3 (mean ± SD)	111.2 ± 6.6*	95.0 ± 11.2	109.4 ± 4.1*	92.8 ± 2.0	<0.001
HAART, number of agents					
NRTI, median (range)	3 (2-4)	2 (1-2)	2 (2-2)	3 (1-3)	
NNRTI, median (range)	1 (0-1)	1 (0-1)	1 (0-1)	1 (0-1)	
PI, median (range)	0 (0-2)	0 (0-3)	0 (0-1)	0 (0-2)	
Total, median (range)	4 (4-6)	3 (3-4)	3 (3-3)	3 (3-4)	

*, *p*-value deemed statistically significant if < 0.05. Representative of one-way ANOVA with post-hoc multiple pair-wise comparisons to the control group by the Student-Newman-Keuls Method.

Peripheral blood lymphocyte populations and activation

To investigate whether using ZDV concurrently with SMX-TMP has any effect on peripheral lymphocyte populations, $CD4^+$ T cell, $CD8^+$ T cell, and $CD19^+$ B cell percentages were determined in blood samples before and after vaccination. Percent $CD4^+$ T cells, $CD8^+$ T cells, and $CD19^+$ B cells of the total peripheral blood cell population (after red cell lysis) are reported in Figure 5.2 (panels A, C, and E, respectively). No significant differences in cell populations in the three treatment groups compared to the control group were demonstrated. Additionally, little difference is noted between pre- and post-vaccination data.

The activated phenotypes of these populations were also determined and reported in Figure 5.2. Percentages of activated $CD4^+$ cells ($CD4^+CD25^+$) and $CD8^+$ cells ($CD8^+CD25^+$) were not significantly different before or after vaccination (panels B and D, respectively). Of note, the percentage of activated $CD8^+$ cells did show a trend toward a decrease in the combination group compared to the control group of subjects

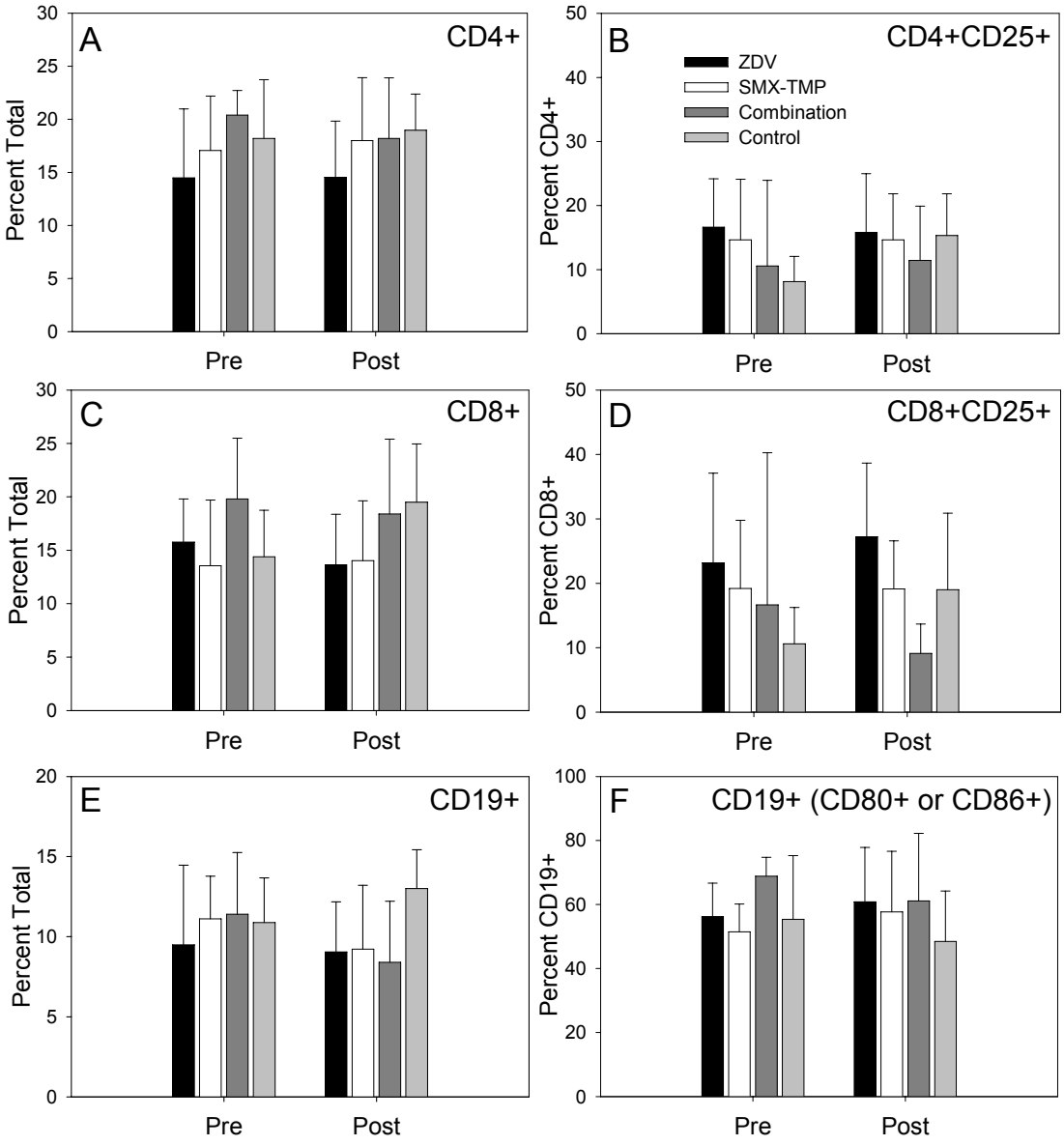

Figure 5.2 Serum percentages of $CD4^+$, $CD8^+$, and $CD19^+$ lymphocytes and their activated phenotypes before and after vaccination with influenza. After being placed in one of four treatment groups: ZDV, SMX-TMP, the combination of both, or neither (control), as detailed in Materials and Methods, blood was drawn from subjects immediately preceding influenza vaccination, and 20-25 days after vaccination. Percentage of total cells in the peripheral blood (after red cell lysis) was determined for $CD4^+$ T cells, $CD8^+$ T cells, and $CD19^+$ B cells by flow cytometry (panels A, C, and E, respectively). The percentage of these cells that were of the activated phenotype are given in panels B, D, and F: $CD4^+CD25^+$ cells, $CD8^+CD25^+$ cells, and $CD19^+$ cells having up-regulated either CD80 or CD86. Statistical significance was not reached in any of the above data when comparing treatment groups to control groups using ANOVA for $p < 0.05$.

(p=0.108). Percentage of activated B cells ($CD19^+$ $CD80^+$ and/or $CD86^+$) also did not show any differences between groups (panel F).

Pre-vaccination influenza-specific IgG was affected by combination drug exposure

We examined antibody titers of the subjects before receiving the influenza vaccine to determine if the drug treatments had any affect on pre-vaccination humoral immune status. Positive IgG reference values (greater than 1.10) specific to either influenza A or B would be indicative of past or current infection or immunization. Subjects in the ZDV only and ZDV plus SMX-TMP groups had influenza A-specific serum IgG values that were significantly lower than the control subjects (Figure 5.3A). This trend was also present in the pre-vaccination influenza B-specific IgG values for each of these groups, although the data did not reach statistical significance (Figure 5.3B). Mean reference values corresponded with a lower percentage of subjects in the positive range for influenza-specific IgG in the combination group (20%) versus the control group (100%). This difference was significantly different (p=0.048, Fisher's Exact Test) (Table 5.2).

Because IgM is an indicator of recent or current infection or immunization, almost all patients tested influenza-IgM negative at pre-vaccination (Figure 5.3A and B). However, patient C04 tested positive to influenza A, and patient D03 tested positive to both influenza A and B. This could indicate recent exposure in each of these individuals, although both reported no recent history of flu-like illness. The mean influenza-specific IgM values were not different among the groups at the pre-vaccination timepoint (Figure 5.3C and D).

Drug exposure affected both post-vaccination influenza-specific IgG and IgM

To determine the humoral response to the vaccine among the patient groups, we measured serum titers of IgG and IgM that were specific to influenza antigens within a window of 20-25 days post-vaccination. Influenza-B specific IgG titers post-vaccination were significantly lower in both the SMX-TMP only and combination treatment groups compared to the control group (Figure 5.3B). This trend was mirrored in the combination treatment group in response to influenza A, although the effect did not

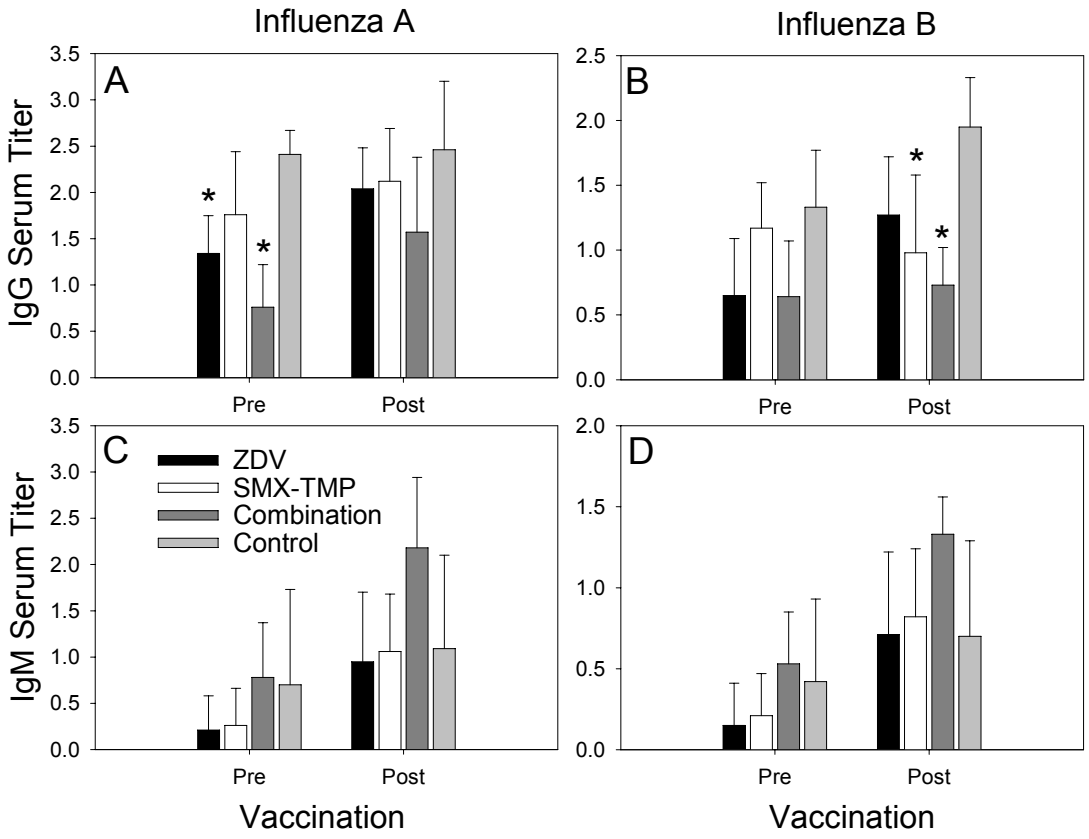

Figure 5.3 Serum antibody titers. After being placed in one of four treatment groups: ZDV, SMX-TMP, the combination of both, or neither (control), as detailed in Materials and Methods, blood was drawn from subjects immediately preceding influenza vaccination, and 20-25 days after vaccination. Serum influenza A and B-specific IgG and IgM titers were obtained by ELISA. *, statistically significant difference detected when compared to control group using ANOVA for $p < 0.05$.

reach statistical significance (Figure 5.3A). Only 60% of patients in the combination treatment group had a positive protective influenza A serum IgG response, compared to 100% in each of the other groups (Table 5.2). With regards to influenza B, serum IgG values only reached the protective range in 1 patient (20%) in the combination group versus 100% of the subjects in the control group, this difference being statistically significant (p=0.048, Fisher's Exact Test).

Interestingly, post-vaccination serum IgM titers reached the positive range in 100% of patients in the combination group for both influenza A and B, versus 40% and 20% in the control group for influenza A and B, respectively (Table 5.2). This corresponded with a trend of an increase in mean IgM values for both influenza A and B in the

combination group versus the control group (Figure 5.3C and D). Due to a high degree of variability in IgM titers among the subjects, there differences did not reach statistical significance (Figure 5.3C and D).

Table 5.2 Subject response to influenza vaccine.

	Influenza A IgG	Influenza B IgG	Influenza A IgM	Influenza B IgM
Pre-vaccination	**Negative + Equivocal / Positive (Percent Positive)**			
ZDV	2/4 (66)	5/1 (16)	6/0 (0)	6/0 (0)
SMX-TMP	1/6 (86)	3/4 (66)	7/0 (0)	7/0 (0)
Combination	4/1 (20)*	4/1 (20)	4/1 (20)	5/0 (0)
Control	0/5 (100)	1/4 (80)	4/1 (20)	4/1 (20)
Post-vaccination				
ZDV	0/6 (100)	2/4 (66)	3/3 (50)	5/1 (16)
SMX-TMP	0/7 (100)	4/3 (43)	3/4 (57)	5/2 (28)
Combination	2/3 (60)	4/1 (20)*	0/5 (100)	0/5 (100)*
Control	0/5 (100)	0/5 (100)	3/2 (40)	4/1 (20)

Influenza-specific antibody reference values were measured in the serum on the day of vaccination (pre) and 20-25 days after vaccination (post). The number of negative (less than 0.89) plus equivocal (0.90-1.10) results are reported, along with the number of subjects that tested positive (greater than 1.11) and the percentage that tested positive. *, *p*-value statistically significant if < 0.05 when treatment groups were compared to the control group using Fisher's Exact Test.

Relationship between IgG response and CD4 count was affected by SMX-TMP exposure

Because antibody production, and specifically class switching, is reliant upon T and B cell interactions, and because T cells exhibit a positive correlation to antigen-specific antibody titers in patients infected with HIV, we compared the strength of this correlation among the different treatment groups before and after vaccination. Influenza A and B-specific serum IgG titers were graphed versus $CD4^+$ cell numbers for the pre-vaccination (Figure 5.4) and post-vaccination (Figure 5.5) blood samples. Figure 5.4

depicts influenza A- (panels A and B) and influenza B- (panels C and D) specific pre-vaccination IgG titers as a function of $CD4^+$ cell count. The combination treatment group was compared to the control group (panels A and C) and the 2 groups that received SMX-TMP were compared to the 2 groups that did not receive SMX-TMP (panels B and D).

Statistical analysis comparing regression lines for these figures are summarized in Table 5.3. Regression analyses of the relationships between antibody response and CD4 count were compared for overall coincidence by calculating the *F*-statistic to determine if a significantly better fit to the data is obtained by fitting it with two separate

Table 5.3 Regression data comparing IgG to CD4.

Pre-vaccination	**n**			**r**			**F**	**Crit F**
Influenza A	**Test**	**Control**	**Pooled**	**Test**	**Control**	**Pooled**		
Combo vs Control	5	5	10	0.636	0.209	0.266	**26.13**	7.26
+/- SMX-TMP	11	11	22	0.080	0.162	0.140	1.69	4.56
Influenza B								
Combo vs Control	5	5	10	0.460	0.248	0.018	3.22	7.26
+/- SMX-TMP	11	11	22	0.144	0.219	0.187	0.05	4.56
Post-vaccination								
Influenza A								
Combo vs Control	5	5	10	0.840	0.804	0.331	**8.72**	7.26
+/- SMX-TMP	11	11	22	0.488	0.427	0.044	3.60	4.56
Influenza B								
Combo vs Control	5	5	10	0.237	0.460	0.422	**11.70**	7.26
+/- SMX-TMP	11	11	22	0.056	0.210	0.110	**5.95**	4.56

Regression analyses of the relationships between antibody response and CD4 count were compared for overall coincidence by calculating the *F*-statistic to determine if a significantly better fit to the data is obtained by fitting it with two separate lines compared to fitting all of the data with one regression line (pooled). This *F*-statistic was then compared to the critical value *F* for $p<0.025$ with the 2,n-4 degrees of freedom. *F* values reaching statistical significance are shown in bold.

lines compared to fitting all of the data with one regression line (pooled). Sample sizes (n) and r values are given for each analysis.

The relationship between influenza A-specific IgG response and $CD4^+$ cell count was significantly different for the subjects receiving ZDV plus SMX-TMP compared to subjects in the control group (Figure 5.4A). This difference corresponded with lower influenza A-specific IgG titers at the corresponding

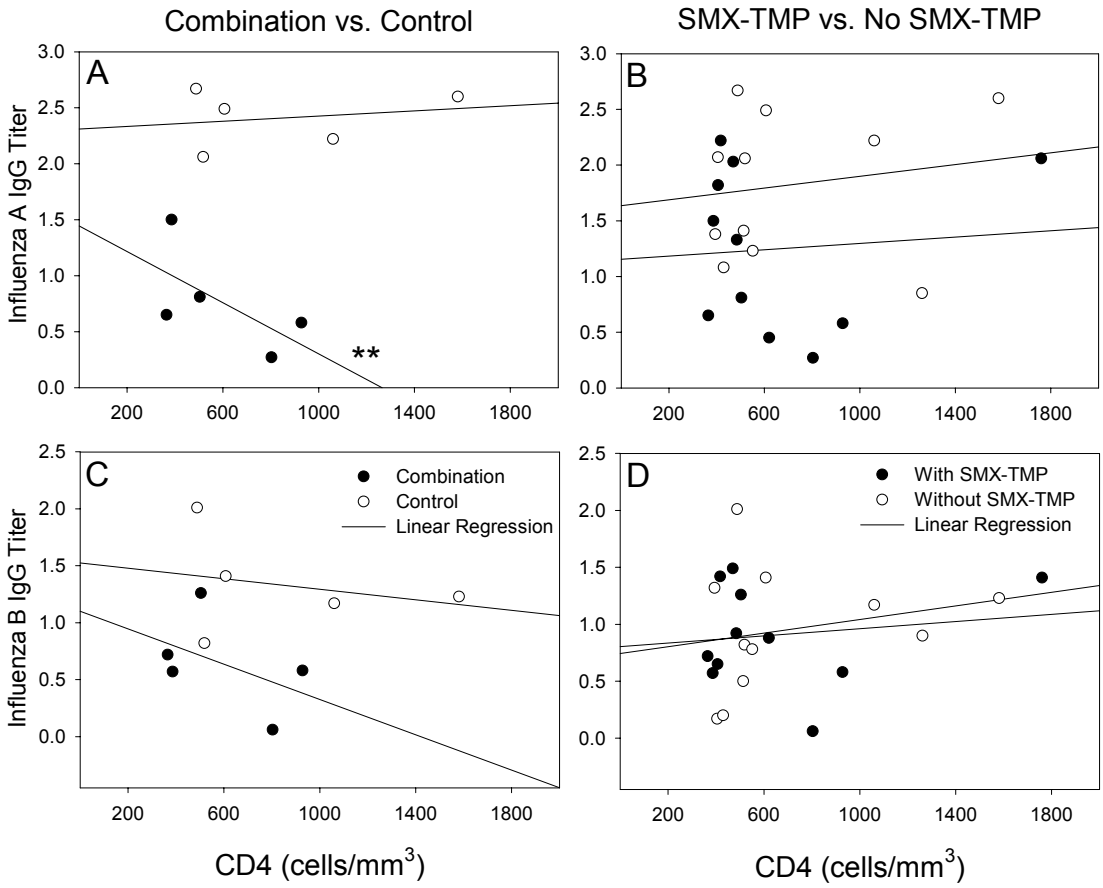

Figure 5.4 Pre-vaccination IgG titer correlation with CD4 cell count. After being placed in one of four treatment groups: ZDV, SMX-TMP, the combination of both, or neither (control), as detailed in Materials and Methods, blood was drawn from subjects immediately preceding influenza vaccination, and serum influenza A and B-specific IgG titers were obtained by ELISA. These titers were plotted versus the corresponding subject's CD4 T cell count for influenza A (panels A and B) and influenza B (panels C and D) comparing the combination treatment group versus the control group (panels A and C) and comparing the groups that received SMX-TMP versus those that did not receive SMX-TMP (panels B and D). **, statistically significant difference when comparing the *F*-statistic to the critical value of *F* for $p<0.05$ when testing regression lines for coincidence.

$CD4^+$ T cell counts. A difference in regression lines was not observed when comparing the combination treatment group versus the control group for influenza B (panel B), or when comparing subjects receiving SMX-TMP versus subjects not receiving SMX-TMP for influenza A or B (panels B and D, respectively).

Figure 5.5 depicts influenza A- (panels A and B) and B- (panels C and D) specific post-vaccination IgG responses as a function of $CD4^+$ cell count, comparing the

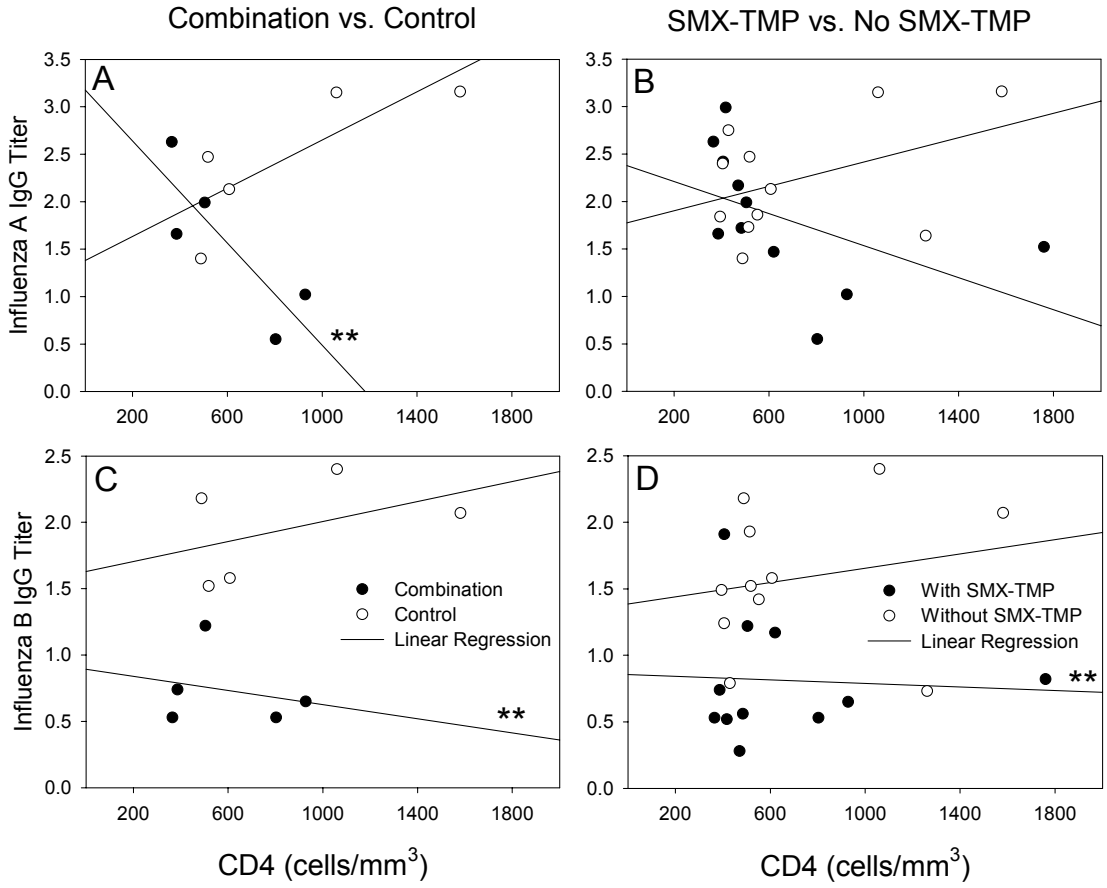

Figure 5.5 Post-vaccination IgG correlation with CD4 cell count. After being placed in one of four treatment groups: ZDV, SMX-TMP, the combination of both, or neither (control), as detailed in Materials and Methods, subjects were vaccinated with the influenza vaccine, and after 20-25 days, blood was drawn and serum influenza A and B-specific IgG titers were obtained by ELISA. These titers were plotted versus the corresponding subject's CD4 T cell count for influenza A (panels A and B) and influenza B (panels C and D) comparing the combination treatment group versus the control group (panels A and C) and comparing the groups that received SMX-TMP versus those that did not receive SMX-TMP (panels B and D). **, statistically significant difference when comparing the *F*-statistic to the critical value of *F* for $p<0.05$ when testing regression lines for coincidence.

combination treatment group versus the control group (panels A and C) and comparing the groups that received SMX-TMP versus group that did not receive SMX-TMP (panels B and D). Regression lines did not coincide with one another in panels A, C, or D. We conclude that the relationship between serum IgG titer and $CD4^+$ count was statistically different for subjects exposed to ZDV plus SMX-TMP versus control subjects for both influenza A and B (panels A and C, respectively). Likewise, the relationship between serum IgG and $CD4^+$ count was different among subjects in who received SMX-TMP and subjects who did not receive SMX-TMP for influenza B (panel D). A significant difference was not observed in panel B. These differences are shown in Table 5.3, with F values greater than the critical F values at $p < 0.025$.

D. CONCLUSIONS

In this chapter we have demonstrated the clinical impact of concurrent treatment with ZDV and SMX-TMP on immune response when using the influenza vaccine to challenge subjects infected with HIV. Peripheral blood lymphocyte percentages were not affected, but despite a lack of differences in demographics between groups, the subjects in the combination treatment group had a lower mean influenza B-specific IgG titer in the serum compared to the control group in response to vaccination. Interestingly, exposure to the combination of agents for 21 days lowered influenza-specific IgG titers at the pre-vaccination sampling as well. Influenza-specific IgM serum titers were actually higher in the group of subjects exposed to ZDV plus SMX-TMP as compared to disease-severity matched control subjects 20-25 days post-vaccination. These differences could be indicative of a suppression of the humoral response, or they could be representative of an alteration in timing of this response.

The majority of the subjects tested positive for influenza-specific IgG, which likely corresponds to the fact that they each received the influenza vaccine during the previous year. Although subjects reported having no flu-like illness during this year's influenza season, recent exposure to the virus cannot be ruled out as a cause for protective IgG levels. Because the assay used cannot distinguish between antigenic

differences from this year's vaccination and those of the previous years, this is a potential source of error for our data. Comparisons of pre-vaccination immune status should therefore be considered cautiously. It would have been helpful to also obtain a blood sample to analyze IgG titers prior to SMX-TMP dosing. Because this was not performed, a true baseline for influenza-specific IgG was not established.

This difference in antibody profile among the groups could indicate an impaired ability of the combination treatment subjects to effectively isotype switch antibody production. B cells constitutively express the IgM isotype in response to an infectious challenge. In order for the host to produce other isotypes, the process of isotype switching must occur, which will then allow cells to produce, among other isotypes, antigen-specific IgG. This process is dependent on B cells interacting with T cells in secondary lymphoid tissues, and will be discussed in detail in Chapter 6. Subjects receiving SMX-TMP had influenza-specific IgG responses that did not positively correlate with $CD4^+$ counts to a similar degree as subjects that did not receive SMX-TMP. These results could indicate that the adverse effects of these drugs could be influencing humoral immune responses to a clinically significant degree.

One limitation to these data concerns the low level of power in statistical analyses comparing CD4 correlation with IgG responses due to the low numbers of subjects in each treatment group. Tests between groups routinely had power levels below the desired power level of 0.80. Although poorly-powered comparisons increase the likelihood of not detecting differences that exist between samples, we were able to detect statistical differences among our treatment groups in several instances. Other differences may exist that were not identified, therefore negative results must be interpreted cautiously. The percentages of subjects with positive influenza-specific antibody titers in the treatment groups were compared to the control group using Fisher's Exact Test, but corrections for multiple comparisons were not utilized. These statistical differences should therefore be interpreted cautiously. A larger study with a higher number of subjects in each group, along with serial timepoints post-vaccination to more accurately describe antibody responses, is warranted.

CHAPTER 6: Discussion

A. RESULTS SUMMARY

Our investigations have characterized the toxicity caused by concurrent ZDV and SMX-TMP exposure. We first began in mice, to define the nature of the toxicity in immune cell populations in primary and secondary lymphoid tissues, as well as a common site of infection, the lungs. We also characterized the effects of this drug combination on the host's response to an immune challenge, using pulmonary *Pneumocystis* as the model of infection. Our investigations then turned in opposing directions. In a series of *in vitro* experiments, we asked basic questions relating to the mechanism of the toxicity to B lymphocytes in the bone marrow. Finally, we explored the clinical relevance of this drug-drug interaction to discover an altered humoral immune response to influenza vaccination in HIV-positive patients exposed to both ZDV and SMX-TMP. Hypotheses generated from this work which will guide the future directions of this project are discussed below.

There are three potential reasons for the synergistic toxicity. First, sequential sites of toxicity along the development pathway could cause synergy to occur, thereby amplifying the overall depletion. Alternatively, combination exposure could cause additive or synergistic DNA damage, increasing the percentage of cells that suffer apoptosis. And finally, one drug could alter the disposition of the other agent or its metabolites, thereby resulting in increased cytotoxicity. These mechanisms are not mutually-exclusive of one another.

B. MECHANISM

Our mechanistic investigation of this drug-drug interaction is in its infancy. There are two categorical elements to the potential cause of the increase in apoptosis observed. First, the presence of the combination of agents could be pharmacodynamically

responsible for the toxicity. It is possible that each drug's unique effect, whether on a molecular or cellular level, when combined cause this synergistic toxicity. Second, the disposition of one agent or its metabolites could be affected by the presence of the other, thereby causing a localized pharmacokinetic interaction in the bone marrow. We have conducted experiments to partially address each element, which are discussed in detail in the points that follow.

Pharmacodynamics

Sequential sites of development. By analyzing specific subpopulations of the B-lineage, we demonstrated that subtypes in the more rapidly-dividing stages of development are the most sensitive to apoptosis induced by ZDV plus SMX-TMP. B lymphocytes serve as an excellent line in which to study this phenomenon because of the extensive work performed by several groups to phenotypically characterize the discrete stages of B-lineage cells and the processes occurring at each of these stages. This allowed us to investigate the characteristics of toxicity to individual cell types as they mature, to consider whether cytotoxicity in sequential stages could cause the synergistic effect of B cell depletion.

We conclude here that the rapidly-dividing early pre-B cell fraction is a focal point of toxicity in mice exposed to the combination of ZDV and SMX-TMP as evidenced by the early block in early pre-B cell proliferation at day 7 of dosing followed by a significant reduction in late pre-B cells by dosing day 15. In addition, by dosing day 21, the more immature cells of the pre-pro-B and pro-B phenotypes were depleted significantly in the single drug treatment groups as well as in the combination treatment group. Therefore, fewer cells reached the proliferative pre-B stages in each of these three groups. However, only mice exposed to the combination of agents had overall B lymphocyte populations depleted in the bone marrow, demonstrating that only with pre-B cell burst-inhibition is the overall number of B cells significantly affected. Two separate sites of toxicity is likely a contributing factor to the synergistic effect observed. The mechanism of toxicity at each point could be the same, because pro-B cells are also proliferating, albeit at a slower rate.

An alternative mechanism of toxicity could be a direct affect on the stromal cells of the bone marrow. This could lead to altered B cell development due to the vital support that stromal cells provide. Stromal cells do not rapidly divide, so if indeed the mechanism of cell death is tied to proliferation, it is unlikely that the stromal cells are involved. However, stromal cells do provide necessary signals to B lineage cells as they develop, the absence of which could induce apoptotic cell death. The impact of combination drug therapy on stromal cells is unknown.

DNA damage. From the analysis of our findings, we hypothesize that the apoptosis in B-lineage cells that results from exposure to ZDV plus SMX-TMP is due to overwhelming DNA damage. We reach this premise for 3 reasons. First, known mechanisms of bone marrow toxicity for each agent individually involve the inhibition of DNA replication. The inhibition of thymidylate kinase by ZDV-monophosphate leading to the depletion of thymidine stores, combined with the inhibition of nucleic acid synthesis by SMX and TMP, could synergistically target highly proliferating early pre-B cells. Furthermore, oxidative stress associated with SMX-NO and SMX-HA could contribute to DNA damage as well.

Second, we have shown that the effect is specific to the proliferation phases of the cell cycle. At dosing day 7 we found a buildup in cell number in these phases in the early pre-B subset and a slight decrease in the number of late pre-B cells, suggesting that they are unable to progress to mitosis. The fact that the percentage of cells in G0/G1 is reduced by the drug combination, in addition to the depletion observed in the late pre-B cell subset (and with extended dosing, in the early pre-B subset also), leads us to believe cells are arrested in the proliferative phases. Cell cycle arrest that causes a buildup of cells in the S and G2 phases results from a failure to proceed through the "checkpoint" to the mitotic stage, prohibiting their division. This step is regulated by the enzyme M phase kinase (228, 229). Cells are prohibited to begin mitosis at this checkpoint if DNA is highly damaged during replication, or if the cell does not have the ability to adequately repair it (230, 231).

The third reason to consider this hypothesis is because the cell death caused by ZDV plus SMX-TMP appears to be caspase-independent. While most forms of

apoptosis induction proceed through either the intrinsic or extrinsic pathways, both of which rely on signaling and effector caspases to induce programmed cell death, there exists a mechanism through which apoptosis can be induced without the requirement of caspases. This caspase-independent apoptosis is triggered by DNA damage. Our results in Chapter 3 support this notion, in that the cytotoxicity was not hindered by pan-caspase inhibition.

Caspase-independent apoptosis. Mitochondria play an important role in programmed cell death through the release of cytochrome c and apoptosis-inducing factor (AIF), which activate caspase-dependent and caspase-independent apoptosis mechanisms, respectively. Poly(ADP-ribose) polymerase 1 (PARP-1) is an important activator of AIF release from the mitochondria. DNA damage causes the up-regulation of PARP-1, which triggers the release of AIF (232). Although caspases may be involved in facilitating cell death mediated by the release of AIF from the mitochondria, they are not required, as broad-spectrum caspase inhibitors do not prevent PARP-1-mediated cell death (67). In addition to PARP-1 up-regulation, AIF release from mitochondria can be stimulated by the intrinsic apoptosis pathway or by changes in mitochondrial membrane potential (233). AIF entering the nucleus causes classic apoptotic features in the cell, including chromatin condensation, phosphatidylserine exposure on the cell surface, and mitochondrial membrane depolarization, all in the absence of caspase activation (67, 234, 235).

PARP-1 activation mediates cell death in ischemia-reperfusion injury, inflammatory injury, and reactive oxygen species-induced injury (236-239). The effects of ZDV and SMX-TMP on DNA replication could be inducing an increase in PARP-1 cleavage leading to induction of apoptosis in B cells.

One caveat that does not support this premise is that ZDV has been demonstrated to cause apoptosis that is caspase-*dependent* (120, 240). The mitochondrial damage associated with ZDV's inhibition of DNA polymerase gamma causes cytochrome c release that triggers the intrinsic apoptosis cascade (120, 240). Further work is needed to investigate each mechanism's contribution to apoptosis when both ZDV and SMX-TMP are present. An ideal next step would be to determine mitochondrial release of

cytochrome c and AIF, as well as mitochondrial membrane potential and permeability, in the setting of combination drug exposure compared to appropriate controls.

Defining this more clearly would not only supply insight into the mechanism of this combined toxicity, but this information could also provide therapeutic potential to this drug combination with respects to cancer treatment. Recently, several papers have given promise to ZDV and its ability to cause apoptosis to occur in several types of malignancy, including lymphoma, multiple myeloma, and parathyroid cancer cells (241-244). Combining this therapeutic effect with SMX-TMP has not been investigated. This could be tested by exposing various B lymphoma cell lines to the combination of ZDV and SMX-TMP *in vitro,* and determining if apoptosis can be induced.

Pharmacokinetics

Alteration of drug disposition. The final possible mechanism that has been addressed is that of drug disposition alteration. Because steady-state serum SMX concentrations were elevated in mice concurrently receiving ZDV, we became interested in the potential causes of this alteration, and the impact that it has on cytotoxicity in the bone marrow. Pharmacokinetic investigations have not previously demonstrated interactions involving combination use of SMX-TMP and ZDV. Although SMX-TMP caused a significant decrease in renal clearance of ZDV and its glucuronide metabolite in a study involving 9 patients infected with HIV, the overall net clearance of ZDV was not affected (158). In another investigation, concomitant SMX-TMP therapy did not alter the AUC of ZDV in 16 HIV-positive patients (245). To our knowledge, our data is the first to suggest that ZDV may affect the disposition of SMX.

Mrp4 expression induced by ZDV could be affecting GSH pools in lymphocytes, thereby increasing the intracellular concentrations of the oxidative metabolites of SMX (see Chapter 3). This would then induce increased amounts of oxidative stress which could lead to DNA damage and caspase-independent apoptosis. This could lead to the alteration in serum concentrations of SMX, as systemic clearance would be delayed by the sequestering of SMX in the intracellular compartment. The fact that it takes 72 hours of exposure for ZDV to contribute to the toxicity in our *in vitro* system could be

due to the time required to up-regulate Mrp4, although the timing of this phenomenon has not been defined (207).

Unfortunately, our study of this premise is in its infancy. Confusing results were reached during our experiments with Mrp1$^{-/-}$ mice, from which no credible conclusions can be drawn at this time. Future studies will involve intracellular concentration determinations of SMX, SMX-NO, and SMX-HA, as well as Mrp4 expression determination on B cells exposed to ZDV. GSH concentrations, as well as GSH-SMX metabolite levels, will also be investigated. It would also be interesting to determine if concurrent dosing of antioxidants would have an inhibitory effect on this drug-drug interaction.

C. EXPERIMENTAL CONSIDERATIONS

Concentration-dependent cytotoxicity *in vitro*

The *in vitro* system utilized in this work is not representative of the B-lineage cellular makeup of the bone marrow in several ways. *In vivo*, B-lineage cells are under the influence of many cytokines and cell-cell interactions as they mature. With the exception of IL-7 (which we supplement), normal stromal cell interactions are absent (see Chapter 1 for a review). The IL-7 therefore biases our population toward the early pre-B and late pre-B cell subtypes that are responsive to its stimulation to proliferate. This forces us to acknowledge that the results that we observe *in vitro* may not be entirely representative of *in vivo* phenomena. However, as demonstrated in Chapter 2, these pre-B cell stages are the primary focus of the combined toxicity observed *in vivo,* so our culture system does have merit.

It is logical to think that this would make cells in our culture system exquisitely sensitive to apoptosis induction by our drug combination. Although serum trough concentrations of the parent SMX reach over 100μg/ml in our *in vivo* experiments, the more relevant information is the intracellular SMX metabolite concentration changes inside B cells. When ZDV exposure was lengthened to 72 hours, B lymphocytes in our culture system underwent rapid apoptosis induction with the addition of SMX-HA.

Intracellular concentrations of SMX-NO and SMX-HA are topics of ongoing investigation.

Comparing Figures 4.2B and 4.4D, we find the percentage of apoptotic B cells to be much higher at low SMX-HA concentrations (and well past its peak at higher SMX-HA concentrations) after exposure to ZDV for 72 hours (Figure 4.4D). Because of this, apoptosis was best studied in the first few hours of SMX-HA exposure, as reflected in the caspase inhibitor experiments.

Dosage relevance

The doses used in the animal experiments corresponded with doses used in studies by other investigators (1, 123, 246). The doses administered to the mice in these experiments were approximately 8-10 times the doses given to humans for *Pneumocystis* pneumonia prophylaxis and HAART; however, the doses were more comparable to humans doses based on body surface area (80, 214). Interspecies scaling in drug dosing has received much attention, as it is a continual problem when using animals to model and investigate human conditions (247, 248). Mice have been shown to require much higher doses of cytotoxic drugs than humans to produce similar levels of cell death (249, 250). The therapeutic range for SMX in humans is 50-200 μg/ml in the serum according to the manufacturer's information for SMX (Hoffman-La Roche, Basel, Switzerland). The serum concentrations of SMX were measured in our mice to be between 45 and 95 μg/ml, which are comparable to those found in humans; although, the mean serum concentrations over the entire dosing interval would be much higher. The extent to which the concentrations of SMX-HA, SMX-NO, and ZDV in mouse bone marrow correlate with humans treated with these agents is unknown. Furthermore, the presence of HIV infection would likely worsen the toxicity of this drug combination, due to the intracellular GSH reductions in HIV patients as outlined previously. This issue makes it difficult to predict the clinical significance of such results, making human investigations extremely important.

D. HOST RESPONSE

Lymphocyte populations in secondary lymphoid tissues

Of note, cells in secondary lymphoid tissues were not studied for apoptotic characteristics associated with combination drug exposure. Apoptotic frequency could be increased here as well, especially in an infectious response, as cells undergo rapid divisions as clonal expansions of T and B cells occur. Along with previous reports by others, we show in Chapter 2 that ZDV plus SMX-TMP do not affect peripheral T cell numbers in the spleens of uninfected mice (1). In the context of infection, however, total and activated $CD4^+$ T cell frequencies were lower in the LN draining the site of infection (Chapter 4).

This could be either a direct effect on expanding T cell populations, or a secondary effect stemming from the B cell depletion. Investigators have shown that T cell responses are dependent on interactions with B cells in secondary lymphoid organs in response to many infectious stimuli, including *Salmonella*, *Bordetella pertussis* vaccine, and *Pneumocystis* (219, 251, 252). By evaluating antigen-specific cytokine secretion by $CD4^+$ cells in normal and B cell-deficient mice, Linton et. al. determined that B cells play a critical role in regulating clonal expansion of $CD4^+$ cells (252). Ugrivovic et. al. suggest that T cell responses to *Salmonella* infection are dependent on B cell antigen presentation (251). Additionally, our group demonstrated that T cell expansion and activation are reduced in TBLN and the lungs of B cell-deficient and CD40 knockout mice in response to *Pneumocystis* infection (219).

Peripheral blood B lymphocytes

No clinical literature exists showing an effect of drug combination treatment on the number of B lymphocytes in the peripheral blood. Consistent with this, we were unable to detect changes in the percentage of peripheral blood B cells in mice treated with the drug combination, or in patients receiving ZDV and SMX-TMP in our clinical study. However, this does not preclude the possibility that the peripheral B cell compartment is altered in patients in the lymph nodes and spleen.

Interesting work has shown that IL-7 knockout mice, which have B lymphocyte production only during fetal and perinatal life, still maintain a stable pool of B cells in peripheral organs including the spleen (253). However, these B cells consist only of the B1 and marginal zone phenotypes, accompanied by a 50-fold increase in the frequency of IgG secreting cells and increased serum antibody titers (253). Folicular B cells, the opposite phenotype, responsible for responding to BCR stimulation to produce high affinity antibodies, are absent in these knockout mice (253). This is extremely similar to patients with advance HIV disease that have altered antibody profiles as discussed earlier. This applies clinically, in that bone marrow depletions of developing B cells may not be reflected in the peripheral blood of patients. A future goal of this project is to determine the effect of ZDV and SMX-TMP on the various peripheral B cell subtypes.

Immune response to *Pneumocystis*

It is not surprising that the abnormalities in the B cell compartment caused by ZDV plus SMX-TMP do not prohibit the clearance of *Pneumocystis*. Pulmonary infection with *Pneumocystis* is cleared in normal mice, requiring the use of a combination of cellular and humoral components of adaptive immunity. It has been shown that mice cannot mount an effective host response to *Pneumocystis* without the presence of $CD4^+$ T cells (215, 216, 254). Alveolar macrophages are the likely effector cells responsible for killing *Pneumocystis* since depletion of alveolar macrophages in rats resulted in the inability to clear infection (255). Additionally, it has been demonstrated that mice deficient in B cells are also susceptible to *Pneumocystis* infection and are rendered unable to resolve a primary infection (217-219, 256). In the present study, the numbers of infiltrating lymphocytes into the site of infection were not altered to a significant degree.

Several investigators have demonstrated that IgG produced by B cells facilitates the clearance of *Pneumocystis* in murine models of infection (257-261). Work from our laboratory recently demonstrated, however, that *Pneumocystis*-specific IgG plays an important, but not critical, role in the defense against *Pneumocystis* (219). This corresponds with the data presented in Chapter 4 in that the mice that received both ZDV and SMX-TMP were able to control the *Pneumocystis* burden in the lungs despite reduced serum IgG concentrations. Our data indicate that clearance of *Pneumocystis*

was able to proceed to a certain point and then stalled. This is consistent with other data from our laboratory in which we found a delay in the clearance of *Pneumocystis* in mice unable to produce *Pneumocystis*-specific isotype class-switched antibody (219). The fact that IgM (which is constitutively expressed) titers were not significantly reduced indicates that B cells from mice receiving both ZDV and SMX-TMP may have a decreased ability to isotype switch to produce IgG.

Isotype switching

All naïve B lymphocytes express IgM and IgD constitutively on their cell surfaces. After interacting with T cells in T cell zones of the LN, B cells begin secreting IgM as well, especially in the initial stages of a primary immune response. Some of these B cells migrate to a primary lymphoid follicle, where they form a germinal center (262). Classes of antibody other than IgM are only produced by B cells that undergo isotype switching, which occurs here in the germinal center. Most antibody in the plasma is class-switched antibody of the IgG isotype. This switch occurs as a result of B cells interacting with helper $CD4^+$ T cells (263, 264). B cells express a particular antigen on their surface in the context of MHC II. This cross-links with the TCR of a T cell that has been primed with the same antigen. CD40 on the B cell surface then ligates to CD40L on the surface of the T cell, providing a secondary signal to the B cells to stimulate class switching and antibody production (263, 264). Additionally, cytokine excretion from T cells (IL-4, IL-5, and TGF-β) also stimulates B cells, to govern which isotypes are produced by that particular cell (265). Combination exposure to ZDV and SMX-TMP could be influencing this interaction in some manner. Although peripheral T cell numbers have not been shown to be affected, Freund et. al. did demonstrate an alteration in T cell function as a result of ZDV plus SMX-TMP exposure (1).

In addition to isotype switching, it is in the germinal center that antibody production also undergoes somatic hypermutation and affinity maturation, in order to produce antibody that displays a high affinity to a specific antigen (266, 267). This occurs as cells are rapidly dividing. The toxicity of ZDV plus SMX-TMP could have an impact on these germinal center cells as they divide. This could account for the lower IgG titers that are observed both in the mice challenged with *Pneumocystis*, and in the HIV-

infected subjects that were vaccinated against influenza. This antibody with high affinity is the very type that is absent in patients with HIV. This drug affect could be contributing to this condition in these patients. Important future work will be to investigate the different B cell phenotypes in the context of infection, to determine whether ZDV plus SMX-TMP exposure results in selective depletion of follicular B cells.

Our data also suggests that IgG antibody titers from previous vaccination or infection are decreased by combination drug exposure. Subjects in the combination drug group had significantly lower pre-vaccination IgG levels. Many factors could have influenced this data since baseline titers before drug treatment were not measured. These include varied exposure to influenza and variable CD4 counts when previously vaccinated. While this should be interpreted conservatively, this data could signify a depletion of plasma cells that have migrated from the germinal centers to the bone marrow, which take up residence there and are very long-lived (268). These cells produce high-affinity, antigen-specific antibody for long periods. Bone marrow toxicity to B lymphocytes could include these plasma cells, although the fact that they are not rapidly dividing could protect them. This hypothesis will be tested in the future by analyzing this subtype of plasma cells that reside in the bone marrow. Additionally, affects on B cell memory as a result of drug exposure would also be interesting to investigate.

Response to vaccination

Immunoprotection is achieved with inactivated influenza vaccination in normal persons at a success rate of 70 to 90% (269). This declines for HIV patients as CD4 counts decrease (223-226, 270). Kroon et. al. measured the proportion of HIV-positive patients with CD4 counts greater than 300 cells/μl that have protective antibody titers from influenza vaccination in a 3-year study (270). At 30 days post-vaccination, 50 to 100% of subjects had protective antibody titers for influenza A, compared to healthy controls with 81-100% protective titer rates (270). Protective titer rates for influenza B were lower; between 64 and 75% versus 86 to 100% for healthy controls (270). This compares with our overall response rates for serum IgG in our subjects of 91% for influenza A and 56% for influenza B (our subjects had $CD4^+$ counts greater than 350 cells/μl). The difference in our study compared to the study conducted by Kroon et. al.

is that subjects cohorted to receive SMX-TMP in our investigation caused this group to have lower response rates of 83% and 33% for influenza A and B, respectively. It appears that SMX-TMP exposure causes protective titers to be reached in a lower percentage of healthy HIV-infected patients.

Further study of this phenomenon in humans is warranted. This data validates the pursuit of a large clinical trial to examine the immunosuppressive effects of concurrent ZDV and SMX-TMP therapy. In addition to a larger sample size and patient randomization, the use of normal healthy volunteers would be useful. This would isolate the effects of the drug combination, eliminating the confounding factors that are associated with HIV-infected patients, including affects of other medications (especially PI, which can decrease ZDV-induced apoptosis), variable $CD4^+$ counts and function, and direct effects of viral immunosuppression. The analysis of serial antibody titers would also be beneficial, because the differences we observed at a single point post-vaccination could be only a reflection of altered timing of the response. In addition, a vaccine to which the subjects were naïve (unlike influenza in most cases) would be more ideal, such as *Haemophilus* b vaccine.

Clinical experience with SMX-TMP

Despite the fact that the clinical significance of this drug-drug interaction is unknown, experience dictates that SMX-TMP must be discontinued in patients due to decreases in overall white blood cells counts. There is a subset of newly-diagnosed patients that, after beginning HAART, have viral loads that proceed to undetectable levels, but that do not have $CD4^+$ T cell counts rebound to safe numbers as usually seen (271). In one study, 17% of patients have a dissociation between viral load reduction to undetectable levels and a complete restoration (>50 cells/μl) after 6 months of HAART (271). Formal investigation of whether discontinuation of SMX-TMP in these patients improves $CD4^+$ T cell numbers has not been conducted.

E. CONCLUSIONS

We conclude that clinicians should consider this drug-drug interaction when treating patients with ZDV and SMX-TMP concurrently. Our findings demonstrate that the host response to infectious challenge is altered in mice and humans having received these agents in combination. This suppression of humoral immunity could affect morbidity and mortality of patients infected with HIV who receive both of these agents. This iatrogenic effect, if clinically significant, could have an impact on outcomes to other opportunistic and true pathogens that afflict this patient population. Additional antiretrovirals are available which cause much less bone marrow toxicity than ZDV, and patients at high risk of bone marrow suppression could potentially benefit from alternative agents in the treatment of their chronic HIV infection. Likewise, clinicians may wish to consider alternatives to SMX-TMP for the treatment and prophylaxis of PCP (such as TMP alone or aerosolized pentamadine) in specific patients.

REFERENCES

1. Freund, Y. R., L. Dousman, J. T. MacGregor, and N. Mohagheghpour. 2000. Oral treatment with trimethoprim-sulfamethoxazole and zidovudine suppresses murine accessory cell-dependent immune responses. *Toxicol Sci 55:335*.
2. McDonnell, P. J., and M. R. Jacobs. 2002. Hospital admissions resulting from preventable adverse drug reactions. *Ann Pharmacother 36:1331*.
3. Colt, H. G., and A. P. Shapiro. 1989. Drug-induced illness as a cause for admission to a community hospital. *J Am Geriatr Soc 37:323*.
4. Miller, R. R. 1974. Hospital admissions due to adverse drug reactions. A report from the Boston Collaborative Drug Surveillance Program. *Arch Intern Med 134:219*.
5. Bates, D. W., D. J. Cullen, N. Laird, L. A. Petersen, S. D. Small, D. Servi, G. Laffel, B. J. Sweitzer, B. F. Shea, R. Hallisey, and et al. 1995. Incidence of adverse drug events and potential adverse drug events. Implications for prevention. ADE Prevention Study Group. *Jama 274:29*.
6. Piscitelli, S. C., and K. D. Gallicano. 2001. Interactions among drugs for HIV and opportunistic infections. *N Engl J Med 344:984*.
7. Stein, D. S., J. A. Korvick, and S. H. Vermund. 1992. CD4+ lymphocyte cell enumeration for prediction of clinical course of human immunodeficiency virus disease: a review. *J Infect Dis 165:352*.
8. Levy, J. A., A. D. Hoffman, S. M. Kramer, J. A. Landis, J. M. Shimabukuro, and L. S. Oshiro. 1984. Isolation of lymphocytopathic retroviruses from San Francisco patients with AIDS. *Science 225:840*.
9. Popovic, M., M. G. Sarngadharan, E. Read, and R. C. Gallo. 1984. Detection, isolation, and continuous production of cytopathic retroviruses (HTLV-III) from patients with AIDS and pre-AIDS. *Science 224:497*.
10. Lifson, J. D., G. R. Reyes, M. S. McGrath, B. S. Stein, and E. G. Engleman. 1986. AIDS retrovirus induced cytopathology: giant cell formation and involvement of CD4 antigen. *Science 232:1123*.

11. Muro-Cacho, C. A., G. Pantaleo, and A. S. Fauci. 1995. Analysis of apoptosis in lymph nodes of HIV-infected persons. Intensity of apoptosis correlates with the general state of activation of the lymphoid tissue and not with stage of disease or viral burden. *J Immunol 154:5555*.
12. Fauci, A. S. 1996. Host factors in the pathogenesis of HIV disease. *Antibiot Chemother 48:4*.
13. Yang, O. O., S. A. Kalams, M. Rosenzweig, A. Trocha, N. Jones, M. Koziel, B. D. Walker, and R. P. Johnson. 1996. Efficient lysis of human immunodeficiency virus type 1-infected cells by cytotoxic T lymphocytes. *J Virol 70:5799*.
14. Cocchi, F., A. L. DeVico, A. Garzino-Demo, S. K. Arya, R. C. Gallo, and P. Lusso. 1995. Identification of RANTES, MIP-1 alpha, and MIP-1 beta as the major HIV-suppressive factors produced by CD8+ T cells. *Science 270:1811*.
15. Deng, H., R. Liu, W. Ellmeier, S. Choe, D. Unutmaz, M. Burkhart, P. Di Marzio, S. Marmon, R. E. Sutton, C. M. Hill, C. B. Davis, S. C. Peiper, T. J. Schall, D. R. Littman, and N. R. Landau. 1996. Identification of a major co-receptor for primary isolates of HIV-1. *Nature 381:661*.
16. Dragic, T., V. Litwin, G. P. Allaway, S. R. Martin, Y. Huang, K. A. Nagashima, C. Cayanan, P. J. Maddon, R. A. Koup, J. P. Moore, and W. A. Paxton. 1996. HIV-1 entry into CD4+ cells is mediated by the chemokine receptor CC-CKR-5. *Nature 381:667*.
17. Alkhatib, G., C. Combadiere, C. C. Broder, Y. Feng, P. E. Kennedy, P. M. Murphy, and E. A. Berger. 1996. CC CKR5: a RANTES, MIP-1alpha, MIP-1beta receptor as a fusion cofactor for macrophage-tropic HIV-1. *Science 272:1955*.
18. Walker, B. D., S. Chakrabarti, B. Moss, T. J. Paradis, T. Flynn, A. G. Durno, R. S. Blumberg, J. C. Kaplan, M. S. Hirsch, and R. T. Schooley. 1987. HIV-specific cytotoxic T lymphocytes in seropositive individuals. *Nature 328:345*.
19. Hoffenbach, A., P. Langlade-Demoyen, G. Dadaglio, E. Vilmer, F. Michel, C. Mayaud, B. Autran, and F. Plata. 1989. Unusually high frequencies of HIV-specific cytotoxic T lymphocytes in humans. *J Immunol 142:452*.
20. Pantaleo, G., C. Graziosi, and A. S. Fauci. 1993. The role of lymphoid organs in the pathogenesis of HIV infection. *Semin Immunol 5:157*.

21. Cease, K. B., H. Margalit, J. L. Cornette, S. D. Putney, W. G. Robey, C. Ouyang, H. Z. Streicher, P. J. Fischinger, R. C. Gallo, C. DeLisi, and et al. 1987. Helper T-cell antigenic site identification in the acquired immunodeficiency syndrome virus gp120 envelope protein and induction of immunity in mice to the native protein using a 16-residue synthetic peptide. *Proc Natl Acad Sci U S A 84:4249*.
22. Kinter, A. L., M. Ostrowski, D. Goletti, A. Oliva, D. Weissman, K. Gantt, E. Hardy, R. Jackson, L. Ehler, and A. S. Fauci. 1996. HIV replication in CD4+ T cells of HIV-infected individuals is regulated by a balance between the viral suppressive effects of endogenous beta-chemokines and the viral inductive effects of other endogenous cytokines. *Proc Natl Acad Sci U S A 93:14076*.
23. Sodroski, J., W. C. Goh, C. Rosen, K. Campbell, and W. A. Haseltine. 1986. Role of the HTLV-III/LAV envelope in syncytium formation and cytopathicity. *Nature 322:470*.
24. Weinhold, K. J., H. K. Lyerly, S. D. Stanley, A. A. Austin, T. J. Matthews, and D. P. Bolognesi. 1989. HIV-1 GP120-mediated immune suppression and lymphocyte destruction in the absence of viral infection. *J Immunol 142:3091*.
25. Manca, F., J. A. Habeshaw, and A. G. Dalgleish. 1990. HIV envelope glycoprotein, antigen specific T-cell responses, and soluble CD4. *Lancet 335:811*.
26. Banda, N. K., J. Bernier, D. K. Kurahara, R. Kurrle, N. Haigwood, R. P. Sekaly, and T. H. Finkel. 1992. Crosslinking CD4 by human immunodeficiency virus gp120 primes T cells for activation-induced apoptosis. *J Exp Med 176:1099*.
27. Folks, T. M., S. W. Kessler, J. M. Orenstein, J. S. Justement, E. S. Jaffe, and A. S. Fauci. 1988. Infection and replication of HIV-1 in purified progenitor cells of normal human bone marrow. *Science 242:919*.
28. Steinberg, H. N., C. S. Crumpacker, and P. A. Chatis. 1991. In vitro suppression of normal human bone marrow progenitor cells by human immunodeficiency virus. *J Virol 65:1765*.
29. Kagi, D., P. Seiler, J. Pavlovic, B. Ledermann, K. Burki, R. M. Zinkernagel, and H. Hengartner. 1995. The roles of perforin- and Fas-dependent cytotoxicity in protection against cytopathic and noncytopathic viruses. *Eur J Immunol 25:3256*.

30. Groux, H., G. Torpier, D. Monte, Y. Mouton, A. Capron, and J. C. Ameisen. 1992. Activation-induced death by apoptosis in CD4+ T cells from human immunodeficiency virus-infected asymptomatic individuals. *J Exp Med 175:331*.
31. Meyaard, L., S. A. Otto, R. R. Jonker, M. J. Mijnster, R. P. Keet, and F. Miedema. 1992. Programmed death of T cells in HIV-1 infection. *Science 257:217*.
32. Perfettini, J. L., M. Castedo, T. Roumier, K. Andreau, R. Nardacci, M. Piacentini, and G. Kroemer. 2005. Mechanisms of apoptosis induction by the HIV-1 envelope. *Cell Death Differ 12 Suppl 1:916*.
33. Pantaleo, G., and A. S. Fauci. 1996. Immunopathogenesis of HIV infection. *Annu Rev Microbiol 50:825*.
34. Clark, S. J., M. S. Saag, W. D. Decker, S. Campbell-Hill, J. L. Roberson, P. J. Veldkamp, J. C. Kappes, B. H. Hahn, and G. M. Shaw. 1991. High titers of cytopathic virus in plasma of patients with symptomatic primary HIV-1 infection. *N Engl J Med 324:954*.
35. Sei, Y., P. H. Tsang, F. N. Chu, I. Wallace, J. P. Roboz, P. S. Sarin, and J. G. Bekesi. 1989. Inverse relationship between HIV-1 p24 antigenemia, anti-p24 antibody and neutralizing antibody response in all stages of HIV-1 infection. *Immunol Lett 20:223*.
36. Lathey, J. L., I. C. Marschner, B. Kabat, and S. A. Spector. 1997. Deterioration of detectable human immunodeficiency virus serum p24 antigen in samples stored for batch testing. *J Clin Microbiol 35:631*.
37. Matthews, T. J., A. J. Langlois, W. G. Robey, N. T. Chang, R. C. Gallo, P. J. Fischinger, and D. P. Bolognesi. 1986. Restricted neutralization of divergent human T-lymphotropic virus type III isolates by antibodies to the major envelope glycoprotein. *Proc Natl Acad Sci U S A 83:9709*.
38. Rusche, J. R., K. Javaherian, C. McDanal, J. Petro, D. L. Lynn, R. Grimaila, A. Langlois, R. C. Gallo, L. O. Arthur, P. J. Fischinger, and et al. 1988. Antibodies that inhibit fusion of human immunodeficiency virus-infected cells bind a 24-amino acid sequence of the viral envelope, gp120. *Proc Natl Acad Sci U S A 85:3198*.

39. Wu, L., N. P. Gerard, R. Wyatt, H. Choe, C. Parolin, N. Ruffing, A. Borsetti, A. A. Cardoso, E. Desjardin, W. Newman, C. Gerard, and J. Sodroski. 1996. CD4-induced interaction of primary HIV-1 gp120 glycoproteins with the chemokine receptor CCR-5. *Nature 384:179*.
40. Pantaleo, G., S. Menzo, M. Vaccarezza, C. Graziosi, O. J. Cohen, J. F. Demarest, D. Montefiori, J. M. Orenstein, C. Fox, L. K. Schrager, and et al. 1995. Studies in subjects with long-term nonprogressive human immunodeficiency virus infection. *N Engl J Med 332:209*.
41. Cao, Y., L. Qin, L. Zhang, J. Safrit, and D. D. Ho. 1995. Virologic and immunologic characterization of long-term survivors of human immunodeficiency virus type 1 infection. *N Engl J Med 332:201*.
42. Robinson, W. E., Jr., D. C. Montefiori, and W. M. Mitchell. 1988. Antibody-dependent enhancement of human immunodeficiency virus type 1 infection. *Lancet 1:790*.
43. Robinson, W. E., Jr., T. Kawamura, M. K. Gorny, D. Lake, J. Y. Xu, Y. Matsumoto, T. Sugano, Y. Masuho, W. M. Mitchell, E. Hersh, and et al. 1990. Human monoclonal antibodies to the human immunodeficiency virus type 1 (HIV-1) transmembrane glycoprotein gp41 enhance HIV-1 infection in vitro. *Proc Natl Acad Sci U S A 87:3185*.
44. Martinez-Maza, O., E. Crabb, R. T. Mitsuyasu, J. L. Fahey, and J. V. Giorgi. 1987. Infection with the human immunodeficiency virus (HIV) is associated with an in vivo increase in B lymphocyte activation and immaturity. *J Immunol 138:3720*.
45. Lane, H. C., H. Masur, L. C. Edgar, G. Whalen, A. H. Rook, and A. S. Fauci. 1983. Abnormalities of B-cell activation and immunoregulation in patients with the acquired immunodeficiency syndrome. *N Engl J Med 309:453*.
46. Ammann, A. J., G. Schiffman, D. Abrams, P. Volberding, J. Ziegler, and M. Conant. 1984. B-cell immunodeficiency in acquired immune deficiency syndrome. *Jama 251:1447*.
47. Simberkoff, M. S., W. El Sadr, G. Schiffman, and J. J. Rahal, Jr. 1984. Streptococcus pneumoniae infections and bacteremia in patients with acquired

immune deficiency syndrome, with report of a pneumococcal vaccine failure. *Am Rev Respir Dis 130:1174*.

48. Bernstein, L. J., H. D. Ochs, R. J. Wedgwood, and A. Rubinstein. 1985. Defective humoral immunity in pediatric acquired immune deficiency syndrome. *J Pediatr 107:352*.
49. Ballet, J. J., G. Sulcebe, L. J. Couderc, F. Danon, C. Rabian, M. Lathrop, J. P. Clauvel, and M. Seligmann. 1987. Impaired anti-pneumococcal antibody response in patients with AIDS-related persistent generalized lymphadenopathy. *Clin Exp Immunol 68:479*.
50. Janoff, E. N., J. M. Douglas, Jr., M. Gabriel, M. J. Blaser, A. J. Davidson, D. L. Cohn, and F. N. Judson. 1988. Class-specific antibody response to pneumococcal capsular polysaccharides in men infected with human immunodeficiency virus type 1. *J Infect Dis 158:983*.
51. Dawood, M. R., B. Conway, P. Patenaude, F. Janmohamed, J. S. Montaner, M. V. O'Shaughnessy, and G. W. Hammond. 1998. Association of phenotypic changes in B cell lymphocytes and plasma viral load in human immunodeficiency virus-infected patients. *J Clin Immunol 18:235*.
52. Wolthers, K. C., S. A. Otto, S. M. Lens, R. A. Van Lier, F. Miedema, and L. Meyaard. 1997. Functional B cell abnormalities in HIV type 1 infection: role of CD40L and CD70. *AIDS Res Hum Retroviruses 13:1023*.
53. De Milito, A., C. Morch, A. Sonnerborg, and F. Chiodi. 2001. Loss of memory (CD27) B lymphocytes in HIV-1 infection. *Aids 15:957*.
54. Heffernan, R. T., N. L. Barrett, K. M. Gallagher, J. L. Hadler, L. H. Harrison, A. L. Reingold, K. Khoshnood, T. R. Holford, and A. Schuchat. 2005. Declining incidence of invasive Streptococcus pneumoniae infections among persons with AIDS in an era of highly active antiretroviral therapy, 1995-2000. *J Infect Dis 191:2038*.
55. Miller, R. 1996. HIV-associated respiratory diseases. *Lancet 348:307*.
56. Katlama, C., and G. M. Dickinson. 1993. Update on opportunistic infections. *Aids 7 Suppl 1:S185*.

57. Hirschtick, R. E., J. Glassroth, M. C. Jordan, T. C. Wilcosky, J. M. Wallace, P. A. Kvale, N. Markowitz, M. J. Rosen, B. T. Mangura, and P. C. Hopewell. 1995. Bacterial pneumonia in persons infected with the human immunodeficiency virus. Pulmonary Complications of HIV Infection Study Group. *N Engl J Med 333:845*.
58. Clarke, P. G. 1990. Developmental cell death: morphological diversity and multiple mechanisms. *Anat Embryol (Berl) 181:195*.
59. Martin, S. J., D. M. Finucane, G. P. Amarante-Mendes, G. A. O'Brien, and D. R. Green. 1996. Phosphatidylserine externalization during CD95-induced apoptosis of cells and cytoplasts requires ICE/CED-3 protease activity. *J Biol Chem 271:28753*.
60. Yuan, J., E. Angelucci, G. Lucarelli, M. Aljurf, L. M. Snyder, C. R. Kiefer, L. Ma, and S. L. Schrier. 1993. Accelerated programmed cell death (apoptosis) in erythroid precursors of patients with severe beta-thalassemia (Cooley's anemia). *Blood 82:374*.
61. Savill, J. S., P. M. Henson, and C. Haslett. 1989. Phagocytosis of aged human neutrophils by macrophages is mediated by a novel "charge-sensitive" recognition mechanism. *J Clin Invest 84:1518*.
62. Fadok, V. A., D. L. Bratton, A. Konowal, P. W. Freed, J. Y. Westcott, and P. M. Henson. 1998. Macrophages that have ingested apoptotic cells in vitro inhibit proinflammatory cytokine production through autocrine/paracrine mechanisms involving TGF-beta, PGE2, and PAF. *J Clin Invest 101:890*.
63. Brancolini, C., M. Benedetti, and C. Schneider. 1995. Microfilament reorganization during apoptosis: the role of Gas2, a possible substrate for ICE-like proteases. *Embo J 14:5179*.
64. Darmon, A. J., D. W. Nicholson, and R. C. Bleackley. 1995. Activation of the apoptotic protease CPP32 by cytotoxic T-cell-derived granzyme B. *Nature 377:446*.
65. Nicholson, D. W., A. Ali, N. A. Thornberry, J. P. Vaillancourt, C. K. Ding, M. Gallant, Y. Gareau, P. R. Griffin, M. Labelle, Y. A. Lazebnik, and et al. 1995. Identification and inhibition of the ICE/CED-3 protease necessary for mammalian apoptosis. *Nature 376:37*.

66. Salvesen, G. S., and V. M. Dixit. 1997. Caspases: intracellular signaling by proteolysis. *Cell 91:443*.
67. Yu, S. W., H. Wang, M. F. Poitras, C. Coombs, W. J. Bowers, H. J. Federoff, G. G. Poirier, T. M. Dawson, and V. L. Dawson. 2002. Mediation of poly(ADP-ribose) polymerase-1-dependent cell death by apoptosis-inducing factor. *Science 297:259*.
68. Majno, G., and I. Joris. 1995. Apoptosis, oncosis, and necrosis. An overview of cell death. *Am J Pathol 146:3*.
69. Pitti, R. M., S. A. Marsters, S. Ruppert, C. J. Donahue, A. Moore, and A. Ashkenazi. 1996. Induction of apoptosis by Apo-2 ligand, a new member of the tumor necrosis factor cytokine family. *J Biol Chem 271:12687*.
70. Pan, G., K. O'Rourke, A. M. Chinnaiyan, R. Gentz, R. Ebner, J. Ni, and V. M. Dixit. 1997. The receptor for the cytotoxic ligand TRAIL. *Science 276:111*.
71. Nagata, S., and T. Suda. 1995. Fas and Fas ligand: lpr and gld mutations. *Immunol Today 16:39*.
72. Rokhlin, O. W., R. A. Glover, and M. B. Cohen. 1998. Fas-mediated apoptosis in human prostatic carcinoma cell lines occurs via activation of caspase-8 and caspase-7. *Cancer Res 58:5870*.
73. Kischkel, F. C., S. Hellbardt, I. Behrmann, M. Germer, M. Pawlita, P. H. Krammer, and M. E. Peter. 1995. Cytotoxicity-dependent APO-1 (Fas/CD95)-associated proteins form a death-inducing signaling complex (DISC) with the receptor. *Embo J 14:5579*.
74. Korsmeyer, S. J., M. C. Wei, M. Saito, S. Weiler, K. J. Oh, and P. H. Schlesinger. 2000. Pro-apoptotic cascade activates BID, which oligomerizes BAK or BAX into pores that result in the release of cytochrome c. *Cell Death Differ 7:1166*.
75. Alimonti, J. B., L. Shi, P. K. Baijal, and A. H. Greenberg. 2001. Granzyme B induces BID-mediated cytochrome c release and mitochondrial permeability transition. *J Biol Chem 276:6974*.
76. Gross, A. 2001. BCL-2 proteins: regulators of the mitochondrial apoptotic program. *IUBMB Life 52:231*.

77. Slee, E. A., M. T. Harte, R. M. Kluck, B. B. Wolf, C. A. Casiano, D. D. Newmeyer, H. G. Wang, J. C. Reed, D. W. Nicholson, E. S. Alnemri, D. R. Green, and S. J. Martin. 1999. Ordering the cytochrome c-initiated caspase cascade: hierarchical activation of caspases-2, -3, -6, -7, -8, and -10 in a caspase-9-dependent manner. *J Cell Biol 144:281*.

78. Zou, H., Y. Li, X. Liu, and X. Wang. 1999. An APAF-1.cytochrome c multimeric complex is a functional apoptosome that activates procaspase-9. *J Biol Chem 274:11549*.

79. Fischl, M. A. 1999. Antiretroviral therapy in 1999 for antiretroviral-naive individuals with HIV infection. *Aids 13 Suppl 1:S49*.

80. Gulick, R. M., J. W. Mellors, D. Havlir, J. J. Eron, A. Meibohm, J. H. Condra, F. T. Valentine, D. McMahon, C. Gonzalez, L. Jonas, E. A. Emini, J. A. Chodakewitz, R. Isaacs, and D. D. Richman. 2000. 3-year suppression of HIV viremia with indinavir, zidovudine, and lamivudine. *Ann Intern Med 133:35*.

81. Montaner, J. S., R. Hogg, J. Raboud, R. Harrigan, and M. O'Shaughnessy. 1998. Antiretroviral treatment in 1998. *Lancet 352:1919*.

82. Autran, B., G. Carcelain, T. S. Li, C. Blanc, D. Mathez, R. Tubiana, C. Katlama, P. Debre, and J. Leibowitch. 1997. Positive effects of combined antiretroviral therapy on CD4+ T cell homeostasis and function in advanced HIV disease. *Science 277:112*.

83. Lederman, M. M., E. Connick, A. Landay, D. R. Kuritzkes, J. Spritzler, M. St Clair, B. L. Kotzin, L. Fox, M. H. Chiozzi, J. M. Leonard, F. Rousseau, M. Wade, J. D. Roe, A. Martinez, and H. Kessler. 1998. Immunologic responses associated with 12 weeks of combination antiretroviral therapy consisting of zidovudine, lamivudine, and ritonavir: results of AIDS Clinical Trials Group Protocol 315. *J Infect Dis 178:70*.

84. Gulick, R. M., J. W. Mellors, D. Havlir, J. J. Eron, C. Gonzalez, D. McMahon, L. Jonas, A. Meibohm, D. Holder, W. A. Schleif, J. H. Condra, E. A. Emini, R. Isaacs, J. A. Chodakewitz, and D. D. Richman. 1998. Simultaneous vs sequential initiation of therapy with indinavir, zidovudine, and lamivudine for HIV-1 infection: 100-week follow-up. *Jama 280:35*.

85. Hammer, S. M., K. E. Squires, M. D. Hughes, J. M. Grimes, L. M. Demeter, J. S. Currier, J. J. Eron, Jr., J. E. Feinberg, H. H. Balfour, Jr., L. R. Deyton, J. A. Chodakewitz, and M. A. Fischl. 1997. A controlled trial of two nucleoside analogues plus indinavir in persons with human immunodeficiency virus infection and CD4 cell counts of 200 per cubic millimeter or less. AIDS Clinical Trials Group 320 Study Team. *N Engl J Med 337:725*.

86. Lu, W., and J. M. Andrieu. 2000. HIV protease inhibitors restore impaired T-cell proliferative response in vivo and in vitro: a viral-suppression-independent mechanism. *Blood 96:250*.

87. Mathez, D., P. Bagnarelli, I. Gorin, C. Katlama, G. Pialoux, G. Saimot, P. Tubiana, P. De Truchis, J. P. Chauvin, R. Mills, R. Rode, M. Clementi, and J. Leibowitch. 1997. Reductions in viral load and increases in T lymphocyte numbers in treatment-naive patients with advanced HIV-1 infection treated with ritonavir, zidovudine and zalcitabine triple therapy. *Antivir Ther 2:175*.

88. Murphy, E. L., A. C. Collier, L. A. Kalish, S. F. Assmann, M. F. Para, T. P. Flanigan, P. N. Kumar, L. Mintz, F. R. Wallach, and G. J. Nemo. 2001. Highly active antiretroviral therapy decreases mortality and morbidity in patients with advanced HIV disease. *Ann Intern Med 135:17*.

89. Verbraak, F. D., R. Boom, P. M. Wertheim-van Dillen, G. J. van den Horn, A. Kijlstra, and M. D. de Smet. 1999. Influence of highly active antiretroviral therapy on the development of CMV disease in HIV positive patients at high risk for CMV disease. *Br J Ophthalmol 83:1186*.

90. Isgro, A., I. Mezzaroma, A. Aiuti, A. Fantauzzi, M. Pinti, A. Cossarizza, and F. Aiuti. 2004. Decreased apoptosis of bone marrow progenitor cells in HIV-1-infected patients during highly active antiretroviral therapy. *Aids 18:1335*.

91. Sloand, E. M., P. N. Kumar, S. Kim, A. Chaudhuri, F. F. Weichold, and N. S. Young. 1999. Human immunodeficiency virus type 1 protease inhibitor modulates activation of peripheral blood CD4(+) T cells and decreases their susceptibility to apoptosis in vitro and in vivo. *Blood 94:1021*.

92. Katsikis, P. D., M. E. Garcia-Ojeda, J. F. Torres-Roca, I. M. Tijoe, C. A. Smith, and L. A. Herzenberg. 1997. Interleukin-1 beta converting enzyme-like protease

involvement in Fas-induced and activation-induced peripheral blood T cell apoptosis in HIV infection. TNF-related apoptosis-inducing ligand can mediate activation-induced T cell death in HIV infection. *J Exp Med 186:1365*.

93. Sloand, E. M., J. Maciejewski, P. Kumar, S. Kim, A. Chaudhuri, and N. Young. 2000. Protease inhibitors stimulate hematopoiesis and decrease apoptosis and ICE expression in CD34(+) cells. *Blood 96:2735*.
94. Clifford, G. M., J. Polesel, M. Rickenbach, L. Dal Maso, O. Keiser, A. Kofler, E. Rapiti, F. Levi, G. Jundt, T. Fisch, A. Bordoni, D. De Weck, and S. Franceschi. 2005. Cancer risk in the Swiss HIV Cohort Study: associations with immunodeficiency, smoking, and highly active antiretroviral therapy. *J Natl Cancer Inst 97:425*.
95. Cheung, T. W. 2004. AIDS-related cancer in the era of highly active antiretroviral therapy (HAART): a model of the interplay of the immune system, virus, and cancer. "On the offensive--the Trojan Horse is being destroyed"--Part B: Malignant lymphoma. *Cancer Invest 22:787*.
96. Jaresko, G. S. 1999. Etiology of neutropenia in HIV-infected patients. *Am J Health Syst Pharm 56 Suppl 5:S5*.
97. Castella, A., T. S. Croxson, D. Mildvan, D. H. Witt, and R. Zalusky. 1985. The bone marrow in AIDS. A histologic, hematologic, and microbiologic study. *Am J Clin Pathol 84:425*.
98. Sun, N. C., P. Shapshak, N. A. Lachant, M. Y. Hsu, L. Sieger, P. Schmid, G. Beall, and D. T. Imagawa. 1989. Bone marrow examination in patients with AIDS and AIDS-related complex (ARC). Morphologic and in situ hybridization studies. *Am J Clin Pathol 92:589*.
99. Aoki, Y., and G. Tosato. 2004. Neoplastic conditions in the context of HIV-1 infection. *Curr HIV Res 2:343*.
100. Volberding, P. A., S. W. Lagakos, M. A. Koch, C. Pettinelli, M. W. Myers, D. K. Booth, H. H. Balfour, Jr., R. C. Reichman, J. A. Bartlett, M. S. Hirsch, and et al. 1990. Zidovudine in asymptomatic human immunodeficiency virus infection. A controlled trial in persons with fewer than 500 CD4-positive cells per cubic

millimeter. The AIDS Clinical Trials Group of the National Institute of Allergy and Infectious Diseases. *N Engl J Med 322:941*.

101. Fischl, M. A., D. D. Richman, N. Hansen, A. C. Collier, J. T. Carey, M. F. Para, W. D. Hardy, R. Dolin, W. G. Powderly, J. D. Allan, and et al. 1990. The safety and efficacy of zidovudine (AZT) in the treatment of subjects with mildly symptomatic human immunodeficiency virus type 1 (HIV) infection. A double-blind, placebo-controlled trial. The AIDS Clinical Trials Group. *Ann Intern Med 112:727*.
102. Tseng, A., J. Conly, D. Fletcher, D. Keystone, I. Salit, and S. Walmsley. 1998. Precipitous declines in hemoglobin levels associated with combination zidovudine and lamivudine therapy. *Clin Infect Dis 27:908*.
103. Richman, D. D., M. A. Fischl, M. H. Grieco, M. S. Gottlieb, P. A. Volberding, O. L. Laskin, J. M. Leedom, J. E. Groopman, D. Mildvan, M. S. Hirsch, and et al. 1987. The toxicity of azidothymidine (AZT) in the treatment of patients with AIDS and AIDS-related complex. A double-blind, placebo-controlled trial. *N Engl J Med 317:192*.
104. McKinney, R. E., Jr., M. A. Maha, E. M. Connor, J. Feinberg, G. B. Scott, M. Wulfsohn, K. McIntosh, W. Borkowsky, J. F. Modlin, P. Weintrub, and et al. 1991. A multicenter trial of oral zidovudine in children with advanced human immunodeficiency virus disease. The Protocol 043 Study Group. *N Engl J Med 324:1018*.
105. Gill, P. S., M. Rarick, R. K. Brynes, D. Causey, C. Loureiro, and A. M. Levine. 1987. Azidothymidine associated with bone marrow failure in the acquired immunodeficiency syndrome (AIDS). *Ann Intern Med 107:502*.
106. Romanelli, F., K. Empey, and C. Pomeroy. 2002. Macrocytosis as an indicator of medication (zidovudine) adherence in patients with HIV infection. *AIDS Patient Care STDS 16:405*.
107. Furman, P. A., J. A. Fyfe, M. H. St Clair, K. Weinhold, J. L. Rideout, G. A. Freeman, S. N. Lehrman, D. P. Bolognesi, S. Broder, H. Mitsuya, and et al. 1986. Phosphorylation of 3'-azido-3'-deoxythymidine and selective interaction of the 5'-

triphosphate with human immunodeficiency virus reverse transcriptase. *Proc Natl Acad Sci U S A 83:8333*.

108. Dainiak, N., M. Worthington, M. A. Riordan, S. Kreczko, and L. Goldman. 1988. 3'-Azido-3'-deoxythymidine (AZT) inhibits proliferation in vitro of human haematopoietic progenitor cells. *Br J Haematol 69:299*.
109. Bogliolo, G., R. Lerza, M. Mencoboni, A. Saviane, and I. Pannacciulli. 1988. Azidothymidine-induced depression of murine hemopoietic progenitor cells. *Exp Hematol 16:938*.
110. Sommadossi, J. P., and R. Carlisle. 1987. Toxicity of 3'-azido-3'-deoxythymidine and 9-(1,3-dihydroxy-2-propoxymethyl)guanine for normal human hematopoietic progenitor cells in vitro. *Antimicrob Agents Chemother 31:452*.
111. Viora, M., G. Di Genova, R. Rivabene, W. Malorni, and A. Fattorossi. 1997. Interference with cell cycle progression and induction of apoptosis by dideoxynucleoside analogs. *Int J Immunopharmacol 19:311*.
112. Barile, M., D. Valenti, E. Quagliariello, and S. Passarella. 1998. Mitochondria as cell targets of AZT (zidovudine). *Gen Pharmacol 31:531*.
113. Foli, A., F. Benvenuto, G. Piccinini, A. Bareggi, A. Cossarizza, J. Lisziewicz, and F. Lori. 2001. Direct analysis of mitochondrial toxicity of antiretroviral drugs. *Aids 15:1687*.
114. Lim, S. E., M. V. Ponamarev, M. J. Longley, and W. C. Copeland. 2003. Structural determinants in human DNA polymerase gamma account for mitochondrial toxicity from nucleoside analogs. *J Mol Biol 329:45*.
115. Rustin, P. 2001. Mitochondrial dysfunction in HIV infection: an overview of pathogenesis. *J HIV Ther 6:4*.
116. Cote, H. C., Z. L. Brumme, K. J. Craib, C. S. Alexander, B. Wynhoven, L. Ting, H. Wong, M. Harris, P. R. Harrigan, M. V. O'Shaughnessy, and J. S. Montaner. 2002. Changes in mitochondrial DNA as a marker of nucleoside toxicity in HIV-infected patients. *N Engl J Med 346:811*.
117. Moyle, G. 2000. Clinical manifestations and management of antiretroviral nucleoside analog-related mitochondrial toxicity. *Clin Ther 22:911*.

118. Zaera, M. G., O. Miro, E. Pedrol, A. Soler, M. Picon, F. Cardellach, J. Casademont, and V. Nunes. 2001. Mitochondrial involvement in antiretroviral therapy-related lipodystrophy. *Aids 15:1643*.
119. Kakuda, T. N. 2000. Pharmacology of nucleoside and nucleotide reverse transcriptase inhibitor-induced mitochondrial toxicity. *Clin Ther 22:685*.
120. Matarrese, P., L. Gambardella, A. Cassone, S. Vella, R. Cauda, and W. Malorni. 2003. Mitochondrial membrane hyperpolarization hijacks activated T lymphocytes toward the apoptotic-prone phenotype: homeostatic mechanisms of HIV protease inhibitors. *J Immunol 170:6006*.
121. Phenix, B. N., J. B. Angel, F. Mandy, S. Kravcik, K. Parato, K. A. Chambers, K. Gallicano, N. Hawley-Foss, S. Cassol, D. W. Cameron, and A. D. Badley. 2000. Decreased HIV-associated T cell apoptosis by HIV protease inhibitors. *AIDS Res Hum Retroviruses 16:559*.
122. Chavan, S. J., S. L. Tamma, M. Kaplan, M. Gersten, and S. G. Pahwa. 1999. Reduction in T cell apoptosis in patients with HIV disease following antiretroviral therapy. *Clin Immunol 93:24*.
123. McKallip, R. J., M. Nagarkatti, and P. S. Nagarkatti. 1995. Immunotoxicity of AZT: inhibitory effect on thymocyte differentiation and peripheral T cell responsiveness to gp120 of human immunodeficiency virus. *Toxicol Appl Pharmacol 131:53*.
124. Gallicchio, V. S., N. K. Hughes, B. C. Hulette, and L. Noblitt. 1991. Effect of interleukin-1, GM-CSF, erythropoietin, and lithium on the toxicity associated with 3'-azido-3'-deoxythymidine (AZT) in vitro on hematopoietic progenitors (CFU-GM, CFU-MEG, and BFU-E) using murine retrovirus-infected hematopoietic cells. *J Leukoc Biol 50:580*.
125. Hengge, U. R., C. Borchard, S. Esser, M. Schroder, A. Mirmohammadsadegh, and M. Goos. 2002. Lymphocytes proliferate in blood and lymph nodes following interleukin-2 therapy in addition to highly active antiretroviral therapy. *Aids 16:151*.
126. Gougeon, M. L., C. Rouzioux, I. Liberman, M. Burgard, Y. Taoufik, J. P. Viard, K. Bouchenafa, C. Capitant, J. F. Delfraissy, and Y. Levy. 2001. Immunological and

virological effects of long term IL-2 therapy in HIV-1-infected patients. *Aids 15:1729*.

127. Moyle, G. J., E. Bouza, F. Antunes, D. Smith, R. Harris, M. Warburg, and M. Walker. 1997. Zidovudine monotherapy versus zidovudine plus zalcitabine combination therapy in HIV-positive persons with CD4 cell counts 300-500 cells/mm3: a double-blind controlled trial. The M50003 Study Group Coordinating and Writing Committee. *Antivir Ther 2:229*.
128. Bakshi, S. S., P. Britto, E. Capparelli, L. Mofenson, M. G. Fowler, S. Rasheed, D. Schoenfeld, B. Zimmer, Y. Frank, R. Yogev, E. Jimenez, M. Salgo, G. Boone, and S. G. Pahwa. 1997. Evaluation of pharmacokinetics, safety, tolerance, and activity of combination of zalcitabine and zidovudine in stable, zidovudine-treated pediatric patients with human immunodeficiency virus infection. AIDS Clinical Trials Group Protocol 190 Team. *J Infect Dis 175:1039*.
129. Yarchoan, R., C. F. Perno, R. V. Thomas, R. W. Klecker, J. P. Allain, R. J. Wills, N. McAtee, M. A. Fischl, R. Dubinsky, M. C. McNeely, and et al. 1988. Phase I studies of 2',3'-dideoxycytidine in severe human immunodeficiency virus infection as a single agent and alternating with zidovudine (AZT). *Lancet 1:76*.
130. Abrams, D. I., A. I. Goldman, C. Launer, J. A. Korvick, J. D. Neaton, L. R. Crane, M. Grodesky, S. Wakefield, K. Muth, S. Kornegay, and et al. 1994. A comparative trial of didanosine or zalcitabine after treatment with zidovudine in patients with human immunodeficiency virus infection. The Terry Beirn Community Programs for Clinical Research on AIDS. *N Engl J Med 330:657*.
131. Schindzielorz, A., I. Pike, M. Daniels, L. Pacelli, and L. Smaldone. 1994. Rates and risk factors for adverse events associated with didanosine in the expanded access program. *Clin Infect Dis 19:1076*.
132. Davey, R. T., Jr., D. G. Chaitt, G. F. Reed, W. W. Freimuth, B. R. Herpin, J. A. Metcalf, P. S. Eastman, J. Falloon, J. A. Kovacs, M. A. Polis, R. E. Walker, H. Masur, J. Boyle, S. Coleman, S. R. Cox, L. Wathen, C. L. Daenzer, and H. C. Lane. 1996. Randomized, controlled phase I/II, trial of combination therapy with delavirdine (U-90152S) and conventional nucleosides in human

immunodeficiency virus type 1-infected patients. *Antimicrob Agents Chemother 40:1657*.

133. Wilde, J. T. 2000. Protease inhibitor therapy and bleeding. *Haemophilia 6:487*.
134. Racoosin, J. A., and C. M. Kessler. 1999. Bleeding episodes in HIV-positive patients taking HIV protease inhibitors: a case series. *Haemophilia 5:266*.
135. Krogstad, P., A. Wiznia, K. Luzuriaga, W. Dankner, K. Nielsen, M. Gersten, B. Kerr, A. Hendricks, B. Boczany, M. Rosenberg, D. Jung, S. A. Spector, and Y. Bryson. 1999. Treatment of human immunodeficiency virus 1-infected infants and children with the protease inhibitor nelfinavir mesylate. *Clin Infect Dis 28:1109*.
136. Deeks, S. G., P. Barditch-Crovo, P. S. Lietman, F. Hwang, K. C. Cundy, J. F. Rooney, N. S. Hellmann, S. Safrin, and J. O. Kahn. 1998. Safety, pharmacokinetics, and antiretroviral activity of intravenous 9-[2-(R)-(Phosphonomethoxy)propyl]adenine, a novel anti-human immunodeficiency virus (HIV) therapy, in HIV-infected adults. *Antimicrob Agents Chemother 42:2380*.
137. Kitchen, V. S., C. Skinner, K. Ariyoshi, E. A. Lane, I. B. Duncan, J. Burckhardt, H. U. Burger, K. Bragman, A. J. Pinching, and J. N. Weber. 1995. Safety and activity of saquinavir in HIV infection. *Lancet 345:952*.
138. Wagstaff, A. J., and H. M. Bryson. 1994. Foscarnet. A reappraisal of its antiviral activity, pharmacokinetic properties and therapeutic use in immunocompromised patients with viral infections. *Drugs 48:199*.
139. Fanning, M. M., S. E. Read, M. Benson, S. Vas, A. Rachlis, V. Kozousek, C. Mortimer, P. Harvey, C. Schwartz, E. Chew, and et al. 1990. Foscarnet therapy of cytomegalovirus retinitis in AIDS. *J Acquir Immune Defic Syndr 3:472*.
140. Jacobson, M. A., J. J. O'Donnell, and J. Mills. 1989. Foscarnet treatment of cytomegalovirus retinitis in patients with the acquired immunodeficiency syndrome. *Antimicrob Agents Chemother 33:736*.
141. Lea, A. P., and H. M. Bryson. 1996. Cidofovir. *Drugs 52:225*.
142. Ognibene, A. J. 1970. Agranulocytosis due to dapsone. *Ann Intern Med 72:521*.
143. Catalano, P. M. 1971. Dapsone agranulocytosis. *Arch Dermatol 104:675*.
144. Foucauld, J., W. Uphouse, and J. Berenberg. 1985. Dapsone and aplastic anemia. *Ann Intern Med 102:139*.

145. Allegra, C. J., J. A. Kovacs, J. C. Drake, J. C. Swan, B. A. Chabner, and H. Masur. 1987. Activity of antifolates against Pneumocystis carinii dihydrofolate reductase and identification of a potent new agent. *J Exp Med 165:926*.
146. Sattler, F. R., C. J. Allegra, T. D. Verdegem, B. Akil, C. U. Tuazon, C. Hughlett, D. Ogata-Arakaki, J. Feinberg, J. Shelhamer, H. C. Lane, and et al. 1990. Trimetrexate-leucovorin dosage evaluation study for treatment of Pneumocystis carinii pneumonia. *J Infect Dis 161:91*.
147. Ansdell, V. E., S. G. Wright, and D. B. Hutchinson. 1976. Megaloblastic anaemia associated with combined pyrimethamine and co-trimoxazole administration. *Lancet 2:1257*.
148. Fleming, A. F., D. A. Warrell, and H. Dickmeiss. 1974. Letter: Co-trimoxazole and the blood. *Lancet 2:284*.
149. Gordin, F. M., G. L. Simon, C. B. Wofsy, and J. Mills. 1984. Adverse reactions to trimethoprim-sulfamethoxazole in patients with the acquired immunodeficiency syndrome. *Ann Intern Med 100:495*.
150. Kovacs, J. A., J. W. Hiemenz, A. M. Macher, D. Stover, H. W. Murray, J. Shelhamer, H. C. Lane, C. Urmacher, C. Honig, D. L. Longo, and et al. 1984. Pneumocystis carinii pneumonia: a comparison between patients with the acquired immunodeficiency syndrome and patients with other immunodeficiencies. *Ann Intern Med 100:663*.
151. Carr, A., B. Tindall, R. Penny, and D. A. Cooper. 1993. Patterns of multiple-drug hypersensitivities in HIV-infected patients. *Aids 7:1532*.
152. Naisbitt, D. J., S. J. Hough, H. J. Gill, M. Pirmohamed, N. R. Kitteringham, and B. K. Park. 1999. Cellular disposition of sulphamethoxazole and its metabolites: implications for hypersensitivity. *Br J Pharmacol 126:1393*.
153. Buhl, R., H. A. Jaffe, K. J. Holroyd, F. B. Wells, A. Mastrangeli, C. Saltini, A. M. Cantin, and R. G. Crystal. 1989. Systemic glutathione deficiency in symptom-free HIV-seropositive individuals. *Lancet 2:1294*.
154. Carr, A., B. Tindall, R. Penny, and D. A. Cooper. 1993. In vitro cytotoxicity as a marker of hypersensitivity to sulphamethoxazole in patients with HIV. *Clin Exp Immunol 94:21*.

155. Cribb, A. E., M. Miller, J. S. Leeder, J. Hill, and S. P. Spielberg. 1991. Reactions of the nitroso and hydroxylamine metabolites of sulfamethoxazole with reduced glutathione. Implications for idiosyncratic toxicity. *Drug Metab Dispos 19:900*.
156. Cribb, A. E., and S. P. Spielberg. 1990. Hepatic microsomal metabolism of sulfamethoxazole to the hydroxylamine. *Drug Metab Dispos 18:784*.
157. Sahai, J., K. Gallicano, A. Pakuts, and D. W. Cameron. 1994. Effect of fluconazole on zidovudine pharmacokinetics in patients infected with human immunodeficiency virus. *J Infect Dis 169:1103*.
158. Chatton, J. Y., A. Munafo, J. P. Chave, F. Steinhauslin, F. Roch-Ramel, M. P. Glauser, and J. Biollaz. 1992. Trimethoprim, alone or in combination with sulphamethoxazole, decreases the renal excretion of zidovudine and its glucuronide. *Br J Clin Pharmacol 34:551*.
159. McCance-Katz, E. F., P. M. Rainey, P. Jatlow, and G. Friedland. 1998. Methadone effects on zidovudine disposition (AIDS Clinical Trials Group 262). *J Acquir Immune Defic Syndr Hum Retrovirol 18:435*.
160. Lee, B. L., M. G. Tauber, B. Sadler, D. Goldstein, and H. F. Chambers. 1996. Atovaquone inhibits the glucuronidation and increases the plasma concentrations of zidovudine. *Clin Pharmacol Ther 59:14*.
161. de Miranda, P., S. S. Good, R. Yarchoan, R. V. Thomas, M. R. Blum, C. E. Myers, and S. Broder. 1989. Alteration of zidovudine pharmacokinetics by probenecid in patients with AIDS or AIDS-related complex. *Clin Pharmacol Ther 46:494*.
162. Kornhauser, D. M., B. G. Petty, C. W. Hendrix, A. S. Woods, L. J. Nerhood, J. G. Bartlett, and P. S. Lietman. 1989. Probenecid and zidovudine metabolism. *Lancet 2:473*.
163. Merry, C., M. G. Barry, F. Mulcahy, M. Ryan, J. Heavey, J. F. Tjia, S. E. Gibbons, A. M. Breckenridge, and D. J. Back. 1997. Saquinavir pharmacokinetics alone and in combination with ritonavir in HIV-infected patients. *Aids 11:F29*.
164. Barry, M., F. Mulcahy, C. Merry, S. Gibbons, and D. Back. 1999. Pharmacokinetics and potential interactions amongst antiretroviral agents used to treat patients with HIV infection. *Clin Pharmacokinet 36:289*.

165. Hochster, H., D. Dieterich, S. Bozzette, R. C. Reichman, J. D. Connor, L. Liebes, R. L. Sonke, S. A. Spector, F. Valentine, C. Pettinelli, and et al. 1990. Toxicity of combined ganciclovir and zidovudine for cytomegalovirus disease associated with AIDS. An AIDS Clinical Trials Group Study. *Ann Intern Med 113:111*.
166. Jacobson, M. A., W. Owen, J. Campbell, C. Brosgart, and D. I. Abrams. 1993. Tolerability of combined ganciclovir and didanosine for the treatment of cytomegalovirus disease associated with AIDS. *Clin Infect Dis 16 Suppl 1:S69*.
167. Group, S. o. O. C. o. A. R. 1992. Mortality in patients with the acquired immunodeficiency syndrome treated with either foscarnet or ganciclovir for cytomegalovirus retinitis. Studies of Ocular Complications of AIDS Research Group, in collaboration with the AIDS Clinical Trials Group. *N Engl J Med 326:213*.
168. Freund, Y. R., L. Dousman, E. S. Riccio, B. Sato, J. T. MacGregor, and N. Mohagheghpour. 2001. Immunohematotoxicity studies with combinations of dapsone and zidovudine. *Int Immunopharmacol 1:2131*.
169. Freund, Y. R., L. Dousman, and N. Mohagheghpour. 2002. Prophylactic clarithromycin to treat mycobacterium avium in HIV patients receiving zidovudine may significantly increase mortality by suppressing lymphopoiesis and hematopoiesis. *Int Immunopharmacol 2:1465*.
170. Slavin, M. A., J. F. Hoy, K. Stewart, M. B. Pettinger, C. R. Lucas, and S. J. Kent. 1992. Oral dapsone versus nebulized pentamidine for Pneumocystis carinii pneumonia prophylaxis: an open randomized prospective trial to assess efficacy and haematological toxicity. *Aids 6:1169*.
171. Matsuoka, N., K. Eguchi, A. Kawakami, M. Tsuboi, Y. Kawabe, T. Aoyagi, and S. Nagataki. 1996. Inhibitory effect of clarithromycin on costimulatory molecule expression and cytokine production by synovial fibroblast-like cells. *Clin Exp Immunol 104:501*.
172. Morikawa, K., F. Oseko, S. Morikawa, and K. Iwamoto. 1994. Immunomodulatory effects of three macrolides, midecamycin acetate, josamycin, and clarithromycin, on human T-lymphocyte function in vitro. *Antimicrob Agents Chemother 38:2643*.

173. Morikawa, K., H. Watabe, M. Araake, and S. Morikawa. 1996. Modulatory effect of antibiotics on cytokine production by human monocytes in vitro. *Antimicrob Agents Chemother 40:1366*.
174. Burman, W. J., B. L. Stone, C. A. Rietmeijer, J. Maslow, D. L. Cohn, and R. R. Reves. 1998. Long-term outcomes of treatment of Mycobacterium avium complex bacteremia using a clarithromycin-containing regimen. *Aids 12:1309*.
175. Chaisson, R. E., C. A. Benson, M. P. Dube, L. B. Heifets, J. A. Korvick, S. Elkin, T. Smith, J. C. Craft, and F. R. Sattler. 1994. Clarithromycin therapy for bacteremic Mycobacterium avium complex disease. A randomized, double-blind, dose-ranging study in patients with AIDS. AIDS Clinical Trials Group Protocol 157 Study Team. *Ann Intern Med 121:905*.
176. Goldberger, M., and H. Masur. 1994. Clarithromycin therapy for Mycobacterium avium complex disease in patients with AIDS: potential and problems. *Ann Intern Med 121:974*.
177. Kadish, J. L., and R. S. Basch. 1976. Hematopoietic thymocyte precursors. I. Assay and kinetics of the appearance of progeny. *J Exp Med 143:1082*.
178. Hardy, R. R., C. E. Carmack, S. A. Shinton, J. D. Kemp, and K. Hayakawa. 1991. Resolution and characterization of pro-B and pre-pro-B cell stages in normal mouse bone marrow. *J Exp Med 173:1213*.
179. Hardy, R. R., and K. Hayakawa. 2001. B cell development pathways. *Annu Rev Immunol 19:595*.
180. Hozumi, N., and S. Tonegawa. 1976. Evidence for somatic rearrangement of immunoglobulin genes coding for variable and constant regions. *Proc Natl Acad Sci U S A 73:3628*.
181. Matthyssens, G., N. Hozumi, and S. Tonegawa. 1976. Somatic generation of antibody diversity. *Ann Immunol (Paris) 127:439*.
182. Schatz, D. G., M. A. Oettinger, and D. Baltimore. 1989. The V(D)J recombination activating gene, RAG-1. *Cell 59:1035*.
183. Oettinger, M. A., D. G. Schatz, C. Gorka, and D. Baltimore. 1990. RAG-1 and RAG-2, adjacent genes that synergistically activate V(D)J recombination. *Science 248:1517*.

184. Sakaguchi, N., and F. Melchers. 1986. Lambda 5, a new light-chain-related locus selectively expressed in pre-B lymphocytes. *Nature 324:579*.
185. Kudo, A., and F. Melchers. 1987. A second gene, VpreB in the lambda 5 locus of the mouse, which appears to be selectively expressed in pre-B lymphocytes. *Embo J 6:2267*.
186. Grawunder, U., T. M. Leu, D. G. Schatz, A. Werner, A. G. Rolink, F. Melchers, and T. H. Winkler. 1995. Down-regulation of RAG1 and RAG2 gene expression in preB cells after functional immunoglobulin heavy chain rearrangement. *Immunity 3:601*.
187. Osmond, D. G., A. Rolink, and F. Melchers. 1998. Murine B lymphopoiesis: towards a unified model. *Immunol Today 19:65*.
188. Goodnow, C. C., J. Crosbie, S. Adelstein, T. B. Lavoie, S. J. Smith-Gill, R. A. Brink, H. Pritchard-Briscoe, J. S. Wotherspoon, R. H. Loblay, K. Raphael, and et al. 1988. Altered immunoglobulin expression and functional silencing of self-reactive B lymphocytes in transgenic mice. *Nature 334:676*.
189. Hartley, S. B., J. Crosbie, R. Brink, A. B. Kantor, A. Basten, and C. C. Goodnow. 1991. Elimination from peripheral lymphoid tissues of self-reactive B lymphocytes recognizing membrane-bound antigens. *Nature 353:765*.
190. Pelanda, R., S. Schwers, E. Sonoda, R. M. Torres, D. Nemazee, and K. Rajewsky. 1997. Receptor editing in a transgenic mouse model: site, efficiency, and role in B cell tolerance and antibody diversification. *Immunity 7:765*.
191. Rosenberg, N., and P. W. Kincade. 1994. B-lineage differentiation in normal and transformed cells and the microenvironment that supports it. *Curr Opin Immunol 6:203*.
192. Ryan, D. H., B. L. Nuccie, C. N. Abboud, and J. M. Winslow. 1991. Vascular cell adhesion molecule-1 and the integrin VLA-4 mediate adhesion of human B cell precursors to cultured bone marrow adherent cells. *J Clin Invest 88:995*.
193. Saeland, S., V. Duvert, D. Pandrau, C. Caux, I. Durand, N. Wrighton, J. Wideman, F. Lee, and J. Banchereau. 1991. Interleukin-7 induces the proliferation of normal human B-cell precursors. *Blood 78:2229*.

194. Kondo, M., I. L. Weissman, and K. Akashi. 1997. Identification of clonogenic common lymphoid progenitors in mouse bone marrow. *Cell 91:661*.
195. Li, Y. S., R. Wasserman, K. Hayakawa, and R. R. Hardy. 1996. Identification of the earliest B lineage stage in mouse bone marrow. *Immunity 5:527*.
196. Kadmon, G., M. Eckert, M. Sammar, M. Schachner, and P. Altevogt. 1992. Nectadrin, the heat-stable antigen, is a cell adhesion molecule. *J Cell Biol 118:1245*.
197. Lin, Q., I. Taniuchi, D. Kitamura, J. Wang, J. F. Kearney, T. Watanabe, and M. D. Cooper. 1998. T and B cell development in BP-1/6C3/aminopeptidase A-deficient mice. *J Immunol 160:4681*.
198. Nielsen, P. J., B. Lorenz, A. M. Muller, R. H. Wenger, F. Brombacher, M. Simon, T. von der Weid, W. J. Langhorne, H. Mossmann, and G. Kohler. 1997. Altered erythrocytes and a leaky block in B-cell development in CD24/HSA-deficient mice. *Blood 89:1058*.
199. Hardy, R. R. 1990. Development of murine B cell subpopulations. *Semin Immunol 2:197*.
200. Burkhart, C., S. von Greyerz, J. P. Depta, D. J. Naisbitt, M. Britschgi, K. B. Park, and W. J. Pichler. 2001. Influence of reduced glutathione on the proliferative response of sulfamethoxazole-specific and sulfamethoxazole-metabolite-specific human CD4+ T-cells. *Br J Pharmacol 132:623*.
201. Daftarian, M. P., L. G. Filion, W. Cameron, B. Conway, R. Roy, F. Tropper, and F. Diaz-Mitoma. 1995. Immune response to sulfamethoxazole in patients with AIDS. *Clin Diagn Lab Immunol 2:199*.
202. Naisbitt, D. J., S. F. Gordon, M. Pirmohamed, C. Burkhart, A. E. Cribb, W. J. Pichler, and B. K. Park. 2001. Antigenicity and immunogenicity of sulphamethoxazole: demonstration of metabolism-dependent haptenation and T-cell proliferation in vivo. *Br J Pharmacol 133:295*.
203. Cribb, A. E., and S. P. Spielberg. 1992. Sulfamethoxazole is metabolized to the hydroxylamine in humans. *Clin Pharmacol Ther 51:522*.

204. Gill, H. J., S. J. Hough, D. J. Naisbitt, J. L. Maggs, N. R. Kitteringham, M. Pirmohamed, and B. K. Park. 1997. The relationship between the disposition and immunogenicity of sulfamethoxazole in the rat. *J Pharmacol Exp Ther 282:795*.

205. Borst, P., R. Evers, M. Kool, and J. Wijnholds. 2000. A family of drug transporters: the multidrug resistance-associated proteins. *J Natl Cancer Inst 92:1295*.

206. Schuetz, J. D., M. C. Connelly, D. Sun, S. G. Paibir, P. M. Flynn, R. V. Srinivas, A. Kumar, and A. Fridland. 1999. MRP4: A previously unidentified factor in resistance to nucleoside-based antiviral drugs. *Nat Med 5:1048*.

207. Jorajuria, S., N. Dereuddre-Bosquet, F. Becher, S. Martin, F. Porcheray, A. Garrigues, A. Mabondzo, H. Benech, J. Grassi, S. Orlowski, D. Dormont, and P. Clayette. 2004. ATP binding cassette multidrug transporters limit the anti-HIV activity of zidovudine and indinavir in infected human macrophages. *Antivir Ther 9:519*.

208. Lai, L., and T. M. Tan. 2002. Role of glutathione in the multidrug resistance protein 4 (MRP4/ABCC4)-mediated efflux of cAMP and resistance to purine analogues. *Biochem J 361:497*.

209. Chou, T. C., and P. Talalay. 1984. Quantitative analysis of dose-effect relationships: the combined effects of multiple drugs or enzyme inhibitors. *Adv Enzyme Regul 22:27*.

210. Vree, T. B., A. J. van der Ven, C. P. Verwey-van Wissen, E. W. van Ewijk-Beneken Kolmer, A. E. Swolfs, P. M. van Galen, and H. Amatdjais-Groenen. 1994. Isolation, identification and determination of sulfamethoxazole and its known metabolites in human plasma and urine by high-performance liquid chromatography. *J Chromatogr B Biomed Appl 658:327*.

211. Wijnholds, J., R. Evers, M. R. van Leusden, C. A. Mol, G. J. Zaman, U. Mayer, J. H. Beijnen, M. van der Valk, P. Krimpenfort, and P. Borst. 1997. Increased sensitivity to anticancer drugs and decreased inflammatory response in mice lacking the multidrug resistance-associated protein. *Nat Med 3:1275*.

212. Jones, J. L., D. L. Hanson, M. S. Dworkin, D. L. Alderton, P. L. Fleming, J. E. Kaplan, and J. Ward. 1999. Surveillance for AIDS-defining opportunistic illnesses, 1992-1997. *MMWR CDC Surveill Summ 48:1*.

213. Morris, A., J. D. Lundgren, H. Masur, P. D. Walzer, D. L. Hanson, T. Frederick, L. Huang, C. B. Beard, and J. E. Kaplan. 2004. Current epidemiology of Pneumocystis pneumonia. *Emerg Infect Dis 10:1713*.

214. Kaplan, J. E., H. Masur, and K. K. Holmes. 2002. Guidelines for preventing opportunistic infections among HIV-infected persons--2002. Recommendations of the U.S. Public Health Service and the Infectious Diseases Society of America. *MMWR Recomm Rep 51:1*.

215. Harmsen, A. G., and M. Stankiewicz. 1990. Requirement for CD4+ cells in resistance to Pneumocystis carinii pneumonia in mice. *J Exp Med 172:937*.

216. Beck, J. M., M. L. Warnock, H. B. Kaltreider, and J. E. Shellito. 1993. Host defenses against Pneumocystis carinii in mice selectively depleted of CD4+ lymphocytes. *Chest 103:116S*.

217. Harmsen, A. G., and M. Stankiewicz. 1991. T cells are not sufficient for resistance to Pneumocystis carinii pneumonia in mice. *J Protozool 38:44S*.

218. Marcotte, H., D. Levesque, K. Delanay, A. Bourgeault, R. de la Durantaye, S. Brochu, and M. C. Lavoie. 1996. Pneumocystis carinii infection in transgenic B cell-deficient mice. *J Infect Dis 173:1034*.

219. Lund, F. E., K. Schuer, M. Hollifield, T. D. Randall, and B. A. Garvy. 2003. Clearance of Pneumocystis carinii in mice is dependent on B cells but not on P carinii-specific antibody. *J Immunol 171:1423*.

220. Cushion, M. T., J. J. Ruffolo, and P. D. Walzer. 1988. Analysis of the developmental stages of Pneumocystis carinii, in vitro. *Lab Invest 58:324*.

221. Garvy, B. A., and A. G. Harmsen. 1996. Susceptibility to Pneumocystis carinii infection: host responses of neonatal mice from immune or naive mothers and of immune or naive adults. *Infect Immun 64:3987*.

222. Harper, S. A., K. Fukuda, T. M. Uyeki, N. J. Cox, and C. B. Bridges. 2004. Prevention and control of influenza: recommendations of the Advisory Committee on Immunization Practices (ACIP). *MMWR Recomm Rep 53:1*.

223. Amendola, A., A. Boschini, D. Colzani, G. Anselmi, A. Oltolina, R. Zucconi, M. Begnini, S. Besana, E. Tanzi, and A. R. Zanetti. 2001. Influenza vaccination of HIV-1-positive and HIV-1-negative former intravenous drug users. *J Med Virol 65:644*.
224. Sorvillo, F. J., and B. L. Nahlen. 1995. Influenza immunization for HIV-infected persons in Los Angeles. *Vaccine 13:377*.
225. Fowke, K. R., R. D'Amico, D. N. Chernoff, J. C. Pottage, Jr., C. A. Benson, B. E. Sha, H. A. Kessler, A. L. Landay, and G. M. Shearer. 1997. Immunologic and virologic evaluation after influenza vaccination of HIV-1-infected patients. *Aids 11:1013*.
226. Kroon, F. P., J. T. van Dissel, J. C. de Jong, K. Zwinderman, and R. van Furth. 2000. Antibody response after influenza vaccination in HIV-infected individuals: a consecutive 3-year study. *Vaccine 18:3040*.
227. Iorio, A. M., D. Francisci, B. Camilloni, G. Stagni, M. De Martino, D. Toneatto, R. Bugarini, M. Neri, and A. Podda. 2003. Antibody responses and HIV-1 viral load in HIV-1-seropositive subjects immunised with either the MF59-adjuvanted influenza vaccine or a conventional non-adjuvanted subunit vaccine during highly active antiretroviral therapy. *Vaccine 21:3629*.
228. Simanis, V., and P. Nurse. 1986. The cell cycle control gene cdc2+ of fission yeast encodes a protein kinase potentially regulated by phosphorylation. *Cell 45:261*.
229. Draetta, G., and D. Beach. 1989. The mammalian cdc2 protein kinase: mechanisms of regulation during the cell cycle. *J Cell Sci Suppl 12:21*.
230. Weinert, T. A., G. L. Kiser, and L. H. Hartwell. 1994. Mitotic checkpoint genes in budding yeast and the dependence of mitosis on DNA replication and repair. *Genes Dev 8:652*.
231. Weinert, T. A., and L. H. Hartwell. 1988. The RAD9 gene controls the cell cycle response to DNA damage in Saccharomyces cerevisiae. *Science 241:317*.
232. Lautier, D., J. Lagueux, J. Thibodeau, L. Menard, and G. G. Poirier. 1993. Molecular and biochemical features of poly (ADP-ribose) metabolism. *Mol Cell Biochem 122:171*.

233. Hong, S. J., T. M. Dawson, and V. L. Dawson. 2004. Nuclear and mitochondrial conversations in cell death: PARP-1 and AIF signaling. *Trends Pharmacol Sci 25:259*.

234. Susin, S. A., H. K. Lorenzo, N. Zamzami, I. Marzo, B. E. Snow, G. M. Brothers, J. Mangion, E. Jacotot, P. Costantini, M. Loeffler, N. Larochette, D. R. Goodlett, R. Aebersold, D. P. Siderovski, J. M. Penninger, and G. Kroemer. 1999. Molecular characterization of mitochondrial apoptosis-inducing factor. *Nature 397:441*.

235. Loeffler, M., E. Daugas, S. A. Susin, N. Zamzami, D. Metivier, A. L. Nieminen, G. Brothers, J. M. Penninger, and G. Kroemer. 2001. Dominant cell death induction by extramitochondrially targeted apoptosis-inducing factor. *Faseb J 15:758*.

236. Endres, M., Z. Q. Wang, S. Namura, C. Waeber, and M. A. Moskowitz. 1997. Ischemic brain injury is mediated by the activation of poly(ADP-ribose)polymerase. *J Cereb Blood Flow Metab 17:1143*.

237. Szabo, C., and V. L. Dawson. 1998. Role of poly(ADP-ribose) synthetase in inflammation and ischaemia-reperfusion. *Trends Pharmacol Sci 19:287*.

238. Eliasson, M. J., K. Sampei, A. S. Mandir, P. D. Hurn, R. J. Traystman, J. Bao, A. Pieper, Z. Q. Wang, T. M. Dawson, S. H. Snyder, and V. L. Dawson. 1997. Poly(ADP-ribose) polymerase gene disruption renders mice resistant to cerebral ischemia. *Nat Med 3:1089*.

239. Pieper, A. A., T. Walles, G. Wei, E. E. Clements, A. Verma, S. H. Snyder, and J. L. Zweier. 2000. Myocardial postischemic injury is reduced by polyADPripose polymerase-1 gene disruption. *Mol Med 6:271*.

240. Collier, A. C., R. J. Helliwell, J. A. Keelan, J. W. Paxton, M. D. Mitchell, and M. D. Tingle. 2003. 3'-azido-3'-deoxythymidine (AZT) induces apoptosis and alters metabolic enzyme activity in human placenta. *Toxicol Appl Pharmacol 192:164*.

241. Ishitsuka, K., T. Hideshima, M. Hamasaki, N. Raje, S. Kumar, K. Podar, S. Le Gouill, N. Shiraishi, H. Yasui, A. M. Roccaro, Y. Z. Tai, D. Chauhan, R. Fram, K. Tamura, J. Jain, and K. C. Anderson. 2005. Novel inosine monophosphate dehydrogenase inhibitor VX-944 induces apoptosis in multiple myeloma cells primarily via caspase-independent AIF/Endo G pathway. *Oncogene*.

242. Falchetti, A., A. Franchi, C. Bordi, C. Mavilia, L. Masi, F. Cioppi, R. Recenti, L. Picariello, F. Marini, F. Del Monte, V. Ghinoi, V. Martineti, A. Tanini, and M. L. Brandi. 2005. Azidothymidine induces apoptosis and inhibits cell growth and telomerase activity of human parathyroid cancer cells in culture. *J Bone Miner Res 20:410*.

243. Ghosh, S. K., C. Wood, L. H. Boise, A. M. Mian, V. V. Deyev, G. Feuer, N. L. Toomey, N. C. Shank, L. Cabral, G. N. Barber, and W. J. Harrington, Jr. 2003. Potentiation of TRAIL-induced apoptosis in primary effusion lymphoma through azidothymidine-mediated inhibition of NF-kappa B. *Blood 101:2321*.

244. Lee, R. K., J. P. Cai, V. Deyev, P. S. Gill, L. Cabral, C. Wood, R. P. Agarwal, W. Xia, L. H. Boise, E. Podack, and W. J. Harrington, Jr. 1999. Azidothymidine and interferon-alpha induce apoptosis in herpesvirus-associated lymphomas. *Cancer Res 59:5514*.

245. Canas, E., J. Pachon, F. Garcia-Pesquera, J. R. Castillo, P. Viciana, J. M. Cisneros, and M. E. Jimenez-Mejias. 1996. Absence of effect of trimethoprim-sulfamethoxazole on pharmacokinetics of zidovudine in patients infected with human immunodeficiency virus. *Antimicrob Agents Chemother 40:230*.

246. McCune, J. M., R. Namikawa, C. C. Shih, L. Rabin, and H. Kaneshima. 1990. Suppression of HIV infection in AZT-treated SCID-hu mice. *Science 247:564*.

247. Boxenbaum, H., and C. DiLea. 1995. First-time-in-human dose selection: allometric thoughts and perspectives. *J Clin Pharmacol 35:957*.

248. Mahmood, I., and J. D. Balian. 1996. Interspecies scaling: a comparative study for the prediction of clearance and volume using two or more than two species. *Life Sci 59:579*.

249. Hertzberg, R. C. 1989. Fitting a model to categorical response data with application to species extrapolation of toxicity. *Health Phys 57 Suppl 1:405*.

250. Paxton, J. W. 1995. The allometric approach for interspecies scaling of pharmacokinetics and toxicity of anti-cancer drugs. *Clin Exp Pharmacol Physiol 22:851*.

251. Ugrinovic, S., N. Menager, N. Goh, and P. Mastroeni. 2003. Characterization and development of T-Cell immune responses in B-cell-deficient (Igh-6(-/-)) mice with Salmonella enterica serovar Typhimurium infection. *Infect Immun 71:6808*.
252. Linton, P. J., J. Harbertson, and L. M. Bradley. 2000. A critical role for B cells in the development of memory CD4 cells. *J Immunol 165:5558*.
253. Carvalho, T. L., T. Mota-Santos, A. Cumano, J. Demengeot, and P. Vieira. 2001. Arrested B lymphopoiesis and persistence of activated B cells in adult interleukin 7(-/)- mice. *J Exp Med 194:1141*.
254. Roths, J. B., and C. L. Sidman. 1992. Both immunity and hyperresponsiveness to Pneumocystis carinii result from transfer of CD4+ but not CD8+ T cells into severe combined immunodeficiency mice. *J Clin Invest 90:673*.
255. Limper, A. H., J. S. Hoyte, and J. E. Standing. 1997. The role of alveolar macrophages in Pneumocystis carinii degradation and clearance from the lung. *J Clin Invest 99:2110*.
256. Macy, J. D., Jr., E. C. Weir, S. R. Compton, M. J. Shlomchik, and D. G. Brownstein. 2000. Dual infection with Pneumocystis carinii and Pasteurella pneumotropica in B cell-deficient mice: diagnosis and therapy. *Comp Med 50:49*.
257. Garvy, B. A., J. A. Wiley, F. Gigliotti, and A. G. Harmsen. 1997. Protection against Pneumocystis carinii pneumonia by antibodies generated from either T helper 1 or T helper 2 responses. *Infect Immun 65:5052*.
258. Harmsen, A. G., W. Chen, and F. Gigliotti. 1995. Active immunity to Pneumocystis carinii reinfection in T-cell-depleted mice. *Infect Immun 63:2391*.
259. Zheng, M., J. E. Shellito, L. Marrero, Q. Zhong, S. Julian, P. Ye, V. Wallace, P. Schwarzenberger, and J. K. Kolls. 2001. CD4+ T cell-independent vaccination against Pneumocystis carinii in mice. *J Clin Invest 108:1469*.
260. Gigliotti, F., and W. T. Hughes. 1988. Passive immunoprophylaxis with specific monoclonal antibody confers partial protection against Pneumocystis carinii pneumonitis in animal models. *J Clin Invest 81:1666*.
261. Gigliotti, F., B. A. Garvy, and A. G. Harmsen. 1996. Antibody-mediated shift in the profile of glycoprotein A phenotypes observed in a mouse model of Pneumocystis carinii pneumonia. *Infect Immun 64:1892*.

262. Brachtel, E. F., M. Washiyama, G. D. Johnson, K. Tenner-Racz, P. Racz, and I. C. MacLennan. 1996. Differences in the germinal centres of palatine tonsils and lymph nodes. *Scand J Immunol 43:239*.

263. Lane, P., A. Traunecker, S. Hubele, S. Inui, A. Lanzavecchia, and D. Gray. 1992. Activated human T cells express a ligand for the human B cell-associated antigen CD40 which participates in T cell-dependent activation of B lymphocytes. *Eur J Immunol 22:2573*.

264. Snapper, C. M., M. R. Kehry, B. E. Castle, and J. J. Mond. 1995. Multivalent, but not divalent, antigen receptor cross-linkers synergize with CD40 ligand for induction of Ig synthesis and class switching in normal murine B cells. A redefinition of the TI-2 vs T cell-dependent antigen dichotomy. *J Immunol 154:1177*.

265. Croft, M., and S. L. Swain. 1991. B cell response to fresh and effector T helper cells. Role of cognate T-B interaction and the cytokines IL-2, IL-4, and IL-6. *J Immunol 146:4055*.

266. Kelsoe, G. 1996. The germinal center: a crucible for lymphocyte selection. *Semin Immunol 8:179*.

267. Gilkeson, G. S., K. Bernstein, A. M. Pippen, S. H. Clarke, T. Marion, D. S. Pisetsky, P. Ruiz, and J. B. Lefkowith. 1995. The influence of variable-region somatic mutations on the specificity and pathogenicity of murine monoclonal anti-DNA antibodies. *Clin Immunol Immunopathol 76:59*.

268. McHeyzer-Williams, M. G., and R. Ahmed. 1999. B cell memory and the long-lived plasma cell. *Curr Opin Immunol 11:172*.

269. Beyer, W. E., A. M. Palache, J. C. de Jong, and A. D. Osterhaus. 2002. Cold-adapted live influenza vaccine versus inactivated vaccine: systemic vaccine reactions, local and systemic antibody response, and vaccine efficacy. A meta-analysis. *Vaccine 20:1340*.

270. Kroon, F. P., G. F. Rimmelzwaan, M. T. Roos, A. D. Osterhaus, D. Hamann, F. Miedema, and J. T. van Dissel. 1998. Restored humoral immune response to influenza vaccination in HIV-infected adults treated with highly active antiretroviral therapy. *Aids 12:F217*.

271. Grabar, S., V. Le Moing, C. Goujard, C. Leport, M. D. Kazatchkine, D. Costagliola, and L. Weiss. 2000. Clinical outcome of patients with HIV-1 infection according to immunologic and virologic response after 6 months of highly active antiretroviral therapy. *Ann Intern Med 133:401*.

VITA

David James Feola, Doctoral Candidate
University of Kentucky, Clinical Pharmaceutical Sciences

Birth

February 2, 1973
Parkersburg, West Virginia, United States of America

Education

University of Kentucky College of Pharmacy
Bachelor of Science in Pharmacy
August 1996

University of Kentucky College of Pharmacy
Doctor of Pharmacy
May 1997

Professional Positions

Appalachian Regional Healthcare Regional Medical Center, Hazard, KY
Clinical Pharmacist, May 1997-May 1998

University of Kentucky Hospital, Lexington, KY
Residency in Pharmacy Practice, July 1998-June 1999

University of Kentucky Hospital, Lexington, KY
Residency in Infectious Disease Pharmacy, July 1999-June 2000

University of Kentucky Clinic, Lexington, KY
Division of Infectious Diseases, Department of Internal Medicine
HIV/AIDS Clinic, July 1999-June 2000 (part-time)

University of Kentucky Hospital, Lexington, KY
Critical Care Clinical Pharmacist, July 1999-August 2000 (part-time)

University of Kentucky Hospital, Lexington, KY
Clinical Staff Pharmacist, July 1998-August 2005 (part-time)

Honors

Dean Earl P. Slone Leadership Award, University of Kentucky College of Pharmacy, 1995, 1996, 1997.

Kappa Psi Graduate Chapter Award, University of Kentucky Graduate Chapter, Kappa Psi Pharmaceutical Fraternity, 1995.

Outstanding Graduating Man Award, University of Kentucky College of Pharmacy, 1997.

Inducted, Rho Chi Pharmaceutical Honor Society, 1997.

University of Kentucky College of Pharmacy and University of Kentucky Hospital Pharmacy Residency Program Impact Award, 2000.

University of Kentucky College of Pharmacy and University of Kentucky Hospital Pharmacy Residency Program Outstanding Resident Award, 2000.

Research Challenge Trust Fund Scholar, University of Kentucky Graduate School, 2000-present.

American Foundation for Pharmaceutical Education Pre-doctoral Fellowship Award, 2002, 2003, and 2004.

Publications

Feola DJ and Rapp RP. Effect of food intake on the bioavailability of itraconazole [letter]. Clinical Infectious Diseases 1997 Aug;25(2):344-5.

Feola DJ. Update on anticoagulation. Current Topics 1999 Jan;29(1):2-3.

Evans ME, Feola DJ, and Rapp RP. Polymyxin B sulfate and colistin: old antibiotics for emerging multiresistant gram-negative bacteria. Annals of Pharmacotherapy 1999;33:960-7.

Feola DJ and Thornton AC. Metronidazole-induced pancreatitis in a patient with recurrent vaginal trichomoniasis. Pharmacotherapy 2002 Nov;22(11):1508-10.

Feola DJ and Garvy BA. Zidovudine plus sulfamethoxazole-trimethoprim adversely affects B lymphocyte maturation in bone marrow of normal mice. International Immunopharmacology 2005. In press.

Feola DJ, Thornton AC, and Garvy BA. Effects of antiretroviral therapy on immunity in patients infected with HIV. Current Pharmaceutical Design 2006 (12). In press.

Thornton AC, Hoven A, Feola DJ, and Murphy B. Diarrheal Diseases, in APIC Text of Infection Control and Epidemiology: Second Edition, Chapter 100, 100-1-100-22, Association for Professionals in Infection Control and Epidemiology, Inc, 2005.